

Nanoparticles and Microorganisms: from Synthesis to Toxicity

THÈSE N° 5614 (2013)

PRÉSENTÉE LE 22 FÉVRIER 2013

À LA FACULTÉ DE L'ENVIRONNEMENT NATUREL, ARCHITECTURAL ET CONSTRUIT
LABORATOIRE DE MICROBIOLOGIE ENVIRONNEMENTALE
PROGRAMME DOCTORAL EN ENVIRONNEMENT

ÉCOLE POLYTECHNIQUE FÉDÉRALE DE LAUSANNE

POUR L'OBTENTION DU GRADE DE DOCTEUR ÈS SCIENCES

PAR

Jan DOBIAS

acceptée sur proposition du jury:

Prof. M. Bierlaire, président du jury
Prof. R. Bernier-Latmani, directrice de thèse
Dr R. Behra, rapporteur
Prof. C. Ludwig, rapporteur
Prof. V. Slaveykova, rapporteur



ÉCOLE POLYTECHNIQUE
FÉDÉRALE DE LAUSANNE

Suisse
2013

Table of Contents

Acknowledgments	5
Summary	7
Résumé	9
Introduction	11
References	15
1 Role of proteins in the formation of selenium nanoparticles	19
1.1 Introduction.....	21
1.2 Materials and Methods.....	23
1.3 Results and discussion	29
1.4 Conclusions.....	35
1.5 Acknowledgments	35
1.6 References.....	37
1.7 Supporting Information.....	39
2 Silver release from silver nanoparticles in natural waters	53
2.1 Introduction.....	55
2.2 Materials and Methods.....	57
2.3 Results and discussion	61
2.4 Associated Content	69
2.5 Acknowledgments	69
2.6 References.....	71
2.7 Supporting Information.....	73
3 Silver nanoparticle toxicity to <i>Escherichia coli</i> and <i>Bacillus subtilis</i>	77
3.1 Introduction.....	79
3.2 Materials and methods	81
3.3 Results and discussion	83
3.4 Acknowledgments	91
3.5 Reference:	93
3.6 Supporting Information.....	96
4 Effect of silver nanoparticles on microbial communities from Lake Geneva	105
4.1 Introduction.....	107
4.2 Materials and methods	109
4.3 Results and discussion	113
4.4 Associated Content	119
4.5 Acknowledgments	119
4.6 References.....	121
4.7 Supporting Information.....	125
5 Conclusions	135
5.1 Chapter 1.....	135
5.2 Chapter 2.....	136
5.3 Chapter 3.....	137
5.4 Chapter 4.....	138
Curriculum Vitae	139

ACKNOWLEDGMENTS

I would first like to thank Prof. Rizlan Bernier-Latmani who is the principal investigator of the EML group and who was my advisor during my doctoral studies.

She provided me with the opportunity to work in a multi-disciplinary field at the edge of biology, microbiology, molecular biology, analytical chemistry, environmental science and field site studies. She has always been available for scientific discussion and her enthusiasm was of great help in moments of doubt.

I also thank the people from central analytical laboratory, and specially Jean-David Teuscher, for their kind assistance with the analytical instruments, Dr. L. Felipe De Alencastro, Dr. Lucas Bragazza, Prof. Tamar Kohn and Dr. Ruud Hovius for granting access to their facilities or equipment.

I would also like to thank all the people I had the chance to work with during my doctoral studies at the EML, former and present members, visiting people or interns.

Lastly, I thank my family and friends whose support and encouragement has been invaluable.

SUMMARY

Nanoscience is a young and growing field of science. It encompasses a diversity of sub-fields such as nanotechnology and nano-medicine, all of them seeking to realize the promises of nanoscale physics. Nano means: “billionth” and conceptually all nano-like terminology implicitly refers to the nano-meter (nm) scale (10^{-9} m). Therefore the size range covered by nanoscience is from 1 to 100 nm, which lays at the boundary of two distinct worlds of physics: the bulk material and the atomic structure. In that particular region, laws of physics transition and while the bulk material exhibits constant physics independently of its size, nanomaterials see their properties and characteristics change as a function of size.

That very specific property makes nanomaterials extremely appealing for a variety of applications. These applications cover areas such as electronics, photonics, catalysts, photography, material coatings, but also biotechnology, medicine, pharmacology, textile embedding, paints, household goods, cosmetics, foods and children goods.

The current dissertation covers the field of metallic nanoparticles, within which, two types have been considered: selenium nanoparticles (SeNPs) and silver nanoparticles (AgNPs). SeNPs are interesting in inorganic semiconductors and crystal respectively used in electronics and photonics, whereas the interest for AgNPs is due to their strong antimicrobial properties.

NPs are not only anthropogenic, but can be produced by a variety of organisms (e.g., bacteria, fungi, yeast or plants). However their biological synthesis remains partially unknown. They can be closely related to chemically produced NPs, but can also exhibit very specific characteristics unobtainable by conventional chemistry. An understanding of the underlying mechanisms of biological synthesis if extended to the industrial level could help achieve better NPs at a lower energetic and environmental cost.

The use of nanomaterials such as AgNPs to protect drinking water from pathogens or prevent microbially derived bad odors, present the risk of their release into the environment. A gap of knowledge remains as to the hazards caused by an increase in AgNPs load in freshwater and sediments on the various biotas.

This thesis addressed these two fundamental questions in Chapter 1 for SeNPs and Chapters 2, 3 and 4 for AgNPs

Keywords : Bacteria, deployment, environment, lake, nanoparticle, river, selenium, silver, “silver loss”, surface water, synthesis, toxicity

RESUME

La nanoscience est une science jeune. Elle couvre une large diversité de domaines comme les nanotechnologies, nanomatériaux ou nanomédecine. Le préfixe Grec nano- signifie un « milliardième » et est souvent implicitement associé à l'unité du mètre. Ainsi les nanosciences s'occupent d'éléments compris entre 1 et 100 nanomètres (nm). Cette gamme de tailles est particulière en ce qu'elle réside à mi-chemin entre le microscopique et l'atomique. Dans ces deux régions de la physique les propriétés des matériaux ne changent pas en fonction de leur taille, ce qui n'est plus vrai au niveau du nanomètre. A ce niveau, les matériaux voient leurs caractéristiques, ainsi que leur propriétés, changer en fonction de leur taille.

Cette propriété est extrêmement intéressante pour une large gamme d'application comme l'électronique, la photonique, les catalyseurs, les biotechnologies, la médecine, la pharmacologie mais aussi le textile, la peinture, la nourriture, les cosmétiques ou les produits pour enfants. Ces produits étant déjà largement répandus, la connaissance de leur comportement une fois relâché dans l'environnement est de première importance.

Ce travail de thèse, s'est intéressé à deux types de nanoparticules : à base de sélénium (AgNPs) ou à base d'argent (AgNPs). Toutes deux ont des propriétés très intéressantes, la première dans le domaine des semi-conducteurs inorganiques et la deuxième dans celui des effets antimicrobiens (bactéricide).

Les NPs ne sont pas seulement d'origine anthropogénique, mais peuvent aussi être produites par de nombreux organismes (e.g. bactérie, levure, lichen, champignon et plante). Leurs propriétés peuvent être proche de NPs synthétiques mais sont souvent spécifiques. Le mécanisme de synthèse est loin d'être compris et sa compréhension permettrait d'être étendu au domaine industriel, permettant d'obtenir de meilleurs produits mais aussi de diminuer le poids énergétique et environnemental des méthodes de synthèse conventionnelles.

Les nanoparticules peuvent par exemple être utilisées dans les textiles pour tuer les bactéries responsables d'odeurs incommodes. Si l'effet toxique des NPs est connu, leur effet à long terme dans l'environnement reste à élucider. Le travail présenté ici questionne ces deux points, dans le chapitre 1 pour le sélénium et les chapitres 2, 3 et 4 pour l'argent.

Mot-clés : Argent, bactérie, déploiement, environnement, eaux de surface, lac, nanoparticule, dissolution d'argent, rivière, sélénium, synthèse, toxicité.

INTRODUCTION

Nanoscience is a rapidly-developing field that covers a wide-range of application in a large variety of areas of science and technology. The greek prefix ‘nano’ used in nanoscience, nanomaterials or nanoparticles means “1 billionth”, while 1 nanometer (1 nm) is $1/10^9$ m. An accepted definition of nanoscale materials is materials that are in the 1-100 nm size range in at least one dimension. The dimension factor is important because it allows materials such as carbon nanotubes, which are several micrometer long by few nanometer wide, to be included in the definition.

Back in 2006, when the nanoparticle project was first discussed, nanomaterials were getting increased attention from academia but also from industry. The number of products available on the market and explicitly referencing the use of nanomaterials in their composition jumped from 54 in 2005 to 336 in 2006¹. New to the field at that time, I would not have predicted a steady increase over the years, but indeed there was, as there are more than 1,300 referenced products in 2011¹. In academia, nanoparticles (NPs), a type of nanomaterials, were getting increasing attention from fields such as biology, microbiology, and geochemistry. Symposia featuring nanoparticles at international conferences grew larger and attracted more scientists from around the world. It was within this appealing and promising new field of nanoscience that this project was started.

One underlying justification for this work was the fundamental observation that nanoparticles of biological origin (biogenic nanoparticles) had the potential to include a wider variety of sizes, shapes, coatings, composition and structure than their chemical counterparts² (chemogenic nanoparticles). Furthermore, they could have additional beneficial properties not obtainable by chemical means. For example, biogenic magnetic nanocrystals (magnetite) were shown to exhibit better crystallographic performance than synthetic ones³. Such observations led to investigating the origin of observed differences between biogenic and chemogenic materials. By extension, if the causative agents could be identified, there might be the potential for the direct synthesis of nanomaterials using biological systems. These were the questions we addressed in the first chapter of this thesis.

The increasing use of nanomaterials represents a yearly production of hundreds of tons^{4, 5}. It has been documented that consumer products containing nanomaterials are likely to release a fraction of those nanosized materials into the environment⁶⁻⁹. An important fraction of nanomaterials used in consumer products is made of silver nanoparticles¹ (AgNPs), which have strong antimicrobial properties¹⁰⁻¹³. Therefore a growing concern for both academia and regulators is emerging about their potentially

harmful impact on prokaryotic and eukaryotic organisms^{8, 14-17} once released in the environment. Chapters 2, 3 and 4 probe the fate of silver NPs (AgNPs) in the environment and their potential inhibitory effect on microorganisms. More specifically, Chapter 2 explores the release of Ag⁺ from AgNPs under environmentally relevant conditions, Chapter 3 investigates the AgNPs characteristics that lead to toxicity to bacteria, and Chapter 4 discusses the impact of AgNPs on the diversity of microbial communities from Lake Geneva.

Progress in the field of nanotechnology has been rapid and a series of innovative synthesis protocols and characterization techniques have been developed¹¹. The products of conventional chemical and physical synthesis methods may result in the synthesis of a mixture of nanoparticles with poor morphology and low synthesis yield¹⁸⁻²⁰. Many of these methods proved to be unfriendly to the environment due to the use of toxic chemicals²¹ but also due the energy consumption related to the need for elevated temperatures and/or pressure during the synthesis process²².

Biogenic synthesis of nanoparticles has been widely documented and can be achieved by several organisms including bacteria, yeast, fungi, lichens, algae, plant and plant extracts^{2, 23}. The involvement of proteins in metal reduction and morphology control has been documented²³. For example, they have been shown to play key roles in nucleation and crystal growth of bacteriogenic metallic NPs²⁴⁻³⁰. Finally, short peptides have been successfully used in biopanning techniques to specifically deliver iron oxide NPs onto titanium patterns³¹⁻³³.

The increasing demand for nanomaterials should be accompanied by “green” synthesis methods in an effort to reduce generated hazardous waste from this industry. Green chemistry would help minimize the use of unsafe products and maximize the efficiency of chemical processes¹¹. An advantage of biogenic synthesis, over conventional chemical synthesis, is the safer and easier handling of microbial cultures and the simpler downstream processing of biomass as compared to synthetic methods². Hence, biogenic NP synthesis represents a very interesting greener and more environmentally friendly manufacturing alternative, due to the use of chemicals of lower toxicity, to the use of lower ambient temperatures and lower pressures in the synthesis^{21, 34, 35}.

In the first chapter of this thesis, the biologically mediated formation of Se NPs is targeted. We used the biologically mediated reduction of selenite to elemental selenium by *E. coli* to evaluate the role of proteins in constraining the properties of the NPs.

Thus, we first tackled the role of proteins in controlling the formation of biogenic NPs (Chapter 1) and then moved on to consider the consequences of AgNPs release in the environment, first from a purely chemical point of view (Chapter 2) and second from the point of view of their impact on microorganisms (Chapters 3 and 4).

Synthesis of nanomaterials is one aspect of interest but their fate in the environment is equally important. It is commonly acknowledged that the use of nanomaterials will result in their release into the environment^{8, 36} potentially causing important damage to natural ecosystems. AgNPs are the most relevant NPs for which to evaluate the effect on ecosystems because they exhibit a high level of toxicity at low concentration to a large diversity of microorganism. Microorganisms are key actors in many environmental, chemical and energetic cycles on which humans are dependent and at least in that respect major attention should be paid to the harmful effects of released anthropogenic nanomaterials into the environment.

Should AgNPs be shown to have the potential to serve as a source of Ag⁺, their stability and persistence in the environment would be the primary focus of research. Should their persistence be extensive, attention would be oriented towards their possible direct interaction with microorganism leading to toxicity.

AgNPs possess several interesting properties for industrial applications (i.e., electrical, optical and catalytic properties)³⁷ but the dominant one is its strong bactericidal effect¹⁰⁻¹³. AgNPs are present in a large number of products spread across a diversity of applications that include: cosmetics, clothing, children goods, biomedical devices and electronics¹.

Several estimations of environmental concentration of AgNPs were conducted and predicted a concentration of 0.3 µg/L for surface water, 6 ppm for sewage treatment plant sludge and 10 ppm for river sediments^{5, 14}. Risk assessment approaches were used to evaluate and confirm the potential risk of AgNPs presence in the environment to living organism¹⁴. A study of Lake Geneva sediments from the Bay of Vidy showed that silver concentrations (1.7-4.6 ppm), near the outlet of a sewage treatment plant, were 10-40 fold higher than background level³⁸. The measured concentrations, although lower than that predicted from modeling studies, suggest that the growing use of AgNPs might become a considerable threat to the environment. Interestingly, while environmental considerations are the justification of many studies, very few have looked at the impact of AgNPs on biota. Hence, the presumed negative effect of AgNPs on biota under realistic conditions remains an open question.

No systematic study has been conducted to look at the physico-chemical characteristics associated with toxicity to microorganism. Previously published findings are extremely valuable but exhibited contradictory results that may be attributed to differences in the considered materials. One example is a recent study that compared citrate-coated AgNPs of 20 nm ± 12 nm to PVP coated AgNPs of 7.6 nm ± 2 nm³⁹. As AgNPs stability is size dependent⁴⁰, the study conclusions are not as strong as they could be, had the authors used a uniform size for all NPs. The absence of a systematic study is salient when the literature is considered carefully.

The effect of some physico-chemical characteristics (e.g., size, coating) has been documented, and while the published findings relative to AgNPs size-mediated toxicity point to a consensus of sub-10nm AgNPs as exhibiting a dramatic effect in microbial inhibition, the effect of the capping agents of AgNPs remains unclear; some studies point to an effect of the coating and some show none^{13, 41, 42}. For studies showing an effect of the capping agent, a proposed explanation for toxicity is the charge associated to the coating and possible electrostatic interactions with the cell membrane^{42, 43}.

Despite the numerous available studies, a large gap still exists in the knowledge of the factors influencing the toxicity of AgNPs under environmental conditions. Among the different physico-chemical characteristics, only size seems to point to consensus of toxicity for sub-10nm AgNPs. The toxicity to environmental microbial consortia is unknown as most of the work considered laboratory planktonic bacterial strains¹³ but effect on *Pseudomonas sp.* biofilms has been reported as well⁴⁴. Finally the mechanism of toxicity is still under debate but three possible alternatives emerge from the literature: (1) release of silver ions from AgNPs^{10, 45-47}, (2) damage of the cell membrane by direct association with AgNPs^{41, 43, 44, 48-50} or uptake of AgNPs (<10nm)⁴⁹ and (3) generation of reactive oxygen species⁵¹⁻⁵⁵.

The goal of Chapters 2, 3 and 4 was to close some of the gaps described above (i.e., persistence in the environment, toxicity factors and impact on bacterial consortia) in order to have a better understanding of realistic consequences from the use and release of AgNPs in natural environment that could help decision making when risk assessment is required.

REFERENCES

- (1) Woodrow Woodrow Wilson Center: Project on Emerging Nanotechnologies Inventory. http://www.nanotechproject.org/inventories/consumer/analysis_draft/.
- (2) Rai, M.; Gade, A.; Yadav, A., Biogenic Nanoparticles: An Introduction to What They Are, How They Are Synthesized and Their Applications. In *Metal Nanoparticles in Microbiology*, Rai, M.; Duran, N., Eds. Springer Berlin Heidelberg: **2011**; pp 1-14.
- (3) Han, L.; Li, S.; Yang, Y.; Zhao, F.; Huang, J.; Chang, J., Comparison of magnetite nanocrystal formed by biomineralization and chemosynthesis. *Journal of Magnetism and Magnetic Materials* **2007**, *313* (1), 236-242.
- (4) Kumar, N.; Shah, V.; Walker, V. K., Influence of a nanoparticle mixture on an arctic soil community. *Environmental Toxicology and Chemistry* **2012**, *31* (1), 131-135.
- (5) Mueller, N. C.; Nowack, B., Exposure modeling of engineered nanoparticles in the environment. *Environmental Science & Technology* **2008**, *42* (12), 4447-4453.
- (6) Benn, T. M.; Westerhoff, P., Nanoparticle Silver Released into Water from Commercially Available Sock Fabrics. *Environmental Science & Technology* **2008**, *42* (11), 4133-4139.
- (7) Durán, N.; Marcato, P.; Alves, O.; Da Silva, J.; De Souza, G.; Rodrigues, F.; Esposito, E., Ecosystem protection by effluent bioremediation: silver nanoparticles impregnation in a textile fabrics process. *Journal of Nanoparticle Research* **2010**, *12* (1), 285-292.
- (8) Gottschalk, F.; Nowack, B., The release of engineered nanomaterials to the environment. *Journal of Environmental Monitoring* **2011**, *13* (5), 1145-1155.
- (9) Kim, B.; Park, C. S.; Murayama, M.; Hochella, M. F., Discovery and Characterization of Silver Sulfide Nanoparticles in Final Sewage Sludge Products. *Environmental Science & Technology* **2010**, *44* (19), 7509-7514.
- (10) Sotiriou, G. A.; Pratsinis, S. E., Antibacterial Activity of Nanosilver Ions and Particles. *Environmental Science & Technology* **2010**, *44* (14), 5649-5654.
- (11) Sharma, V. K.; Yngard, R. A.; Lin, Y., Silver nanoparticles: Green synthesis and their antimicrobial activities. *Advances in Colloid and Interface Science* **2009**, *145* (1-2), 83-96.
- (12) Lok, C. N.; Ho, C. M.; Chen, R.; He, Q. Y.; Yu, W. Y.; Sun, H.; Tam, P. K. H.; Chiu, J. F.; Che, C. M., Silver nanoparticles: partial oxidation and antibacterial activities. *Journal of Biological Inorganic Chemistry* **2007**, *12* (4), 527-534.
- (13) Marambio-Jones, C.; Hoek, E., A review of the antibacterial effects of silver nanomaterials and potential implications for human health and the environment. *Journal of Nanoparticle Research* **2010**, *12* (5), 1531-1551.
- (14) Blaser, S. A.; Scheringer, M.; MacLeod, M.; Hungerbühler, K., Estimation of cumulative aquatic exposure and risk due to silver: Contribution of nano-functionalized plastics and textiles. *Science of The Total Environment* **2008**, *390* (2-3), 396-409.
- (15) Handy, R. O.; Richard, Viewpoint: Formulating the Problems for Environmental Risk Assessment of Nanomaterials. *Environmental Science & Technology* **2007**, *41* (16), 5582-5588.
- (16) Nowack, B.; Bucheli, T. D., Occurrence, behavior and effects of nanoparticles in the environment. *Environmental Pollution* **2007**, *150* (1), 5-22.
- (17) Wiesner, M. R.; Lowry, G. V.; Jones, K. L.; Hochella, J. M. F.; Di Giulio, R. T.; Casman, E.; Bernhardt, E. S., Decreasing Uncertainties in Assessing Environmental Exposure, Risk, and Ecological Implications of Nanomaterials. *Environmental Science & Technology* **2009**, *43* (17), 6458-6462.
- (18) Sau, T. K.; Rogach, A. L., Nonspherical Noble Metal Nanoparticles: Colloid-Chemical Synthesis and Morphology Control. *Advanced Materials* **2010**, *22* (16), 1781-1804.
- (19) Dimitrijevic, N. M.; Kamat, P. V., Photoelectrochemistry in particulate systems. 8. Photochemistry of colloidal selenium. *Langmuir* **1988**, *4* (3), 782-784.
- (20) Jeong, U.; Xia, Y., Synthesis and Crystallization of Monodisperse Spherical Colloids of Amorphous Selenium. *Advanced Materials* **2005**, *17* (1), 102-106.
- (21) Pearce, C. I.; Coker, V. S.; Charnock, J. M.; Patrick, R. A. D.; Mosselmans, J. F. W.; Law, N.; Beveridge, T. J.; Lloyd, J. R., Microbial manufacture of chalcogenide-based nanoparticles via the reduction of selenite using *Veillonella atypica*: an in situ EXAFS study. *Nanotechnology* **2008**, *19* (15), 155603.

- (22) Birla, S. S.; Tiwari, V. V.; Gade, A. K.; Ingle, A. P.; Yadav, A. P.; Rai, M. K., Fabrication of silver nanoparticles by *Phoma glomerata* and its combined effect against *Escherichia coli*, *Pseudomonas aeruginosa* and *Staphylococcus aureus*. *Letters in Applied Microbiology* **2009**, *48* (2), 173-179.
- (23) Thakkar, K. N.; Mhatre, S. S.; Parikh, R. Y., Biological synthesis of metallic nanoparticles. *Nanomedicine: Nanotechnology, Biology and Medicine* **2010**, *6* (2), 257-262.
- (24) Abdelouas, A.; Gong, W. L.; Lutze, W.; Shelnutt, J. A.; Franco, R.; Moura, I., Using Cytochrome c3 To Make Selenium Nanowires. *Chemistry of Materials* **2000**, *12* (6), 1510-1512.
- (25) Gorby, Y. A.; Beveridge, T. J.; Blakemore, R. P., Characterization of the bacterial magnetosome membrane. *J Bacteriol* **1988**, *170* (2), 834-41.
- (26) Leinfelder, W.; Forchhammer, K.; Zinoni, F.; Sawers, G.; Mandrand-Berthelot, M. A.; Bock, A., *Escherichia coli* genes whose products are involved in selenium metabolism. *J Bacteriol* **1988**, *170* (2), 540-6.
- (27) Tanaka, M.; Okamura, Y.; Arakaki, A.; Tanaka, T.; Takeyama, H.; Matsunaga, T., Origin of magnetosome membrane: proteomic analysis of magnetosome membrane and comparison with cytoplasmic membrane. *Proteomics* **2006**, *6* (19), 5234-47.
- (28) Arakaki, A.; Webb, J.; Matsunaga, T., A novel protein tightly bound to bacterial magnetic particles in *Magnetospirillum magneticum* strain AMB-1. *The Journal of biological chemistry* **2003**, *278* (10), 8745-50.
- (29) Brown, S., Engineered iron oxide-adhesion mutants of the *Escherichia coli* phage lambda receptor. *Proc Natl Acad Sci U S A* **1992**, *89* (18), 8651-5.
- (30) Brown, S.; Sarikaya, M.; Johnson, E., A genetic analysis of crystal growth. *J Mol Biol* **2000**, *299* (3), 725-35.
- (31) Sano, K.; Shiba, K., A hexapeptide motif that electrostatically binds to the surface of titanium. *J Am Chem Soc* **2003**, *125* (47), 14234-5.
- (32) Lower, B. H.; Lins, R. D.; Oestreicher, Z.; Straatsma, T. P.; Hochella, M. F., Jr.; Shi, L.; Lower, S. K., In vitro evolution of a peptide with a hematite binding motif that may constitute a natural metal-oxide binding archetype. *Environmental science & technology* **2008**, *42* (10), 3821-7.
- (33) Yamashita, I.; Kirimura, H.; Okuda, M.; Nishio, K.; Sano, K.; Shiba, K.; Hayashi, T.; Hara, M.; Mishima, Y., Selective nanoscale positioning of ferritin and nanoparticles by means of target-specific peptides. *Small* **2006**, *2* (10), 1148-52.
- (34) Dobias, J.; Suvorova, E. I.; Bernier-Latmani, R., Role of proteins in controlling selenium nanoparticle size. *Nanotechnology* **2011**, *22* (19), 195605.
- (35) Mukherjee, P.; Roy, M.; Mandal, B. P.; Dey, G. K.; Mukherjee, P. K.; Ghatak, J.; Tyagi, A. K.; Kale, S. P., Green synthesis of highly stabilized nanocrystalline silver particles by a non-pathogenic and agriculturally important fungus *T. asperellum*. *Nanotechnology* **2008**, *19* (7), 075103.
- (36) Klaine, S. J.; Alvarez, P. J. J.; Batley, G. E.; Fernandes, T. F.; Handy, R. D.; Lyon, D. Y.; Mahendra, S.; McLaughlin, M. J.; Lead, J. R., Nanomaterials in the environment: Behavior, fate, bioavailability, and effects. *Environmental Toxicology and Chemistry* **2008**, *27* (9), 1825-1851.
- (37) Dallas, P.; Sharma, V. K.; Zboril, R., Silver polymeric nanocomposites as advanced antimicrobial agents: Classification, synthetic paths, applications, and perspectives. *Advances in Colloid and Interface Science* **2011**, *166* (1-2), 119-135.
- (38) Poté, J.; Haller, L.; Loizeau, J.-L.; Garcia Bravo, A.; Sastre, V.; Wildi, W., Effects of a sewage treatment plant outlet pipe extension on the distribution of contaminants in the sediments of the Bay of Vidy, Lake Geneva, Switzerland. *Bioresource Technology* **2008**, *99* (15), 7122-7131.
- (39) Gondikas, A. P.; Morris, A.; Reinsch, B. C.; Marinakos, S. M.; Lowry, G. V.; Hsu-Kim, H., Cysteine-Induced Modifications of Zero-valent Silver Nanomaterials: Implications for Particle Surface Chemistry, Aggregation, Dissolution, and Silver Speciation. *Environmental Science & Technology* **2012**, *46* (13), 7037-7045.
- (40) Ma, R.; Levard, C.; Marinakos, S. M.; Cheng, Y. W.; Liu, J.; Michel, F. M.; Brown, G. E.; Lowry, G. V., Size-Controlled Dissolution of Organic-Coated Silver Nanoparticles. *Environmental Science & Technology* **2012**, *46* (2), 752-759.
- (41) Dror-Ehre, A.; Mamane, H.; Belenkova, T.; Markovich, G.; Adin, A., Silver nanoparticle - *E. coli* colloidal interaction in water and effect on *E. coli* survival. *Journal of Colloid and Interface Science* **2009**, *339* (2), 521-6.
- (42) El Badawy, A. M.; Luxton, T. P.; Silva, R. G.; Scheckel, K. G.; Suidan, M. T.; Tolaymat, T. M., Impact of Environmental Conditions (pH, Ionic Strength, and Electrolyte Type) on the Surface Charge and Aggregation of Silver Nanoparticles Suspensions. *Environmental Science & Technology* **2010**, *44* (4), 1260-1266.

-
- (43) El Badawy, A. M.; Silva, R. G.; Morris, B.; Scheckel, K. G.; Suidan, M. T.; Tolaymat, T. M., Surface Charge-Dependent Toxicity of Silver Nanoparticles. *Environmental Science & Technology* **2011**, *45* (1), 283-287.
- (44) Fabrega, J.; Renshaw, J. C.; Lead, J. R., Interactions of Silver Nanoparticles with *Pseudomonas putida* Biofilms. *Environmental Science & Technology* **2009**, *43* (23), 9004-9009.
- (45) Lok, C. N.; Ho, C. M.; Chen, R.; He, Q. Y.; Yu, W. Y.; Sun, H. Z.; Tam, P. K. H.; Chiu, J. F.; Che, C. M., Proteomic analysis of the mode of antibacterial action of silver nanoparticles. *Journal of Proteome Research* **2006**, *5* (4), 916-924.
- (46) Kittler, S.; Greulich, C.; Diendorf, J.; Köller, M.; Epple, M., Toxicity of Silver Nanoparticles Increases during Storage Because of Slow Dissolution under Release of Silver Ions. *Chemistry of Materials* **2010**, *22* (16), 4548-4554.
- (47) Navarro, E.; Piccapietra, F.; Wagner, B.; Marconi, F.; Kaegi, R.; Odzak, N.; Sigg, L.; Behra, R., Toxicity of silver nanoparticles to *Chlamydomonas reinhardtii*. *Environmental Science & Technology* **2008**, *42* (23), 8959-64.
- (48) Sondi, I.; Salopek-Sondi, B., Silver nanoparticles as antimicrobial agent: a case study on *E-coli* as a model for Gram-negative bacteria. *Journal of Colloid and Interface Science* **2004**, *275* (1), 177-182.
- (49) Morones, J. R.; Elechiguerra, J. L.; Camacho, A.; Holt, K.; Kouri, J. B.; Ramirez, J. T.; Yacaman, M. J., The bactericidal effect of silver nanoparticles. *Nanotechnology* **2005**, *16* (10), 2346-2353.
- (50) Pal, S.; Tak, Y. K.; Song, J. M., Does the Antibacterial Activity of Silver Nanoparticles Depend on the Shape of the Nanoparticle? A Study of the Gram-Negative Bacterium *Escherichia coli*. *Applied and Environmental Microbiology* **2007**, *73* (6), 1712-1720.
- (51) Kim, J. S.; Kuk, E.; Yu, K. N.; Kim, J.-H.; Park, S. J.; Lee, H. J.; Kim, S. H.; Park, Y. K.; Park, Y. H.; Hwang, C.-Y.; Kim, Y.-K.; Lee, Y.-S.; Jeong, D. H.; Cho, M.-H., Antimicrobial effects of silver nanoparticles. *Nanomedicine: Nanotechnology, Biology and Medicine* **2007**, *3* (1), 95-101.
- (52) Hwang, E. T.; Lee, J. H.; Chae, Y. J.; Kim, Y. S.; Kim, B. C.; Sang, B. I.; Gu, M. B., Analysis of the toxic mode of action of silver nanoparticles using stress-specific bioluminescent bacteria. *Small* **2008**, *4* (6), 746-750.
- (53) Choi, O.; Hu, Z., Size dependent and reactive oxygen species related nanosilver toxicity to nitrifying bacteria. *Environmental Science & Technology* **2008**, *42* (12), 4583-8.
- (54) Park, M. V. D. Z.; Neigh, A. M.; Vermeulen, J. P.; de la Fonteyne, L. J. J.; Verharen, H. W.; Briedé, J. J.; van Loveren, H.; de Jong, W. H., The effect of particle size on the cytotoxicity, inflammation, developmental toxicity and genotoxicity of silver nanoparticles. *Biomaterials* **2011**, *32* (36), 9810-9817.
- (55) Su, H. L.; Chou, C. C.; Hung, D. J.; Lin, S. H.; Pao, I. C.; Lin, J. H.; Huang, F. L.; Dong, R. X.; Lin, J. J., The disruption of bacterial membrane integrity through ROS generation induced by nanohybrids of silver and clay. *Biomaterials* **2009**, *30* (30), 5979-5987.

Chapter

1 Role of proteins in the formation of selenium nanoparticles*

J Dobias, E I Suvorova and R Bernier-Latmani

Abstract. This work investigates the potential for harnessing the association of bacterial proteins to biogenic selenium nanoparticles (Se NPs) to control the size distribution and the morphology of the resultant SeNPs. We conducted a proteomic study and compared proteins associated with biogenic SeNPs produced by *E. coli* and chemically synthesized SeNPs as well as to magnetite nanoparticles. We identified four proteins (AdhP, Idh, OmpC, AceA) that bound specific to SeNPs and observed a narrower size distribution as well as more spherical morphology when the particles were synthesized chemically in the presence of proteins. A more detailed study of AdhP (alcohol dehydrogenase propanol preferring) confirmed the strong affinity of this protein for the SeNP surface and revealed that this protein controlled the size distribution of the SeNPs and yielded a narrow size distribution with a three-fold decrease in the median size. These results support the assertion that protein may become an important tool in the industrial-scale synthesis of SeNPs of uniform size and properties.

Keywords: Selenium nanoparticle, proteins, bacteria, nanomaterial synthesis

* This chapter has been published in the peer review journal "NANOTECHNOLOGY" in 2011 (doi:10.1088/0957-4484/22/19/195605) and has been selected by the editors for inclusion in the exclusive "2011 Highlights" collection.

1.1 Introduction

Biological systems can produce a tremendous variety of potential nanomaterial products. If fully deciphered, these biological systems could be harnessed for industrial nanomaterial manufacturing. Biologically-aided synthesis could help decrease the consumption of energy and toxic chemicals, opening the path for more environmentally friendly green manufacturing¹.

Bacteria, among all biological systems, are well known to produce metal and metal oxide nanoparticles (NPs) of various compositions, sizes and morphologies. For instance, *Bacillus selenitireducens* can reduce tellurium to rosette-aggregated rods of 30x200 nm and selenium to 200 nm spherical particles^{2, 3}; *Shewanella oneidensis* MR-1 reduces tellurium to 50-80 nm spherical particles⁴; *Magnetospirillum magneticum* AMB-1 produces 30-120 nm cubic magnetic particles⁵ and *Veillonella atypica* produces 30 nm ZnSe and CdSe particles¹.

However, there is a significant knowledge gap in our collective understanding of the mechanism of formation of those NPs: it is unclear how the control of the final product is achieved. This knowledge gap precludes mass production on an industrial scale using bacterially-based nanomanufacturing. Therefore, there is a salient need to develop a mechanistic understanding of the processes leading to the formation of solid-state nanoparticles by bacteria.

Bacterial synthesis of metallic NPs is often achieved by a reduction step followed by a precipitation step with the latest composed of two parts: nucleation and crystal growth. To date, only the reduction step has been studied extensively and the biological processes responsible for nucleation and crystal growth are not fully understood. Several studies provide evidence that proteins might play a key role in the nucleation and crystal growth of bacteriogenic metal NPs. A bacterial protein -cytochrome *c*₃- was found to reduce selenate (SeO₄²⁻) in aqueous solution leading to the formation of one-dimensional chainlike aggregates of monoclinic selenium nanoparticles⁶. Secondly, in magnetosomes of the magnetotactic bacterium, *Magnetospirillum magneticum* AMB-1, membrane proteins are tightly bound to the magnetic NPs⁷⁻⁹ and a single protein (Mms6) was shown to control the shape of the final nanomagnetite particles¹⁰. Similarly, the rate of crystal growth and the morphology of Au NPs were shown to be controlled by proteins. These proteins able to constrain the speed of Au NPs crystal growth as well as to direct particle morphology were identified from a random phage-display peptide library^{11, 12}. Finally, short peptide-based biopanning techniques^{13, 14} showed the strong adhesion of some peptides to titanium NPs surfaces.

In order to better understand the role of proteins in controlling of the formation of nanoparticles, we studied the reduction of selenite to elemental selenium by *E. coli*.

This microorganism offers the advantage of being well-studied and genetically-tractable, which allows the ready use of genetic engineering and molecular biology. Additionally, it is able to reduce tetravalent and hexavalent selenium to elemental selenium, Se(0).

Selenium (Se) is an element of interest for electronics and photonics applications. Its attractiveness stems from its high refractive index (>2.5)¹⁵ and its high reactivity: the reduction and disproportionation of elemental selenium allow the coating of selenium nanostructures with other metals (Pt, Cd) and can be used to produce core/shell nanostructure as inverted opaline lattices¹⁵ or other functional materials such as silver selenide¹⁵. In order to be used at an industrial scale, it requires an efficient and affordable method of production of monodispersed nanospheres of amorphous selenium (a-Se).

To date, several synthetic techniques exist to produce spherical selenium nanoparticles (SeNPs). These include: (a) exposing selenious acid to gamma-radiation¹⁶, (b) reducing selenious acid by various reagents such as hydrazine (N₂H₄)¹⁷, (c) oxidizing selenide ions electrochemically¹⁸, (d) crystallizing melt-quenched amorphous selenium¹⁹, (e) using a reverse micelle method²⁰ or (f) using laser ablation²¹. However these techniques have limitations. The most significant of which are the absence of narrow size distributions (size variation of less than 5%)¹⁵ that are important for industrial applications and the production of NPs that are subject to extreme photocorrosion¹⁷. In order to overcome the limitations of the previous techniques (high temperature, high pressure or use of catalysts), biologically-based, semi-synthetic methods have been explored to produce nanomaterials⁶.

This work focuses on pinpointing the role of naturally-occurring *E. coli* proteins in controlling the structure and morphology of SeNPs. We identified proteins that bind strongly to biogenic SeNPs and subsequently selected a single protein for a detailed study of its effect on the morphology and size distribution of these NPs.

The long-term goal of this work is to identify proteins that play a role in the bacteria-dependent biomineralization of selenium and other metals, to unravel their binding mechanism and to help develop protocols for industrial applications. We believe that the biologically-based, semi-synthetic production of NPs may be a viable economic alternative to existing nanomaterial production processes due to the added value of avoiding the production and use of environmentally hazardous chemicals and promoting green manufacturing.

1.2 Materials and Methods

All chemicals were of analytical grade and obtained from Sigma-Aldrich (Basel, Switzerland), unless otherwise stated.

1.2.1 Bacterial strains and growth conditions

In this study, we used *Escherichia coli* K-12 obtained from DSMZ (DSM-No. 498). Bacterial cultures were grown aerobically at 30°C in liquid Luria-Bertani (LB) broth [10 g/l Tryptone, 10 g/l sodium chloride, 5 g/l yeast extract] in 250 ml Erlenmeyer flasks containing 125 ml of medium, inoculated from a 10% (v/v) overnight culture in LB and placed on a rotary shaker (140 rpm).

1.2.2 Production of zerovalent selenium nanoparticles (SeNPs)

To test the hypothesis that proteins are associated to NPs *in vivo* and that they can bind them *in vitro*, we produced chemogenic SeNPs (ChSeNPs) as previously described²² as well as biogenic SeNPs (BioSeNPs) using *E. coli* K-12. Briefly, ChSeNPs were produced by mixing sodium thiosulfate ($\text{Na}_2\text{O}_3\text{S}_2$) and selenous acid [Se(IV)] in 0.01% (final concentration) sodium dodecyl sulfate (SDS) solution. Purified protein or *E. coli* cell free extract were added at a concentration of 0.1 mg/ml final concentration in appropriate experiments. The speed of the reaction and the size of the particles are controlled by the ratio of Se(IV) to sodium thiosulfate. We worked with two ratios of Se(IV) to $\text{Na}_2\text{O}_3\text{S}_2$: 1:150, 1:30. The respective concentrations of Se(IV) were: 0.7 mM, 5.2 mM. Particle size can be visually estimated based on the color of the solution due to size-specific plasmon phenomenon²².

BioSeNPs were produced as follows: an overnight culture of *E. coli* K-12 was supplemented with filter-sterilized selenous acid (H_2SeO_3) as the source of Se(IV) to a final concentration of 4 mM and incubated for two days. Se(IV) reduction to Se(0) was visible with the appearance of a dark red coloration in the culture. We measured the reduction of Se(IV) by sampling the culture over time, filtering the samples with a 0.2 μm pore diameter syringe filter followed by filtration with a 0.02 μm pore diameter syringe filter. The filtrate (1 ml) was acidified with 0.1N HNO_3 (9 ml) and measured for total Se in solution by inductively coupled plasma optical emission spectroscopy (ICP-OES; Perkin Elmer Optima 3000).

To separate BioSeNPs from biomass, cells were lysed by adding NaOH to a final concentration of 1N and heating the suspension in a boiling water bath for 20 min. The resultant mixture was amended with n-hexane and placed in a separatory funnel. The solvent phase contained the biomass and the aqueous phase contained the NPs. The pH of the collected aqueous fraction containing the SeNPs was then lowered to 7.2 using

6M HCl and NPs were collected by centrifugation (16'000 rcf, room temperature (RT), 30 min), washed 3 times with ultrapure water (Milli-Q, 18M Ω cm water: ddH₂O) and stored in ddH₂O for further use. BioSeNPs free of biomass are hereafter abbreviated BioSeNPsBF.

1.2.3 Cell free extract (CFX) of *E. coli* K-12

E. coli cells were grown until the mid logarithmic phase (OD₆₀₀ = 0.4 - 0.6), transferred to 50 ml centrifuge tubes, centrifuged (3'000 rcf, 15 min, 4°C) and washed twice with phosphate buffered saline (PBS). The cell pellet was frozen at -80°C if not used immediately. Cells were resuspended in ice-cold 100mM Tris-Cl pH 7.4 (10 ml per 40 ml of cell culture) and kept on ice. They were sonicated (Branson sonifier 150D, Branson ultrasonic corporation, CT, USA) on ice at 100 W 5 times for 5 minutes (4 sec. pulse, 2 sec. pause) and the temperature was monitored to remain under 20°C. After each cycle of 5 minutes, cells were cooled down to 4°C. Cells were observed under an optical microscope to verify the efficiency of sonication. Unbroken cells and cell debris were removed by centrifugation (16'000 rcf, 30 min, 4°C). The supernatant was aliquoted into 1 ml samples and stored at -80°C. Protein concentration was measured using Bradford assay from Bio-Rad (Munich, Germany) according to the manufacturer's protocol.

1.2.4 Protein-NPs association

In order to identify the proteins that are natively associated with SeNPs, cells of *E. coli* K-12 that had reduced Se(IV) to Se(0) were ultrasonicated to release the SeNPs and the lysate was centrifuged on an 80% sucrose solution. The heavy fraction containing the BioSeNP was separated from the light ones and washed with 100 mM Tris pH 7.4 to remove sucrose.

We also tested the association of proteins present in *E. coli* K-12 cell free extract with ChSeNP, BioSeNPBF and magnetite (Fe(II)/Fe(III) oxide) nanoparticles (FeNPs). FeNPs is a commercially available nanopowder made of spherical particles (< 50 nm). FeNPs were washed and resuspended in ddH₂O. We mixed cell free extract with ChSeNP, BioSeNPBF or FeNPs to a final ratio of 1-1.6 mg/ml of proteins to 0.7-1.0 mg of NPs and agitated overnight on a rotary shaker. SeNPs were collected by centrifugation (16'000 rcf, 4°C, 30 min) and FeNPs were collected using a magnet.

To resolve the protein composition, samples were mixed with gel loading buffer containing (final concentration): 50 mM Tris-HCl (pH 6.8), 100 mM 1,4-dithiothreitol (DTT), 2% SDS, 10% glycerol and 0.01% bromophenol blue. Samples were heated at 95°C for 5 min to denature the proteins and subjected to SDS-polyacrylamide gel

electrophoresis (SDS-PAGE) in a 12% (wt/vol) polyacrylamide gel. The gel was stained with “ProtoBlue™ Safe” from National Diagnostics (Atlanta, USA).

1.2.5 *Stripping-off proteins from NPs*

When proteins were found associated with NPs, the strength of the association was tested by a series of increasingly denaturing treatments. NPs were mixed with *E. coli* cell free extract at a ratio of 1 mg to 1-1.5 mg/ml respectively and left overnight at room temperature on a rotator. NPs were collected by centrifugation (16'000 g, 4°C, 30 min) and the supernatant transferred to a fresh tube. The pelleted NPs were washed twice with 100 mM Tris-Cl pH 7.4 to remove free proteins. Subsequently NPs were treated either sequentially or individually with six different solutions (from least to most denaturing): (1) 2% Triton X-100, (2) 2% SDS, (3) a solution composed of 7 M urea, 2 M thiourea, 4% CHAPS (Biochemica, Applichem GmbH, Germany), 40 mM Trisbase (abbreviated “Urea 7 M”), (4) 10% SDS, (5) 10% SDS and boiling for 10 min and (6) 10% SDS and boiling for 30 min. For the individually treated samples, the NPs were resuspended in the adequate stringent solution and gently shaken 20 min at room temperature on a rotary shaker. For the sequentially treated samples, each step was performed as follows: an aliquot was collected and washed with the previous solution. The remaining sample was centrifuged (16000 rcf, 10 min, RT) to collect the NPs and the supernatant was stored. The NPs were resuspended in the washing solution of the next stringency and agitated (20 min, RT) on a rotary shaker. The collected fractions (aliquot, supernatants and NPs) were characterized by the Bradford assay and SDS polyacrylamide gel electrophoresis (SDS-PAGE) techniques²³.

1.2.6 *Protein Identification*

Proteins within a given sample were separated by SDS-PAGE. To identify individual proteins, the bands of interest were cut out, sliced into 1 mm slices and sent for protein identification to EPFL’s Protein Core Facility (PCF). Samples were reduced and alkylated with dithioerythritol (DTE) and iodoacetamide (IAA) respectively in order to reduce and block disulfide bonds. Samples were dried and in-gel digested with Trypsin for at least 12 hours at 37°C. Peptides were then extracted from gel pieces and concentrated by Speed-Vac evaporation. Samples were finally resuspended and analyzed by Liquid Chromatography Ion Trap Mass Spectrometry (LC-IT-MS/MS). Reverse Phase LC separation was performed on a nano-HPLC quaternary pump (Rheos 2200) at a flow rate of 700 nl/min using a C18 capillary column (100 µm id x 100 mm). MS analysis was performed on a Finnigan/Thermo LTQ Ion-Trap MS instrument. An *Escherichia coli* UniProt (SwissProt) sub-database and the Matrix Science (Ltd.)

Mascot search engine were used to perform identifications using the mass fragments detected. Mascot's discriminating factors p and ionic score (IS) were chosen such as $p < 10^{-6}$ and $IS > 40$.

1.2.7 *Electron Microscopy (EM)*

Transmission Electron Microscopy (TEM) samples were prepared by washing NPs and depositing a drop of the sample suspension on a carbon-coated copper grid. Samples were air-dried at room temperature overnight in a dust-free box.

Local analysis to investigate the morphology and structure of particles was performed by TEM, scanning TEM (STEM), selected area electron diffraction (SAED) and energy-dispersive X-ray spectroscopy (EDS) in a FEI CM 300FEG-UT analytical transmission electron microscope (300 kV field emission gun, 0.18nm Scherzer resolution, 20° X-ray take-off angle). The images were recorded with a Gatan 797 slow scan CCD camera (1024 pixels x 1024 pixels x 14 bits) and processed with the Gatan Digital Micrograph 3.11.0 software. The chemical composition of particles was obtained from X-ray EDS in STEM mode with 2 to 50 nm diameter electron probes and interpreted with the INCA (Oxford) software.

1.2.8 *Particle size measurement*

We used EM to measure sizes of individual particles but, in addition, in order to have representative values of particle populations, we used two dynamic light scattering (DLS) instruments: (1) Beckman Coulter LS 13320 Laser diffraction Particle Size analyzer that can measure spherical particles from 40 nm to 2 mm and (2) Malvern Zetasizer nano ZS which size range is 0.3 nm – 10 μ m.

1.2.9 *AdhP cloning*

Alcohol dehydrogenase propanol preferring (AdhP) is one of the proteins identified in the cell free extract to bind strongly to SeNP. We tested its effect on ChSeNPs during NP formation. To do so, we produced purified protein by cloning and overexpressing it in *E. coli*. We cloned *adhP* with an Invitrogen™ (Basel, Switzerland) Champion™ pET-D200/TOPO® Expression kit by strictly following the supplied protocol. The gene encoding AdhP was generated by Polymerase Chain Reaction (PCR) amplification using genomic DNA from *E. coli* K-12 as the template with the primers DJ-adhp_F2 (5'-cac cAT GAA GGC TGC AGT TGT TA-3') and DJ-adhp_R2 (5'-TTA GTG ACG GAA ATC AAT CAC CAT GC-3') and New England Biolabs (Ipswich, MA, USA) Vent polymerase.

Positive colonies containing the cloned gene were selected on kanamycin (50 µg/ml) agar plates, the plasmid was purified using Sigma Aldrich (Basel, Switzerland) GeneElute™ plasmid mini prep kit and sequenced by FASTERIS SA (Geneva, Switzerland).

Bacteria overexpressing AdhP (BL21AdhP) were grown in Invitrogen™ MagicMedia supplemented with kanamycin (50 µg/ml). Cells were collected, washed and lysed according to a protocol from the Bio-Rad (Reinach, Switzerland) Profinia protein purification system that was used to purify the His-tagged AdhP (His-ADHP). Invitrogen™ InVision™ His-tag in-gel stain was used to specifically stain His-ADHP on protein gels. Finally the N-terminal 6xHIS fragment was removed with Invitrogen™ EnterokinaseMax™ system by strictly following the supplied protocol (we used 1U of EKMax™ for the His-tag cleavage) and the purified protein is referred to as pAdhP herein after.

1.2.10 AdhP activity assay

To test the proper conformation and the activity of pAdhP, we used the alcohol dehydrogenase enzymatic assay protocol from Sigma Aldrich based on Kägi and Vallee (1960). It consists of following the reduction of β-NAD to NADH by measuring the absorbance of the latter at 340nm overtime. One unit (U) is equal to the production of one µmole per min of NADH and the specific activity of the enzyme is 1U per µg of protein.

1.3 Results and discussion

1.3.1 Characterization of bacteriogenic NPs

ICP-OES measurements (figure S1) showed that *E. coli* could reduce 4 mM of selenite over 2 days. In absence of cells or in the presence of heat-killed cells, the reduction does not occur. No toxic effect of selenite or SeNPs was observed as spent medium supplemented with yeast extract and peptone didn't impair the growth of a fresh *E. coli* inoculum, and the inoculation of fresh medium with bacteria grown in the presence of selenite for more than two days showed bacterial growth (data not shown). The apparition of a dark red color indicated the formation of amorphous elemental selenium particles (figures S2 and S3). Electron microscopy analysis revealed spheroidal particles (figure S2-A) with no crystalline structure (figure S2-B) and a size range of 10 nm to 90 nm. DLS Measurements gave an average size of 62 nm \pm 15 nm (figure S4), which is an overestimate as the Beckmann DLS instrument used has a detection limit of 40 nm at the lower end.

1.3.2 Protein Identification

The goal was to identify proteins potentially involved in the biomineralization of Se(0). Our approach was to assay for the association of proteins to biogenic SeNPs. The assumption inherent in this approach is that proteins involved in nanoparticle formation are tightly associated with the produced NPs^{6, 10, 11, 13, 14, 24}. The assay involved growing *E. coli* bacteria in the presence of selenite until the appearance of a brick red color representative of the presence of Se(0) particles. The Se(0) NPs and associated proteins were then collected by lysing the cells via ultrasonication and centrifuging the lysate through an 80% sucrose solution leading to four fractions (figure S5). Fractions 1 and 3 were transparent and considered NP-free as opposed to fractions 2 and 4 (figure S5), which were orange-red and therefore considered to contain a significant amount of SeNPs. Fraction 4 was a brick red SeNP pellet which was the focus of further work. The protein content in these fractions was analyzed by SDS-PAGE (figure 1).

The proteins of fraction 1 were distributed throughout the entire size range and were representative of the entire proteome. This distribution pattern differed significantly from those of fractions 2 and 4 (figure 1) and fraction 3 did not exhibit any proteins. Fractions 2 and 4 differed from fractions 1, 3 and P, suggesting a specific enrichment of certain proteins through their association with Se NPs.

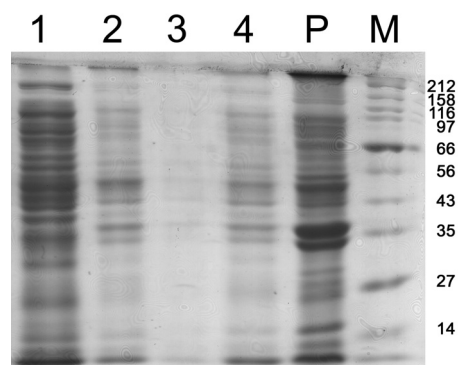


Figure 1: 12% SDS-PAGE of fractions 1-4 of the sucrose separation (figure S5), P (pellet fraction from lysed cells) and M (protein ladder with sizes in kDa). Fractions 2 and 4 include SeNPs.

To test the strength of protein binding to NPs, the NPs from fraction 4 were washed with increasingly stringent denaturing solutions. Some proteins remained attached to the NPs even after 30 minutes of boiling in 10% SDS (figure 2) which implies a very strong interaction between these proteins and the NPs. The experiment was repeated with (a) BioSeNPsBF exposed to CFX (figure S6), (b) FeNPs exposed to CFX (figure S7) and (c) ChSeNPs formed in presence of CFX (figure S8). The FeNPs were used to differentiate between specific and non-specific association of proteins to NPs. The bands delimited by black boxes in figures 2 and S6-S8 were cut out of the gel and proteins were identified by nano-LC-IT-MS/MS. Results of protein identification are given in Tables S1-S4.

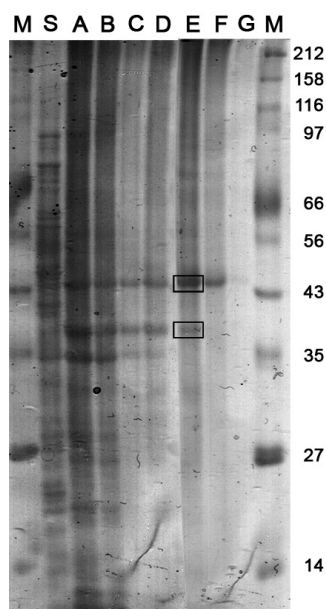


Figure 2: 12% SDS-PAGE of BioNPs from *E. coli* grown in selenite. A (no treatment), B (Triton 2%), C (SDS 2%), D (urea 7M), E (SDS 10%), F (boiled 10min in SDS10%), G (boiled 30min in SDS10%), S (supernatant from centrifuged lysed cells) and M (protein ladder with sizes in kDa). The square boxes are the bands that were cut out and identified by mass spectrometry.

None of the identified NPs associated proteins are known to be involved in selenium or iron metabolism. Instead, they are related to energy production and carbohydrate or fatty acid metabolism. ADHP, ACEA, ENO, KPYK1, IDH and GLPK require metallic cofactors (respectively Zn, divalent cations, Mg, Mg-K, Mn-Mg and Zn) and DCEA, ASTC and TNAA require non-metallic cofactors (pyridoxal phosphate). One could speculate that the binding to cofactors could explain their strong association with SeNPs.

Only two proteins were found to be common to all tested conditions (including FeNPs): elongation factor Tu (EFTU) and 3-oxoacyl synthase (FABB), suggesting a non-specific binding of those proteins to metallic and metal oxide NPs.

Four proteins were found to be associated specifically and solely to SeNPs (table 1). These four proteins vary in size (36 to 48 kDa), in function (enzyme or structural protein) as well as in isoelectric point (4.58 to 5.94). Additionally, there is no obvious similarity in amino acid sequence between the four proteins. Thus, no evidence of a clear mechanism leading to the binding of these specific proteins to SeNPs can be gleaned from the information currently available.

Table 1. Identified proteins specific to Selenium NPs (IP: isoelectric point).

Name		Size [kDa]	IP	Cofactor	Function
ACEA	Isocitrate lyase	48	5.16	divalent cations	Glyoxylate and dicarboxylate metabolism
IDH	Isocitrate dehydrogenase [NADP]	46	5.15	Mg or Mn	Tricarboxylic acid cycle and glyoxylate bypass
OMPC	Outer membrane protein C precursor (Porin ompC)	40	4.58		Passive pore formation
ADHP	Alcohol dehydrogenase, propanol-preferring	36	5.94	Zn	Fermentation (Aldehyde/ketone formation)

1.3.3 Role of CFX proteins in SeNPs formation

In the previous section we showed that some proteins are strongly attached to SeNPs. In order to identify the potential effect of proteins on SeNPs, we chemically synthesized SeNPs (ChSeNPs at a 1:30 ratio of Se(IV) to sodium thiosulfate) in the presence and the absence of *E. coli* cell free extract and performed TEM, SAED and EDS analyses. The cell free extract appears to restrict the size distribution of NPs yielding a more tightly controlled size distribution of 106.7 ± 8.7 nm (figure 3B) versus 10 to 90 nm (figure 3A). Furthermore, NPs formed in the presence of cell free extract are almost perfectly spherical as opposed to the one formed in its absence. In both cases, NPs are made of non-crystalline selenium (data not shown).

Unfortunately, the extreme effect of CFX on ChSeNP synthesis was difficult to reproduce for more detailed study. One of the main issues was the composition of CFX. Because there is variation in the exact composition of the CFX as a function of the batch of grown bacteria, it is not practically feasible to use CFX as an experimental reagent. Nonetheless, every batch of CFX tested decreased the size distribution range of synthesized SeNPs but to varying extents. Secondly, careful selection of the selenite concentration and the selenite to thiosulfate ratio was needed to avoid the formation of sulfur-containing polymer structures.

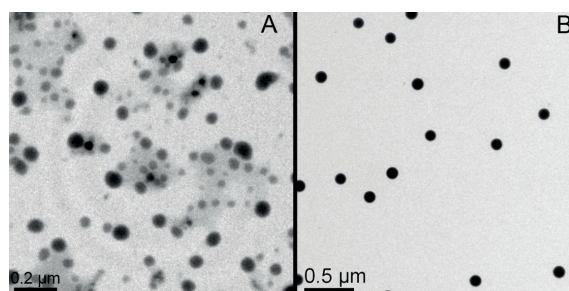


Figure 3: TEM of chemogenic NPs produced at a 1:30 Se(IV):thiosulfate ratio in absence (A) and presence (B) of cell free extract.

1.3.4 *AdhP* effect on *SeNPs*

In order to tackle the mechanism of binding of proteins to NPs in a more tractable experimental system, we resolved to study proteins individually. We tested the effect of a single purified protein on the reduction-nucleation-growth process during chemical production of elemental selenium. We choose to work with alcohol dehydrogenase propanol preferring (*AdhP*) for two reasons: (1) it was found to be associated only to selenium NPs (table 1) and (2) we can ensure that its three dimensional conformation is correct by quantifying its enzymatic activity. We tested the binding ability of His-*AdhP* to BioSeNPs, the enzymatic activity of p*AdhP* and the effect of p*AdhP* on the formation of ChSeNPs synthesized at a selenite to sodium thiosulfate ratio of 1 to 150.

As stated previously, we selected *AdhP* as the target protein to study due to its preferential binding to SeNPs as determined from incubations with *E. coli* CFX. We confirmed this characteristic of *AdhP* by quantifying the binding of the recombinant protein His-*AdhP* to BioSeNPs by protein gel (figure 4). As is evident from the protein gel, lanes corresponding to purified His-*AdhP* and BioSeNPs exposed to His-*AdhP* both show a clear band at the correct size. In contrast, the supernatant derived from the centrifugation of a suspension of BioSeNPs and His-*AdhP* shows no evidence for the protein, suggesting the removal of His-*AdhP* from solution through binding to SeNPs. Thus, there is overwhelming evidence for the strong binding of His-*AdhP* to BioSeNPs.

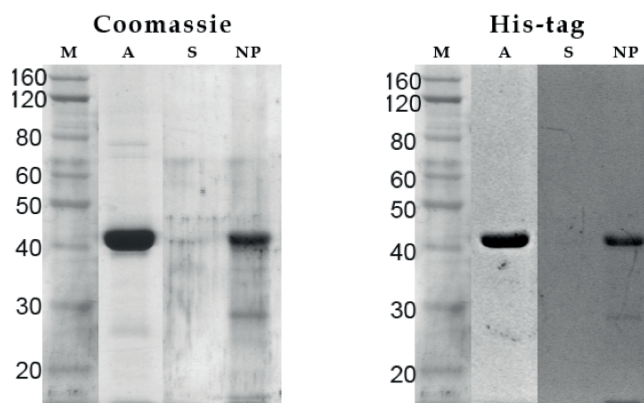


Figure 4: Binding of His-AdhP to bacteriogenic SeNPs. (A) Purified His-AdhP, (S) supernatant, (NP) NP exposed to His-AdhP and (M) protein ladder (sizes are in kDa). The left gel was stained with coomassie blue and the right gel with Invision™ His-tag stain.

For a meaningful comparison of the effect of recombinant AdhP and native *E. coli* AdhP on NP formation, the two proteins have to be structurally similar. To test the similarity of the proteins, we used the enzymatic activity as an indicator of their spatial conformation. Therefore, we measured the enzymatic activity of pAdhP and found 108 and 126 $\text{U} \times \text{min}^{-1} \times \text{mg}^{-1}$ for ethanol and propanol substrates, respectively. These values are in the range of reported activities for alcohol dehydrogenase enzymes from various species [unit: $\text{U} \times \text{min}^{-1} \times \text{mg}^{-1}$]: 43 for *E. coli*, 40-184 for *Drosophila melanogaster* and 210-7300 for *Saccharomyces cerevisiae*²⁵⁻²⁷. Therefore, we concluded that the recombinant protein was active and that its spatial conformation corresponded to that of the native protein. Hence, we could reliably compare *in-vivo* and *in-vitro* systems.

We evaluated the effect of pAdhP on ChSeNPs formation. We synthesized ChSeNPs in the presence of pAdhP and observed a three-fold decrease of their size as compared to that of NPs synthesized in the protein's absence (100 vs. 300 nm) (figure 5).

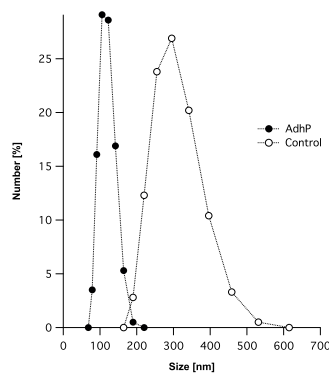


Figure 5: DLS size measurement of ChSeNP synthesized in the presence (AdhP) and in the absence (control) of pAdhP.

The difference in size distribution was even more visually striking by STEM analysis (figure 6). The SeNPs produced in the presence of pAdhP were clearly smaller and with a narrower size distribution (figure 6A and 6C) as compared to those produced in the absence of pAdhP (figure 6B and 6D). EDS mapping confirmed that the SeNP were made only of selenium (figure 6) and SAED showed no crystalline structure for the NPs (data not shown). Overall, these data show that among possible effects of proteins on NPs (e.g., shape, size, crystallinity), only the size distribution was modified – albeit three-fold – when pAdhP was present in the solution of the chemical reduction of selenite by sodium thiosulfate.

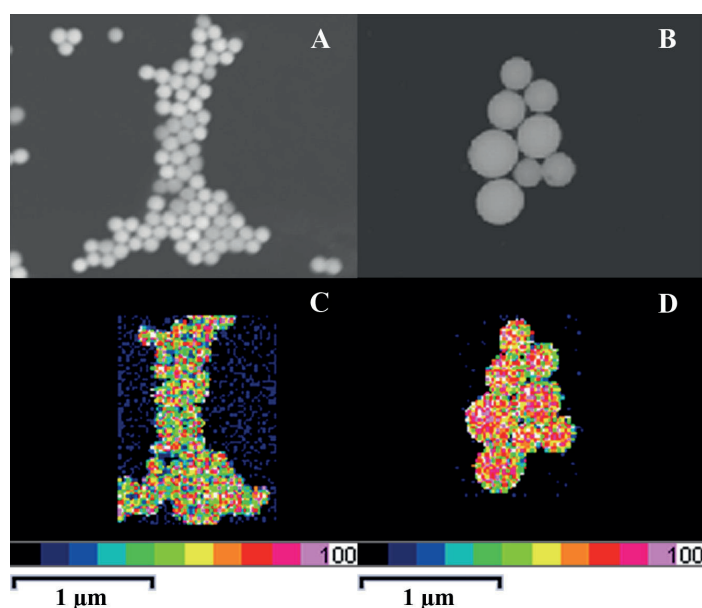


Figure 6: STEM (A, B) and EDS selenium mapping (C, D; colors represent the abundance percentage of the mapped element from 0% (black) to 100% (white)) of ChSeNP produced in the presence of AdhP (A, C) or in absence of AdhP (B, D).

1.4 Conclusions

In biological systems, the synthesis of NPs by bacteria is equivalent to simple reactions occurring in a complex chemical environment. These environments are rich in biomolecules such as proteins, exopolysaccharides, nucleic acids, fatty acid or sugars. In this work, we studied the interaction between proteins and metallic NPs and the role of proteins in the formation of NPs. In preliminary experiments, we observed that CFX (a complex matrix of biomolecules) was able to affect the size distribution of ChSeNPs by narrowing their size distribution. We also observed that in biological matrices, SeNPs and FeNPs are associated with a large number of proteins and that several of these are strongly bound to the NPs. The identification of these strongly associated proteins revealed that, among the identified proteins, none has a reported function that is related to NP formation or metal reduction. These proteins are primarily implicated in energy, carbohydrate or fatty acid metabolism but do not share chemical properties such as isoelectric point, cofactor or size. We conclude that the binding ability of the proteins depends either on their spatial configuration or/and on physico-chemical properties of some amino acid.

We tested the effect of a single purified protein, AdhP, on the formation of ChSeNPs and found an effect on size distribution: a three-fold decrease in the average size of ChSeNPs.

Overall, this work shows that the control of the size distribution of synthetic SeNPs produced in a simple aqueous system and under standard ambient temperature and pressure conditions is possible through harnessing the interactions of naturally-occurring proteins with these NPs. The protein-derived control of NPs size could have great implication for industrial-scale production.

1.5 Acknowledgments

We would like to acknowledge the Protein core facility (PCF), the Protein elution core facility (PECF) and the Centre interdisciplinaire de microscopie électronique (CIME) at EPFL for equipment use and technical advice.

1.6 References

- (1) Pearce, C. I.; Coker, V. S.; Charnock, J. M.; Patrick, R. A. D.; Mosselmanns, J. F. W.; Law, N.; Beveridge, T. J.; Lloyd, J. R., Microbial manufacture of chalcogenide-based nanoparticles via the reduction of selenite using *Veillonella atypica*: an in situ EXAFS study. *Nanotechnology* **2008**, *19* (15), 155603.
- (2) Oremland, R. S.; Herbel, M. J.; Blum, J. S.; Langley, S.; Beveridge, T. J.; Ajayan, P. M.; Sutto, T.; Ellis, A. V.; Curran, S., Structural and spectral features of selenium nanospheres produced by Se-respiring bacteria. *Appl Environ Microbiol* **2004**, *70* (1), 52-60.
- (3) Baesman, S. M.; Bullen, T. D.; Dewald, J.; Zhang, D.; Curran, S.; Islam, F. S.; Beveridge, T. J.; Oremland, R. S., Formation of tellurium nanocrystals during anaerobic growth of bacteria that use Te oxyanions as respiratory electron acceptors. *Appl Environ Microbiol* **2007**, *73* (7), 2135-43.
- (4) Klonowska, A.; Heulin, T.; Vermiglio, A., Selenite and tellurite reduction by *Shewanella oneidensis*. *Appl Environ Microbiol* **2005**, *71* (9), 5607-9.
- (5) Lang, C.; Schuler, D., Biogenic nanoparticles: production, characterization, and application of bacterial magnetosomes. *Journal of Physics: Condensed Matter* **2006**, *18* (38), S2815-S2828.
- (6) Abdelouas, A.; Gong, W. L.; Lutze, W.; Shelnett, J. A.; Franco, R.; Moura, I., Using Cytochrome c3 To Make Selenium Nanowires. *Chemistry of Materials* **2000**, *12* (6), 1510-1512.
- (7) Gorby, Y. A.; Beveridge, T. J.; Blakemore, R. P., Characterization of the bacterial magnetosome membrane. *J Bacteriol* **1988**, *170* (2), 834-41.
- (8) Leinfelder, W.; Forchhammer, K.; Zinoni, F.; Sawers, G.; Mandrand-Berthelot, M. A.; Bock, A., *Escherichia coli* genes whose products are involved in selenium metabolism. *J Bacteriol* **1988**, *170* (2), 540-6.
- (9) Tanaka, M.; Okamura, Y.; Arakaki, A.; Tanaka, T.; Takeyama, H.; Matsunaga, T., Origin of magnetosome membrane: proteomic analysis of magnetosome membrane and comparison with cytoplasmic membrane. *Proteomics* **2006**, *6* (19), 5234-47.
- (10) Arakaki, A.; Webb, J.; Matsunaga, T., A novel protein tightly bound to bacterial magnetic particles in *Magnetospirillum magneticum* strain AMB-1. *The Journal of biological chemistry* **2003**, *278* (10), 8745-50.
- (11) Brown, S., Engineered iron oxide-adhesion mutants of the *Escherichia coli* phage lambda receptor. *Proc Natl Acad Sci U S A* **1992**, *89* (18), 8651-5.
- (12) Brown, S.; Sarikaya, M.; Johnson, E., A genetic analysis of crystal growth. *J Mol Biol* **2000**, *299* (3), 725-35.
- (13) Sano, K.; Shiba, K., A hexapeptide motif that electrostatically binds to the surface of titanium. *J Am Chem Soc* **2003**, *125* (47), 14234-5.
- (14) Lower, B. H.; Lins, R. D.; Oestreicher, Z.; Straatsma, T. P.; Hochella, M. F., Jr.; Shi, L.; Lower, S. K., In vitro evolution of a peptide with a hematite binding motif that may constitute a natural metal-oxide binding archetype. *Environmental science & technology* **2008**, *42* (10), 3821-7.
- (15) Jeong, U.; Xia, Y., Synthesis and Crystallization of Monodisperse Spherical Colloids of Amorphous Selenium. *Advanced Materials* **2005**, *17* (1), 102-106.
- (16) Zhu, Y. J.; Qian, Y. T.; Hai, H. A.; Zhang, M. W., Preparation of nanometer-size selenium powders of uniform particle size by gamma-irradiation. *Mater Lett* **1996**, *28* (1-3), 119-122.
- (17) Dimitrijevic, N. M.; Kamat, P. V., Photoelectrochemistry in particulate systems. 8. Photochemistry of colloidal selenium. *Langmuir* **1988**, *4* (3), 782-784.
- (18) Franklin, T. C.; Adeniyi, W. K.; Nnodimele, R., The Electro-oxidation of Some Insoluble Inorganic Sulfides, Selenides, and Tellurides in Cationic Surfactant-Aqueous Sodium Hydroxide Systems. *Journal of The Electrochemical Society* **1990**, *137* (2), 480-484.
- (19) Zhang, H. Y.; Hu, Z. Q.; Lu, K., Transformation from the Amorphous to the Nanocrystalline State in Pure Selenium. *Nanostructured Materials* **1995**, *5* (1), 41-52.
- (20) Johnson, J. A.; Saboungi, M. L.; Thiyagarajan, P.; Csencsits, R.; Meisel, D., Selenium nanoparticles: A small-angle neutron scattering study. *Journal of Physical Chemistry B* **1999**, *103* (1), 59-63.
- (21) Jiang, Z. Y.; Xie, Z. X.; Xie, S. Y.; Zhang, X. H.; Huang, R. B.; Zheng, L. S., High purity trigonal selenium nanorods growth via laser ablation under controlled temperature. *Chemical Physics Letters* **2003**, *368* (3-4), 425-429.
- (22) Lin, Z.-H.; Wang, C. R., Evidence on the size-dependent absorption spectral evolution of selenium nanoparticles. *Materials Chemistry and Physics* **2005**, *92* (2-3), 591-594.
- (23) Laemmli, U. K., Cleavage of Structural Proteins during the Assembly of the Head of Bacteriophage T4. *Nature* **1970**, *227* (5259), 680-685.

- (24) Aryal, B. P.; Benson, D. E., Polyhistidine fusion proteins can nucleate the growth of CdSe nanoparticles. *Bioconjugate Chemistry* **2007**, *18* (2), 585-9.
- (25) Shafqat, J.; Hoog, J. O.; Hjelmqvist, L.; Oppermann, U. C. T.; Ibanez, C.; Jornvall, H., An ethanol-inducible MDR ethanol dehydrogenase/acetaldehyde reductase in *Escherichia coli* - Structural and enzymatic relationships to the eukaryotic protein forms. *European Journal of Biochemistry* **1999**, *263* (2), 305-311.
- (26) Blandino, A.; Caro, I.; Cantero, D., Comparative study of alcohol dehydrogenase activity in flor yeast extracts. *Biotechnology Letters* **1997**, *19* (7), 651-654.
- (27) Bozcuk, A. N.; Sumer, S.; Ozsoy, E. D.; Arisoy, M., Age-related enzyme activity in different genotypes of alcohol dehydrogenase (ADH) in *Drosophila melanogaster*. *Biogerontology* **2004**, *5* (4), 243-247.

1.7 Supporting Information

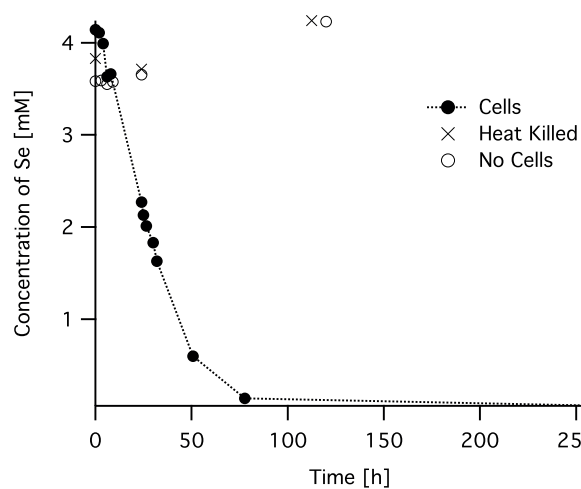


Figure S1: ICP-OES measurement of selenite reduction by *E. coli*.

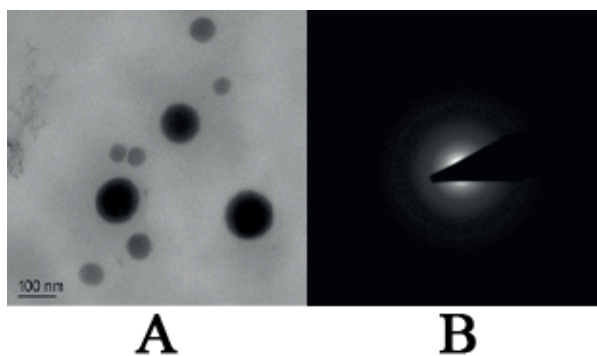


Figure S2: TEM (A) and SAED (B) of bacteriogenic SeNPs.

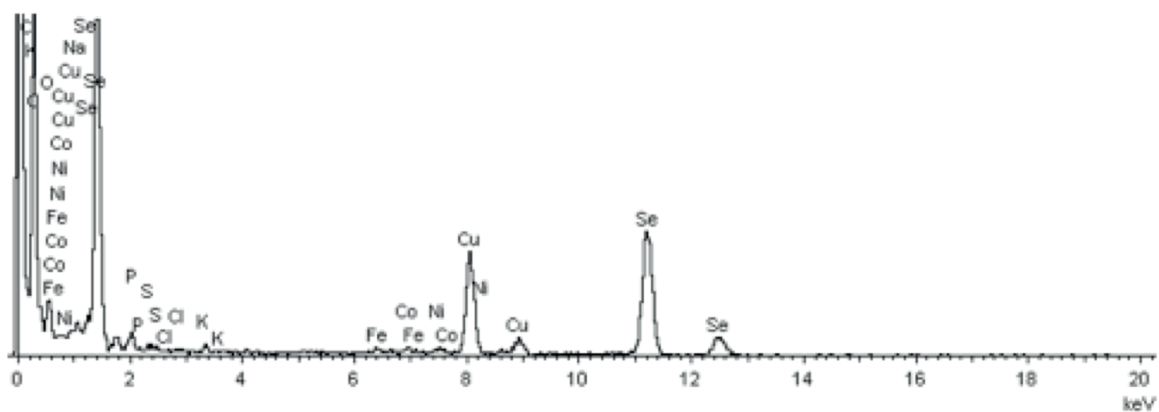


Figure S3: Electron Dispersive Spectroscopy of BioSeNPs.

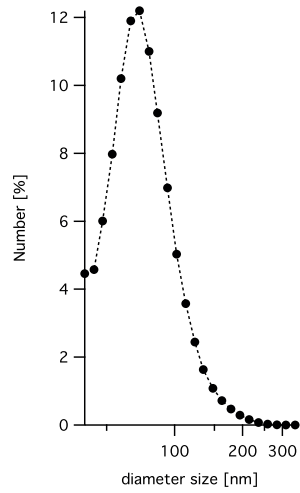


Figure S4: DLS measurement of BioSeNPs.

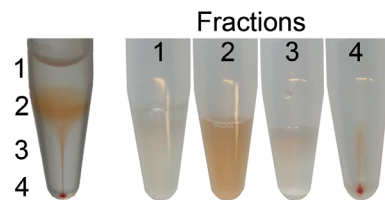


Figure S5: Fractions obtained after the centrifugation in an 80% sucrose solution of cell free extract from *E. coli* grown in selenite. Fractions are labeled 1-4 with 1 being the top layer containing the lighter molecules. Fraction 4 is a brick red pellet.

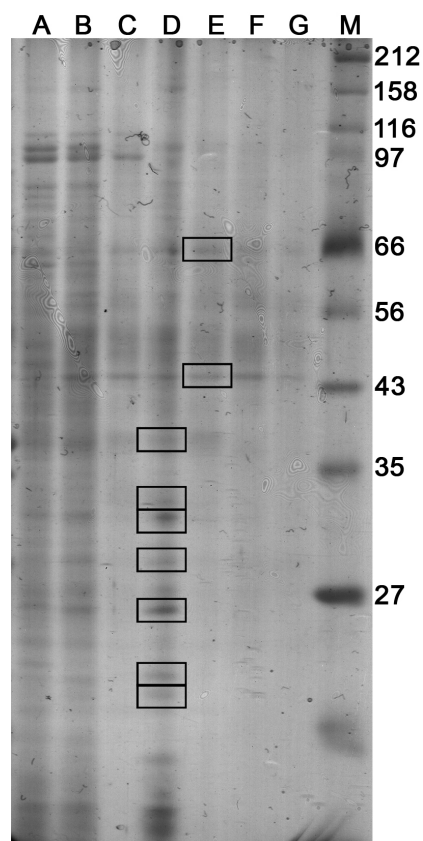


Figure S6: 12% SDS-PAGE of proteins from *E. coli* cell free extract captured by BioSeNPsBF. A (no treatment), B (Triton 2%), C (SDS 2%), D (urea 7M), E (SDS 10%), F (boiled 10min in SDS10%), G (boiled 30min in SDS10%), M (protein ladder with sizes in kDa). The square boxes are the bands that were cut out and identified by mass spectrometry.

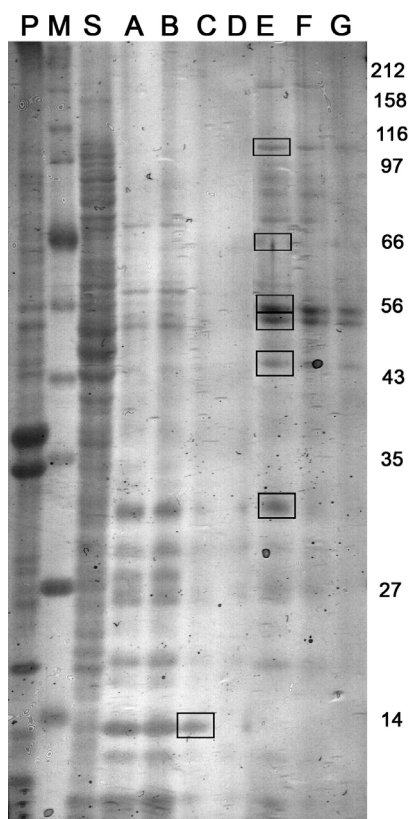


Figure S7: 12% SDS-PAGE of *E. coli* cell free extract proteins captured by FeNPs. A (no treatment), B (Triton 2%), C (SDS 2%), D (urea 7M), E (SDS 10%), F (boiled 10min in SDS10%), G (boiled 30min in SDS10%), P (pellet fraction from centrifuged lysed cells), S (supernatant fraction from centrifuged lysed cells) and M (protein ladder with sizes in kDa). The square boxes are the bands that were cut out and identified by mass spectrometry.

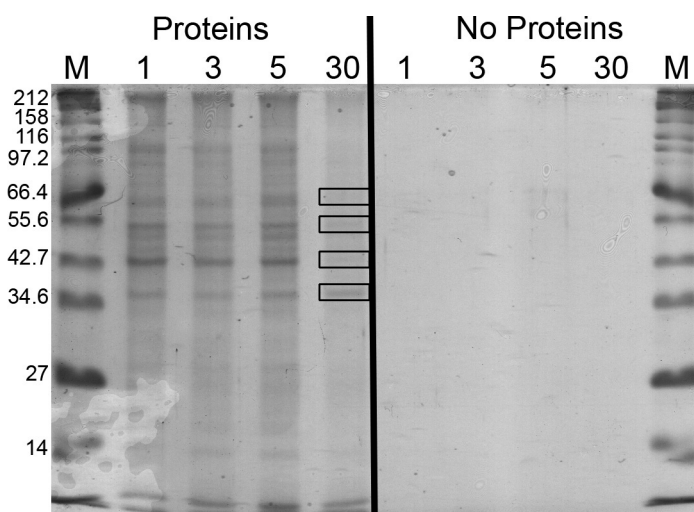


Figure S8: 12% SDS-PAGE of chemogenic particles produced at 1 to: 1, 3, 5, 30 ratio of selenite to sodium thiosulfate in the presence (left panel) or the absence (right panel) of cell free extract. M (Protein ladder with sizes in kDa). The square boxes are the bands that were cut out and identified by mass spectrometry.

Table S1. Identified proteins from *E. coli* CFX exposed to FeNPs. The –bands- column correspond to boxes present on figure S7. The –Score- column is the overall score of the identified protein based on all detected fragment. The -Queries Matched- column is the number of peptide that could match the equivalent protein and that relies on individual peptide scores.

Bands [kDa]	Name	Short name	Size [Da]	Score	Queries Matched
	Aldehyde-alcohol dehydrogenase	ADHE_ECOLI	96580	216	38
100	Pyruvate dehydrogenase E1 component	ODP1_ECO57	99948	98	16
	NADH-quinone oxidoreductase chain G	NUOG_ECOLI	101148	87	8
	30S ribosomal protein S1	RS1_ECO57	61235	202	29
66	Translation initiation factor IF-2	IF2_ECO57	97461	149	13
	2,4-dienoyl-CoA reductase [NADPH]	FADH_ECOLI	73203	84	1
	Glutamate decarboxylase alpha	DCEA_ECOLI	53221	181	27
	Glutamate decarboxylase beta	DCEB_ECOLI	53204	181	24
53	Soluble pyridine nucleotide transhydrogenase	STHA_ECOLI	51984	88	3
	ATP synthase subunit beta	ATPB_ECOLI	50351	79	4
	Tryptophanase	TNAA_ECO57	53155	79	14
	Glutamate decarboxylase alpha	DCEA_ECOLI	53221	145	9
	Tryptophanase	TNAA_ECOLI	53155	144	33
50	ATP synthase subunit beta	ATPB_ECOLI	50351	130	8
	Hypothetical GTP-binding protein yhbZ	YHBZ_ECOLI	43487	91	3
	3-oxoacyl-[acyl-carrier-protein] synthase 1	FABB_ECOLI	42928	80	1
	Elongation factor Tu	EFTU_ECOLI	43457	139	24
	N-acetylglucosamine repressor	NAGC_ECOLI	44970	134	3
	Ribosomal large subunit pseudouridine synthase D	RLUD_ECOLI	37155	114	3
45	Enolase	ENO_ECOLI	45683	109	11
	Glutamate decarboxylase alpha	DCEA_ECOLI	53221	102	2
	3-oxoacyl-[acyl-carrier-protein] synthase 1	FABB_ECOLI	42928	88	10
	Hypothetical protein ygeY	YGEY_ECOLI	45228	81	6

Continued on next page

Table S1 continued

	Elongation factor Tu	EFTU_ECOLI	43457	104	9
	Hypothetical protein yfeX	YFEX_ECOLI	33260	94	3
	Hypothetical protein yffS	YFFS_ECOLI	31250	91	4
30	30S ribosomal protein S3	RS3_ECO57	25967	89	1
	50S ribosomal protein L2	RL2_ECO57	29956	86	12
	Enoyl-[acyl-carrier-protein] reductase [NADH]	FABI_ECOLI	28074	84	7
14	DNA protection during starvation protein	DPS_ECOLI	18684	132	31

Table S2: Identified proteins from *E. coli* CFX exposed to BioNPsBF. The bands column correspond to boxes present on figure S6. The -Score- column is the overall score of the identified protein based on all detected fragment. The -Queries Matched- column is the number of peptide that could match the equivalent protein and that relies on individual peptide scores.

Bands [KDa]	Name	Short name	Size [Da]	Score	Queries Matched
66	Pyruvate dehydrogenase [cytochrome]	POXB_ECOLI	62542	86	3
	Phosphoenolpyruvate-protein phosphotransferase	PT1_ECOLI	63750	84	1
44	Glutamate decarboxylase beta (GAD-beta)	DCEB_ECOLI	53204	195	7
	3-oxoacyl-[acyl-carrier-protein] synthase 1	FABB_ECOLI	42928	159	3
	Elongation factor Tu (EF-Tu) (P-43)	EFTU_ECOLI	43457	122	13
	Tryptophanase	TNAA_ECOLI	53139	116	7
	Hypothetical protein ygeW	YGEW_ECOLI	44501	96	4
	Isocitrate lyase	ACEA_ECOLI	47777	88	1
37	Isocitrate dehydrogenase [NADP]	IDH_ECOLI	46070	87	2
	Elongation factor Tu (EF-Tu) (P-43)	EFTU_ECOLI	43457	112	6
	Glutamate decarboxylase beta (GAD-beta)	DCEB_ECOLI	53204	103	2
	3-dehydroquinate synthase	AROB_ECOLI	39141	102	1
	Hypothetical tRNA/rRNA methyltransferase yfiF	YFIF_ECOLI	37989	98	3
	Alcohol dehydrogenase, propanol-preferring	ADHP_ECOLI	35870	92	4
	Outer membrane protein C precursor (Porin ompC)	OMP_C_ECOLI	40343	84	6
Ribosomal large subunit pseudouridine synthase C	RLUC_ECOLI	36118	84	7	
33	Naphthoate synthase	MENB_ECOLI	32069	162	7
	Elongation factor Tu (EF-Tu) (P-43)	EFTU_ECOLI	43457	127	2
32	Naphthoate synthase	MENB_ECOLI	32069	123	4
	Enoyl-[acyl-carrier-protein] reductase [NADH]	FABI_ECOLI	28074	120	8
	Succinyl-CoA ligase [ADP-forming] subunit alpha	SUCD_ECOLI	30044	101	10
	3-oxoacyl-[acyl-carrier-protein] synthase 1	FABB_ECOLI	42928	101	3
	Glucokinase	GLK_ECOLI	35043	86	3
	Probable manno(fructo)kinase	MAK_ECOLI	32821	85	1

Continued on next page

Table S2 continued

	Elongation factor Tu (EF-Tu) (P-43)	EFTU_ECOLI	43457	78	6
32	Ribosomal large subunit pseudouridine synthase B	RLUB_ECOLI	32862	78	3
	ProP effector	PROQ_ECOLI	25991	86	2
30	30S ribosomal protein S2	RS2_ECO57	26784	83	3
	Outer membrane protein A precursor	OMPA_ECOLI	37292	82	1
	30S ribosomal protein S4	RS4_ECO57	23512	132	15
	UPF0135 protein ybgI - Escherichia coli	YBGI_ECOLI	26990	109	1
	Elongation factor Tu (EF-Tu) (P-43)	EFTU_ECOLI	43457	104	4
	Glutamate decarboxylase beta	DCEB_ECOLI	53204	99	2
	50S ribosomal protein L3	RL3_ECO57	22230	99	4
	30S ribosomal protein S3	RS3_ECO57	25967	91	10
27	Succinate dehydrogenase iron-sulfur protein	DHSB_ECOLI	27379	79	3
	Dihydrolipoyllysine-residue acetyltransferase component of pyruvate dehydrogenase complex	ODP2_ECOLI	66112	79	1
	50S ribosomal protein L1	RL1_ECO57	24714	78	3
	Hypothetical protein ykgE	YKGE_ECOLI	26500	78	1
	Succinyl-CoA synthetase beta chain	SUCC_ECOLI	41652	78	1
	Elongation factor Tu (EF-Tu) (P-43)	EFTU_ECOLI	43457	113	1
	30S ribosomal protein S3	RS3_ECO57	25967	103	4
	Phosphoheptose isomerase	GMHA_ECOLI	20973	103	2
20	50S ribosomal protein L6	RL6_ECO57	18949	92	18
	30S ribosomal protein S4	RS4_ECO57	23512	84	5
	Glutamate decarboxylase alpha	DCEA_ECOLI	53221	82	1
	50S ribosomal protein L5	RL5_ECO57	20346	79	5
	Translation initiation factor IF-3	IF3_ECO57	20608	79	7
	Elongation factor Tu (EF-Tu) (P-43)	EFTU_ECOLI	43457	105	3
	30S ribosomal protein S3	RS3_ECO57	25967	97	5
20	50S ribosomal protein L5	RL5_ECO57	20346	95	10
	50S ribosomal protein L6	RL6_ECO57	18949	92	6
	30S ribosomal protein S4	RS4_ECO57	23512	89	8
	30S ribosomal protein S7	RS7_ECO57	17593	84	6

Table S3. Identified proteins associated to *E. coli* BioSeNPs. The bands column correspond to boxes present on figure 2. The -Score- column is the overall score of the identified protein based on all detected fragment. The -Queries Matched- column is the number of peptide that could match the equivalent protein and that relies on individual peptide scores.

Bands [KDa]	Name	Short name	Size [Da]	Score	Queries Matched
	Elongation factor Tu (EF-Tu) (P-43)	EFTU_ECOLI	43457	490	63
	Isocitrate dehydrogenase [NADP]	IDH_ECOLI	46070	170	11
	Isocitrate lyase	ACEA_ECOLI	47777	144	9
	3-oxoacyl-[acyl-carrier-protein] synthase 1	FABB_ECOLI	42928	133	8
	Succinylornithine transaminase	ASTC_ECOLI	43980	109	7
	Putative tagatose 6-phosphate kinase gatZ	GATZ_ECOLI	47535	101	9
45	D-amino acid dehydrogenase small subunit	DADA_ECOLI	47919	91	3
	Phosphopentomutase	DEOB_ECOLI	44684	83	2
	30S ribosomal protein S3	RS3_ECO57	25967	82	1
	4-aminobutyrate aminotransferase	GABT_ECOLI	46202	81	5
	Molybdopterin biosynthesis protein moeA	MOEA_ECOLI	44382	81	1
	Tryptophanase	TNAA_ECOLI	53139	79	6
	Outer membrane protein C precursor	OMPC_ECOLI	40343	196	40
	Outer membrane protein C precursor	OMPC_ECO57	40483	179	26
	Outer membrane protein F precursor	OMPF_ECOLI	39039	161	8
	Transaldolase A	TALA_ECOLI	35865	131	8
	Elongation factor Tu (EF-Tu) (P-43)	EFTU_ECOLI	43457	130	15
	Glyceraldehyde-3-phosphate dehydrogenase A	G3P1_ECO57	35681	109	9
38	6-phosphogluconolactonase	6PGL_ECO57	36653	102	5
	Alcohol dehydrogenase, propanol-preferring	ADHP_ECOLI	35870	99	6
	tRNA-modifying protein ygfZ	YGFZ_ECOLI	36185	97	3
	Isocitrate lyase	ACEA_ECOLI	47777	96	2
	Oligopeptide transport ATP-binding protein oppF	OPPF_ECOLI	37573	96	9
	Oligopeptide transport ATP-binding protein oppD	OPPD_ECOLI	37506	91	3

Continued on next page

Table S3 continued

	Hypothetical ABC transporter ATP-binding protein yejF	YEJF_ECOLI	58918	91	1
	Transaldolase B	TALB_ECOLI	35368	89	4
38	Pyruvate kinase I	KPYK1_ECO57	51039	87	2
	Rod shape-determining protein mreB	MREB_ECOLI	37100	82	16
	Hypothetical oxidoreductase yajO	YAJO_ECOLI	36569	82	7
	50S ribosomal protein L4	RL4_ECO57	22073	81	1

Table S4. Identified proteins from *E. coli* CFX exposed to ChSeNPs. The bands column correspond to boxes present on figure S8. The -Score- column is the overall score of the identified protein based on all detected fragment. The -Queries Matched- column is the number of peptide that could match the equivalent protein and that relies on individual peptide scores.

Bands [KDa]	Name	Short name	Size [Da]	Score	Queries Matched
	Aconitate hydratase 2 (Citrate hydro-lyase 2)	ACON2_ECOLI	94009	147	4
	60 kDa chaperonin (groEL protein)	CH60_ECO57	57464	139	11
	Pyruvate dehydrogenase E1 component	ODP1_ECO57	99948	122	7
	NAD-dependent malic enzyme	MAO1_ECO57	63435	111	6
	Malate synthase A	MASY_ECOLI	60521	109	22
	Elongation factor Tu (EF-Tu) (P-43)	EFTU_ECOLI	43457	101	13
66	Phosphoenolpyruvate-protein phosphotransferase	PT1_ECOLI	63750	100	7
	Long-chain-fatty-acid-CoA ligase	LCFA_ECOLI	62521	98	4
	ATP-dependent Clp protease ATP-binding subunit clpA	CLPA_ECOLI	84326	91	1
	Pyruvate dehydrogenase [Contains: Alpha-peptide]	POXB_ECOLI	62542	89	10
	Sulfite reductase [NADPH] hemoprotein beta-component	CYSI_ECOLI	64300	80	1
	30S ribosomal protein S4	RS4_ECO57	23512	80	1
	Enolase (2-phosphoglycerate dehydratase)	ENO_ECOLI	45683	158	7
	Aldehyde dehydrogenase A	ALDA_ECOLI	52411	147	12
	Elongation factor Tu (EF-Tu) (P-43)	EFTU_ECOLI	43457	140	19
	Succinylornithine transaminase (Carbon starvation)	ASTC_ECOLI	43980	129	5
	Mannitol-1-phosphate 5-dehydrogenase	MTLD_ECOLI	41171	112	2
55	Phosphoribosylglycinamide formyltransferase 2	PURT_ECOLI	42692	110	3
	2-methylcitrate synthase	PRPC_ECOLI	43246	105	9
	Hypothetical protein ygeY	YGEY_ECOLI	45288	105	3
	3-oxoacyl-[acyl-carrier-protein] synthase 1	FABB_ECOLI	42928	100	4
	Isocitrate lyase (EC 4.1.3.1)	ACEA_ECOLI	47777	100	5
	Isocitrate dehydrogenase (NADP(+)-specific ICDH)	IDH_ECOLI	46070	100	3

Continued on next page

Table S4 continued

	Aconitate hydratase 2	ACON2_ECOLI	94009	96	4
	Tyrosyl-tRNA synthetase	SYT_ECOLI	47896	95	4
	N-acetylglucosamine repressor - Escherichia coli	NAGC_ECOLI	44970	94	4
	Pyruvate dehydrogenase E1 component	ODP1_ECO57	99948	92	2
	Protein recA (Recombinase A)	RECA_ECOLI	38121	85	5
	Citrate synthase (EC 2.3.3.1)	CISY_ECOLI	48383	85	1
	Malate synthase A (EC 2.3.3.9) (MSA)	MASY_ECOLI	60521	85	2
55	Succinyl-CoA synthetase beta chain	SUCC_ECOLI	41652	84	6
	Phosphoenolpyruvate synthase	PPSA_ECOLI	87836	84	2
	Bifunctional protein putA (Proline dehydrogenase)	PUTA_ECOLI	144467	81	1
	Aldehyde dehydrogenase B	ALDB_ECOLI	56670	79	2
	S-adenosylmethionine synthetase	METK_ECOLI	42153	78	2
	ATP-dependent Clp protease ATP-binding subunit clpX	CLPX_ECOLI	46726	78	3
	30S ribosomal protein S3	RS3_ECO57	25967	77	1
	Fructose-1,6-bisphosphatase	F16P_ECOL6	37153	118	5
	Oligopeptide transport ATP-binding protein oppD	OPPD_ECOLI	37506	117	4
	Hypothetical ABC transporter ATP- binding protein yejF	YEJF_ECOLI	58918	117	1
	HTH-type transcriptional repressor purR (Purine)	PURR_ECOLI	38378	116	4
	Lipoate-protein ligase A	LPLA_ECOLI	38244	113	1
	Nucleoid-associated protein ndpA	NDPA_ECOLI	37913	109	3
	6-phosphofructokinase isozyme 1	K6PF1_ECO57	35162	98	1
43	Pyruvate dehydrogenase E1 component	ODP1_ECO57	99948	96	3
	Outer membrane protein C precursor (Porin ompC)	OMPC_ECOLI	40343	96	17
	Phosphopentomutase	DEOB_ECOLI	44684	94	2
	UTP-glucose-1-phosphate uridylyltransferase	GALU_ECOLI	33206	94	4
	Catalase HPII (Hydroxyperoxidase II)	CATE_ECOLI	84224	91	3
	Nicotinate-nucleotide pyrophosphorylase	NADC_ECOLI	32856	91	2
	Phenylalanyl-tRNA synthetase alpha chain	SYFA_ECOLI	36866	90	2

Continued on next page

Table S4 continued

	DNA protection during starvation protein	DPS_ECOLI	18684	90	2
	Aconitate hydratase 2	ACON2_ECOLI	94009	88	3
	Outer membrane protein F precursor (Porin ompF)	OMPF_ECOLI	39309	88	4
	Isocitrate lyase	ACEA_ECOLI	47777	88	3
	Glyceraldehyde-3-phosphate dehydrogenase A	G3P1_ECO57	35681	87	8
	L-asparaginase 2 precursor	ASPG2_ECOLI	36942	86	1
	Alcohol dehydrogenase, propanol-preferring	ADHP_ECOLI	35870	85	5
	Protein mrp	MRP_ECOLI	40084	85	1
43	Outer membrane protein C precursor (Porin ompC)	OMPC_ECO57	40483	85	12
	Probable GTPase engC precursor	ENGC_ECOLI	39454	85	1
	Phosphoribosylformylglycinamide cyclo-ligase	PUR5_ECO57	37226	85	1
	30S ribosomal protein S4	RS4_ECO57	23512	84	2
	Formate acetyltransferase 1	PFLB_ECOLI	85588	84	3
	50S ribosomal protein L11	RL11_ECO57	14923	80	1
	Hypothetical protein ynhG precursor	YNHG_ECOLI	36117	80	1
	Succinyl-CoA synthetase beta chain	SUCC_ECOLI	41652	78	3
	Fructose-bisphosphate aldolase class 1	ALF1_ECOL6	38313	78	2
	Galactitol-1-phosphate 5-dehydrogenase	GATD_ECOLI	37822	77	2
	Aldehyde dehydrogenase A	ALDA_ECOLI	52411	230	29
	Aldehyde dehydrogenase B	ALDB_ECOLI	56670	167	20
	Elongation factor Tu (EF-Tu) (P-43)	EFTU_ECOLI	43457	161	12
	ATP synthase subunit alpha	ATPA_ECOLI	55416	154	18
	Glycerol kinase	GLPK_ECOLI	56480	149	13
35	Gamma-aminobutyraldehyde dehydrogenase	ABDH_ECOLI	51197	144	3
	Glutamate decarboxylase alpha	DCEA_ECOLI	53221	123	1
	Isocitrate lyase	ACEA_ECOLI	47777	98	1
	Trk system potassium uptake protein trkA	TRKA_ECOLI	50393	96	1
	Pyruvate dehydrogenase E1 component	ODP1_ECO57	99948	93	3
	Catalase HPII (Hydroxyperoxidase II)	CATE_ECOLI	84224	92	3

Continued on next page

Table S4 continued

	Pyruvate kinase II	KPYK2_ECOLI	51553	89	11
	Dihydrolipoyl dehydrogenase	DLDH_ECOLI	50942	87	4
	Malate synthase A	MASY_ECOLI	60521	85	6
35	Aminoacyl-histidine dipeptidase	PEPD_ECOLI	53110	84	5
	Elongation factor G (EF-G)	EFG_ECOLI	77704	80	2
	Succinate-semialdehyde dehydrogenase [NADP+]	GABD_ECOLI	52030	79	2

Chapter

2 Silver release from silver nanoparticles in natural waters

J. Dobias and R. Bernier-Latmani

Abstract: Silver nanoparticles (AgNPs) are used increasingly in consumer products for their antimicrobial properties. This increased use raises ecological concern due to the release of AgNPs into the environment. Once released, zerovalent silver may be oxidized to Ag^+ and the cation liberated or it may persist as AgNPs. The chemical form of Ag has implications for its toxicity. It is therefore crucial to characterize the persistence of AgNPs to predict their ecotoxicological potential.

In this study, we evaluated the release of Ag from AgNPs of various sizes exposed to river and lake water for up to four months. Several AgNP capping agents were also considered: polyvinylpyrrolidone (PVP), tannic acid (Tan) and citric acid (Cit). We observed a striking difference between 5-10 nm and 50 nm AgNPs with the latter being more resistant to dissolution in oxic water on a mass basis. However, the difference decreased when Ag was surface area-normalized, suggesting an important role of surface area in determining Ag loss. We propose that rapid initial Ag^+ release was attributable to desorption of Ag^+ from nanoparticle surfaces. In addition, it is likely that oxidative dissolution also occurs but at a slower rate. We also observed an effect of the coating on dissolution, with PVP- and Tan-AgNPs being more prone to Ag^+ release than Cit-AgNPs. This study clearly shows that small AgNPs (5 nm - PVP and Tan) dissolve rapidly and almost completely, while larger ones (50 nm) and ones coated with citric acid have the potential to persist for at least a year and could serve as a continuous source of silver ions.

Keywords: Silver, nanoparticles, dissolution, freshwater, polyvinylpyrrolidone, tannic, citrate

2.1 Introduction

The use of nanomaterials in consumer goods has increased significantly over the last decade to reach approximately 1,300 referenced products distributed across numerous categories including appliances, clothing, electronics, toys, housing materials, as well as health and fitness products^{1, 2}. Among consumer products that include nanomaterials, nanoparticulate silver-containing products are most numerous¹. This is because of silver's antimicrobial properties³⁻⁶. It has been shown that some of these consumer products release silver nanoparticles (AgNPs) in the environment during their production, useful life^{7, 8} or upon final disposal^{9, 10}. Hence, there is a concern that AgNP release would adversely affect natural microbial communities, potentially causing a significant impact on aqueous ecosystems^{9, 11}.

The mechanism of AgNP toxicity to microorganisms is not well understood. It is unclear whether AgNP toxicity is mechanistically linked to Ag⁺ ion toxicity or whether additional nanoparticle-specific mechanisms are important. AgNPs may serve as a source of Ag⁺ under oxic conditions through the oxidation of zerovalent Ag^{5, 12, 13}. Ag⁺ may be released into solution or may be sorbed by the AgNPs and delivered locally at high doses to the cell (i.e., the Trojan horse effect^{14, 15}). Ag⁺ release was found to correlate to AgNP size^{13, 16} but also to other factors such as water chemistry or NP surface coating¹⁷⁻²². Additional toxicity mechanisms include the association of AgNPs with bacterial membranes and consequent membrane damage²³⁻²⁵, the intracellular uptake of AgNPs (<10 nm)²⁶ and the release of reactive oxygen species that induce a stress response in bacterial cells^{27, 28}. In order to unravel the potential contribution of these toxicity pathways in the environment and, in particular, to evaluate whether the non-ionic toxicity routes are relevant in such a context, it is essential to have a good understanding of AgNP persistence in the environment. To our knowledge, only three studies evaluated AgNP dissolution over a time course of several months^{12, 13, 29}.

The first study predicts that, based on thermodynamic calculations, AgNPs will not persist in an oxic solution and will undergo complete oxidative dissolution¹². If the thermodynamic characteristics of AgNPs alone did, in fact, control the oxidative dissolution of AgNPs, we would expect that AgNPs released into the environment would rapidly dissolve and the contaminant of concern would be Ag⁺ ions¹². However various factors such as dissolved oxygen, organic matter or water chemistry play an important but unclear role in AgNPs dissolution. In contrast, the second study shows a variable extent of dissolution (1-70% depending on AgNP size) after 3 months under oxic aqueous conditions¹³. Moreover, the authors state that surface area alone cannot explain the dissolution of AgNPs, suggesting that not only the primary particle characteristics, but also the chemical composition of the water, the concentration of NPs

as well as the capping agents are to be considered when attempting to understand the dissolution of AgNPs¹³. In the third study, the release of Ag from AgNPs incubated in ultrapure water was quantified over time³⁰. The findings clearly show that the coating (polyvinylpyrrolidone or citrate) and the incubation temperature greatly impact the release of Ag⁺.

These studies provide a helpful framework to investigate the release of Ag from AgNPs in the environment as they collectively suggest that this release varies greatly depending on nanoparticle properties and environmental parameters. Hence, these studies underscore the need to consider the complexity of the environment in its entirety by carrying out field deployments of AgNPs.

In this study, we investigated the persistence of AgNPs under environmental conditions by deploying them in a lake and two rivers for a maximum of four months. The effect of size and capping agent was studied by considering AgNPs of 5nm, 10nm and 50nm coated with polyvinylpyrrolidone (PVP), tannic acid (Tan) or citric acid (Cit). Complementary laboratory experiments were carried out to support conclusions from field observations.

2.2 Materials and Methods

2.2.1 *Preparation of nanoparticles for deployment*

Spherical silver nanoparticles of various sizes and surface coatings were considered in this study: 5 and 50 nm polyvinylpyrrolidone (PVP)-coated AgNPs (6.5 ± 0.8 nm and 53.4 ± 5.0 nm), 5 and 50 nm tannic acid-coated AgNPs (4.3 ± 1.3 nm and 52.1 ± 7.1 nm) and 10 and 50 nm citric-acid coated AgNPs (8.2 ± 1.2 nm and 49.1 ± 4.5 nm) were obtained from nanoComposix (San Diego, CA) as water suspensions of 20 mg/L and characterized by TEM and DLS (Figure S1 and S2). In order to expose AgNPs to natural waters and to quantify silver loss overtime, we embedded the nanoparticles in 4% low-melt agarose (Applichem GmbH, Darmstadt, Germany) at a concentration of 1,000 $\mu\text{g/L}$ by gently stirring a mixture of melted gel and AgNPs and aspirating the mixture into PVC tubing (3 mm ID) with a syringe. The tubing was then placed on ice to accelerate gelation, pushed out of the tube with a flow of N_2 , cut into 3.5 cm-long pieces and placed into individual deployment tubes. As the gel puck preparation requires melting the agarose at 60°C , a control experiment was carried out to ascertain the effect of temperature and no release of silver was measured after the preparation step (S1).

The deployment tubes consisted of 1.5 mL polypropylene microcentrifuge screw cap tubes into the side of which six slits (2 mm x 45 mm) were cut lengthwise (Figure S3). The tubes were placed in holders made of two polypropylene square plates (10 cm x 10 cm x 1.2 cm), equipped with twelve depressions (10 mm x 6 mm for the upper plate and 8 mm x 6 mm for the lower plate) equidistant from the plate center and held together with cable ties (Figure S3). For river deployment, the holders were attached to galvanize steel poles (3.5 cm x 180 cm) with nylon wires. The poles were hammered down into the riverbed to a depth of about 50 cm (Figure S4-A). For lake deployment, the holders were attached to a cable (Figure S4-B) at about 100 m below the water surface. Individual gel puck weights were recorded before and after deployment.

2.2.2 *Deployment sites*

The selected sites are located in Switzerland at the following coordinates (latitude-longitude-elevation): NG1 [46.494463 - 6.579595 - 372], R1 [46.504598 - 6.430565 - 455], R2 [46.549241 - 6.541399 - 395]. NG1 is located in lake Geneva, R1 is a small river (Le Boiron) and R2 a mid-size river (La Venoge) both located in the region of Morges, VD. Physico-chemical characteristics of the waters are presented in the SI (S5 and S6). The two rivers are protected from direct sunlight exposure as they are running in a small forest shaded environment.

2.2.3 *Sample retrieval and processing*

The samples were deployed between October and March, covering western European fall and winter seasons. The lake samples were retrieved after 1 and 4 months and the river samples after 2 weeks, and 1 month for R1 and 2 weeks, 1 month and 4 months for R2. Water samples were collected for chemical analysis at deployment and retrieval times. Retrieved gel pucks were placed in epitubes, weighed, dried at 60°C for at least two days and weighed again. 1 mL of nitric acid (12%) was added to the dry gel pucks and the mixture incubated for at least 3 days to dissolve the remaining AgNPs. The loss of silver was determined by comparing the mass of silver normalized to dry gel puck weight before and after deployment.

The last retrieval of the R1 samples was made impossible by the removal of the deployment system by river shore workers.

2.2.4 *Laboratory experiments*

Laboratory experiments were used to test hypotheses generated by the field experiments. Gel pucks were prepared as described above. Water from river R1 was collected, filtered through a 3 µm and then a 0.22 µm pore size filter (GSWP 47 mm, Merck Millipore, Billerica, Ma). Serum bottles were amended with 200 mL of water. For anoxic conditions, water in the bottles was bubbled with N₂ for 2h and incubated overnight in an anoxic glovebox. The next day, the measured dissolved oxygen (DO) concentration was 0.09 +/- 0.05 mg/L.

All the bottles were sealed, cooled down to and maintained at 10°C (river water temperature) in an ice water bath. Several gel pucks or a control AgNO₃ solution were added to the bottles and incubated under either oxic or anoxic conditions. At 5, 30 and 60 min, a water sample was retrieved for ultracentrifugation (see below) and the gel pucks collected from the corresponding bottle. The aqueous concentration of Ag was taken to represent released Ag and the gel puck analysis post-deployment allowed the evaluation of Ag loss (as described for field deployment). The remaining solution was acidified with HNO₃ (0.5% final concentration) to desorb Ag from the walls and analyzed for Ag content. A mass balance was calculated and ≥ 90% of Ag was accounted for.

Ultracentrifugation was carried out to differentiate between AgNPs (pellet) and solution silver (supernatant). It was performed using a Beckman coulter LX80P system with a swinging bucket rotor SW60-TI at 60,000 rpm (485,000 rcf) for 2 hours at 20°C. Centrifuge tubes were tested for Ag sorption by amending filtered river water or 18MΩ cm H₂O with silver nitrate (1.8 µg/L) and incubating for 3 hours. No sorption was observed.

The effect of NaCl on the release of Ag from AgNPs was evaluated by measuring Ag release from gel pucks containing AgNPs into R1 water either unaltered or amended with 25 mg/L of NaCl to represent R2 water. The incubations were sampled after 5 min, 1 day, 1 week and 2 weeks.

2.2.5 *Analytical approaches*

Total organic carbon (TOC) in water was measured on a Shimadzu total organic carbon analyzer TOC-V CPH coupled to an autosampler ASI-V. Anions and cations in water were measured by ion chromatography (DX-3000, Dionex, Sunnyvale, CA) with an IonPac AS11-HC column. Elution was carried out using a gradient of 0.5–30 mM KOH. Ag solution concentrations originating from the gel pucks digestion were determined using an ICP-OES (Shimadzu ICPE 9000) and the samples and standards were prepared in 1.2% HNO₃ (final concentration).

Ag solution concentrations in aqueous samples were measured using an ICP-MS (Perkin Elmer DRCII) with a detection limit of 0.09 ppt for silver. Samples and standards were prepared in 0.5% HNO₃ (final concentration). Dissolved oxygen (DO), pH and temperature were measured on site with a portable meter HQ40d (Hack Company, Loveland, CO, USA) with pH (PHC101) and DO (LDO101) probes that included integrated temperature probes.

2.3 Results and discussion

The release of Ag from commercial AgNPs, characterized by TEM and DLS (Figure S3 and S4), in natural aquatic environments was studied using agarose gel pucks deployed in a lake and two rivers for up to four months. The advantage of *in situ* deployment is that it captures the natural variability of the aqueous environment over time and hence, the results are taken to be representative of environmental processes. Ag release was quantified by comparing the initial silver concentrations in unexposed gel pucks to those remaining after incubation (Figures 1-3). There are several obvious trends: (a) small (5 nm) nanoparticles release more Ag (normalized to mass of gel) than large (50 nm) nanoparticles; (b) the largest amount of silver loss occurs primarily between deployment and the first time point; (c) In the lake and R2, there is sustained loss of Ag from 5 nm AgNPs after the first time point; and (d) Ag loss is more prevalent for tannic acid- and PVP-coated than citric acid-coated AgNPs. We considered each of these observations to extract conclusions about the behavior of AgNPs in natural waters.

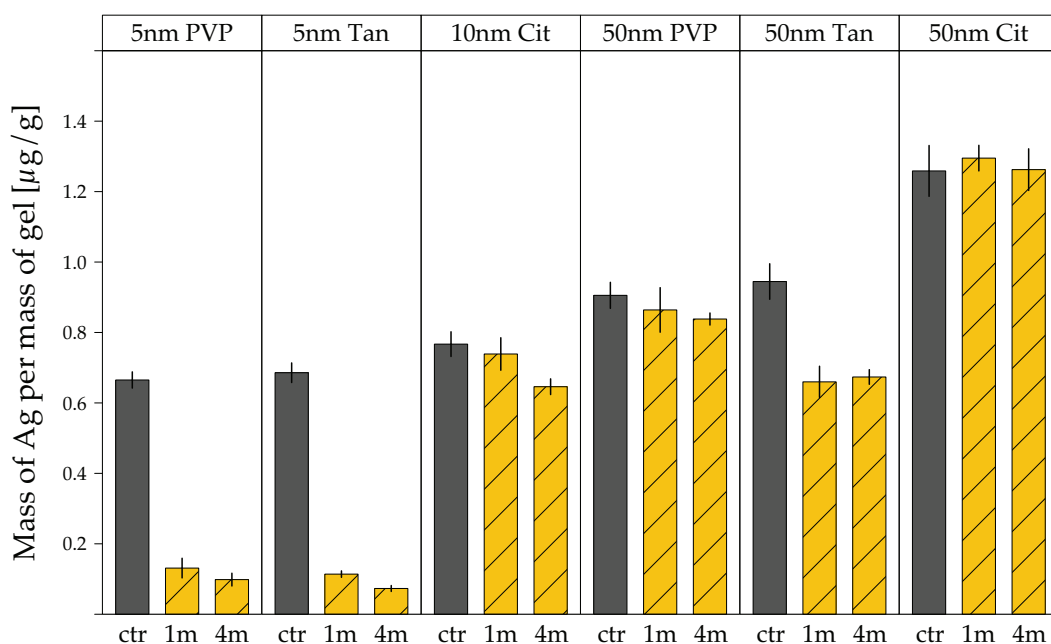


Figure 1: Silver content of gel pucks (in μg of Ag per g of dry gel) deployed in lake Geneva for 1 and 4 months (hatched bars: 1m and 4m). The first bar in each panel represents the undeployed gel pucks (ctr). Error bars represent the range of measurements for duplicate deployed gel pucks and 5 unexposed gel pucks.

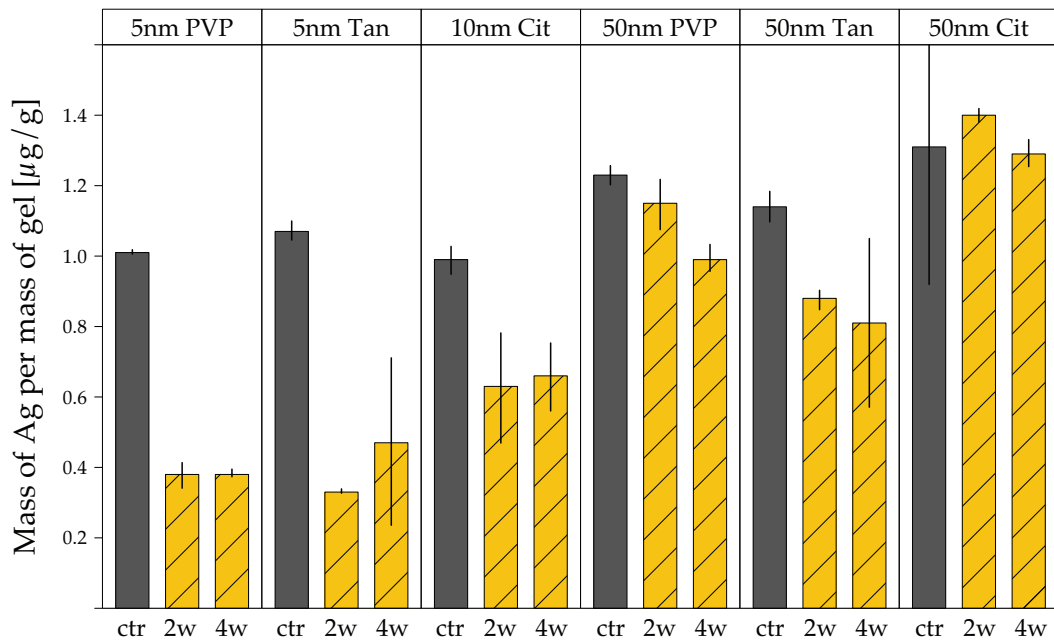


Figure 2: Silver content of gel pucks (in μg of Ag per g of dry gel) deployed in R1 river for 2 and 4 weeks (hatched bars: 2w and 4w). The first bar in each panel represents the undeployed gel pucks (ctr). Error bars represent the range of measurements for duplicate deployed gel pucks and 5 undeployed gel pucks.

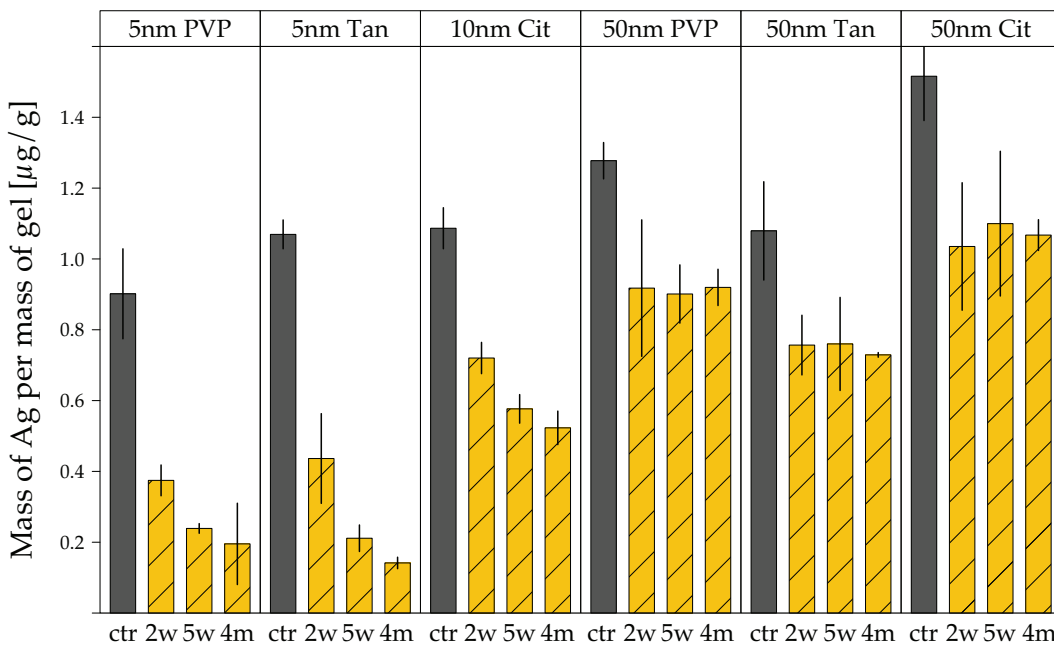


Figure 3: Silver content of gel pucks (in μg of Ag per g of dry gel) deployed in R2 river for 2 weeks, 5 weeks and 4 months (hatched bars: 2w, 5w and 4m). The first bar in each panel represents the undeployed gel pucks (ctr). Error bars represent the range of measurements for duplicate deployed gel pucks and 5 undeployed gel pucks.

2.3.1 Size-dependent release of Ag

Loss of Ag is clearly related to AgNP size when the data are presented as a function of mass loss. At all three deployment sites (Figures 1-3), 5 nm AgNPs display significantly more loss (85-89%) than 50 nm AgNPs over the same time frame. A similar size dependency – where the mass-normalized dissolution rate is greater for small AgNPs – was observed previously when the dissolution of citrate-coated AgNPs was studied in the presence of the oxidant H_2O_2 ³⁰. However, if the process were surface-controlled, we would expect similar loss regardless of size when the data are normalized to surface area. We calculated time-resolved silver loss (Figure 4-A) and silver loss normalized to the surface-area for all cases (Figure 4-B). The difference in the fraction of silver lost observed, when comparing 5 nm and 50 nm AgNPs in Figure 4-A and Figure 4-B, drops below a seven-fold factor. In the absence of surface area effect the ratio of 50 nm to 5 nm in figure 4-B should be of two orders of magnitude corresponding to the ratio of the respective spheres' surface area. This finding suggests a dominant effect of surface area in determining Ag loss and confirms findings by other studies³¹.

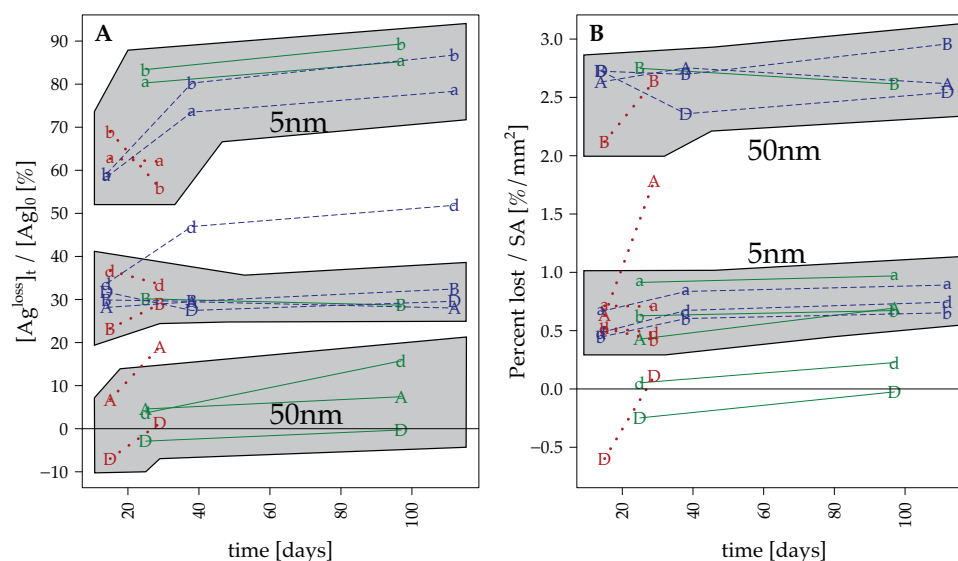


Figure 4: Time-resolved silver loss in percent (A) and in percent per surface area (B) from lake (plain lines), R1 river (dotted lines) and R2 river (dashed lines) deployments. $[Ag]_{t}^{loss} = Ag$ loss from gel in μg Ag/g gel; $[Ag]_0$ = initial concentration of silver in gel in μg Ag/g gel, SA= surface area per gram of gel in mm^2/g gel. Legends: a, A= 5 and 50 nm PVP AgNPs, b, B= 5 and 50 nm tannic AgNPs, d, D= 10 and 50 nm citric AgNPs.

The majority of the data obtained fall between values of 0.5 and 3 $\%/mm^2$ regardless of size and deployment site (Figure 4-B). However, we note that the surface area-normalized values were clustered around 2.5 $\%/mm^2$ for 50 nm AgNPs and around 0.6 $\%/mm^2$ for 5 nm AgNPs. This difference runs counter to the published result that smaller AgNPs have higher solubility as a result of their size¹³. In our findings, smaller

AgNPs have lower solubility (surface area normalized) than larger AgNPs but the effect of size is considerably lower than the surface area effect as shown above. This confirms the dominance of surface area as a control of Ag release but also suggests that other unidentified factors also play a role.

In contrast to all the other AgNPs, 50 nm Cit AgNPs in two of the three sites (lake and R1) and 10 nm Cit AgNPs in the lake site displayed almost no loss (Figure 4A). Hence, it appears that a citric acid surface coating may play an important role in modulating Ag loss from the AgNPs.

2.3.2 Mechanism of release of Ag

In most cases, we observed a rapid loss of Ag at the first time point after deployment, which suggests a rapid initial loss rate (Figures 1-3). We explored two hypotheses to account for that initial loss: (1) an oxidative dissolution process with O_2 as the oxidant as described in Liu *et al.*¹² or (2) the release of chemisorbed Ag^+ as described in Lok *et al.*⁵.

The first hypothesis was explored by carrying out Ag release experiments with gel pucks embedded with 5 nm and 50 nm PVP-coated AgNPs in oxic or anoxic 0.22 μm prefiltered R1 water. After 5 minutes of exposure, approximately 30% of the Ag is lost from 5 nm AgNPs gel pucks regardless of the oxygen content of the solution (Figure 5). The lack of difference in Ag release between oxic and anoxic conditions suggests that oxidative dissolution cannot explain this rapid initial silver release. A more likely explanation is the release of sorbed Ag^+ from the surface of the AgNPs.

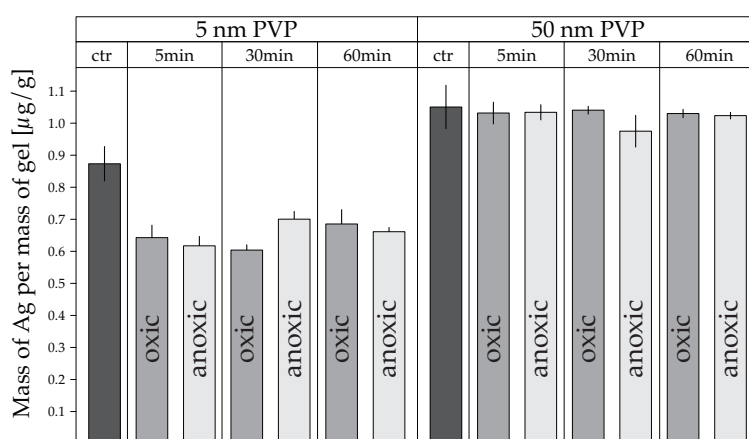


Figure 5: Mass of silver (μg) per gram of gel remaining in gel pucks loaded with 5nm and 50nm PVP-coated AgNPs after exposure to oxic and anoxic filtered R1 water for 5, 30 and 60 minutes and unexposed to filtered water (ctr). Error bars represent the standard deviation for five gel pucks.

In the case of 50 nm AgNPs, consistent with results from the field deployment, no significant Ag loss and no effect of oxic/anoxic conditions was observed. Hence, we conclude that oxidative dissolution likely plays a minor role in the initial release of Ag

from the AgNPs deployed in the field. A calculation of the fraction of sorbed Ag that is released upon exposure to water yields 2% and 6% for 5 nm and 50 nm AgNPs, respectively (Table S1). Thus, it is realistic to consider that the released Ag was initially present as sorbed Ag.

Nonetheless, we cannot exclude the possibility that in addition to the rapid release of sorbed Ag⁺, a slower process of oxidative dissolution takes place. The sustained release of Ag after the first time point which is observed for 10 nm citric acid-coated AgNPs (Figure 1), for 50 nm tannic acid-coated AgNPs (Figure 2) and 5 nm PVP- or tannic-acid coated and 10 nm citric acid-coated AgNPs (Figure 3) is consistent with a slow oxidative dissolution step.

Previous studies¹² have shown a large difference in Ag release under oxic and anoxic conditions. We attribute the different outcome of our findings to the specific solution chemistry in our study. Desorption may be predominant in our study because the rate of oxidative dissolution is very slow due to the pH values of lake and river water (7.9-8.4). It has been shown¹² that the rate of release of Ag from AgNPs decreases rapidly at pH values ≥ 8 . In contrast, the study showing extensive oxidative dissolution¹² under oxic conditions was carried out at a pH value of 5.68, pH at which oxidative dissolution is approximately 3-fold faster than at pH 8.

In order to test the second hypothesis and to exclude the possibility of physical release of AgNPs from the gel, we exposed gel pucks to 0.22 μm prefiltered R1 water for 5 or 60 minutes. At each time point, water was collected and ultracentrifuged at 485,000 rcf for 2 hours and the supernatant fraction analyzed for silver content by ICP-MS. A control experiment indicated that 5 nm PVP-coated AgNPs were localized in the pellet under these condition. At both time points, there was no measurable difference in concentration before and after ultracentrifugation, indicating that silver is in a soluble form (Figure 6).

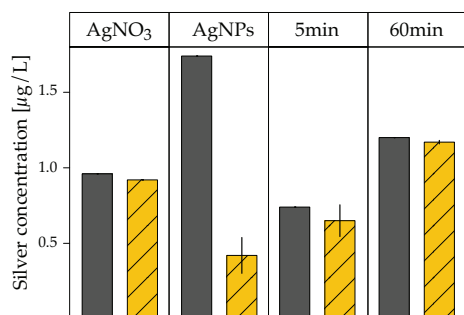


Figure 6: Concentration of silver in solutions amended with AgNO₃ (AgNO₃), with 5nm PVP-AgNPs (AgNP) or incubated for 5 or 60 min with gel pucks containing 5 nm PVP-AgNPs (5min, 60min). Silver concentration were measured prior (plain bar) and after (hatched bar) ultracentrifugation. Error bars on the yellow bars represent replicate ultracentrifugation runs.

Hence, the rapid release of Ag from the AgNPs cannot be attributed to an experimental artifact of physical loss of AgNPs from the gel but rather is likely due to the release of sorbed Ag^+ species from the surface of Ag nanoparticles. The presence of chemisorbed Ag^+ at the surface of AgNPs under oxic conditions is well documented^{5, 32} and the desorption of Ag^+ upon incubation of these AgNPs in Ag-free oxic or anoxic aqueous solution is expected as a result of mass action.

2.3.3 Role of the aqueous chemical composition in Ag release

When comparing the two river sites, we note that R2 displays the sustained loss of Ag beyond the first time point for the smaller (5 and 10 nm) AgNPs but that R1 does not. We hypothesize that oxidative dissolution is more rapid in R2 than in R1 and that these differences in the chemical composition of the two river waters account for this disparity in behavior. To evaluate this hypothesis, we compared the major ion and organic carbon (TOC) content of both waters (Figure S5). We found that sodium, chloride and TOC were present in higher concentrations in R2 water. We chose to evaluate the impact of sodium chloride on oxidative dissolution, and therefore compared the release of Ag from PVP-coated AgNPs embedded in gel pucks incubated in R1 water to those incubated in R1 water amended with 25 mg/L NaCl at 10°C. Overall, we observe little difference in the release of Ag^+ between the two conditions for up to 2 weeks (Figure 7). After two weeks, the soluble silver in solution reached an equilibrium corresponding to 40-50% of total silver in the gel pucks, hence no additional increase in silver was measured.

This result points to factors other than NaCl as being important in explaining differences between R1 and R2. We propose that natural organic matter (NOM) measured as TOC (Figure S5) rather than NaCl content may be a critical parameter in Ag release in these freshwaters. However, complementary experiment should be carried out to answer that hypothesis.

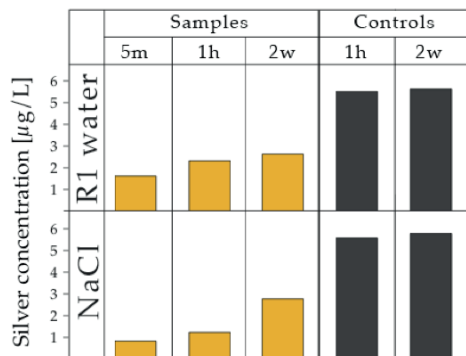


Figure 7: Ag released from gel pucks containing 5 nm PVP AgNPs (Samples) exposed to filtered R1 water unaltered or amended with NaCl after an incubation of 5 min, 1 hour, and 2 weeks. An Ag_2SO_4 solution serves as silver ions control (Controls).

2.3.4 *Role of AgNP coating on Ag release*

The final observation gleaned from the field deployment is that there are significant differences in Ag release from AgNPs depending on the surface coating. Notably, a citric acid coating leads to lower Ag loss as compared to a PVP or tannic acid coating (Figures 1-3). Similar observations have emerged from several studies. A comparison of citric acid- and PVP-coated AgNPs showed that PVP-coated AgNPs (8 nm) released almost an order of magnitude higher Ag concentration than citrate-coated AgNPs of comparable size (7 nm)³⁶. There appear to be several mechanisms by which the surface coating impacts AgNP dissolution. In the case of citrate, Ag⁺ binding to the carboxylic groups of the organic acid has been proposed¹² as a process that leads to the retention of Ag⁺, hence lowering solubility. Additionally, citrate may act as a reducing agent at the AgNP surface, reducing the oxide layer back to zerovalent Ag and decreasing solubility³⁵.

2.3.5 *Environmental implications*

The present work focuses on observing the release of Ag⁺ from AgNPs in natural waters under field conditions. Extensive Ag loss was documented for small (5 nm) AgNPs but complete dissolution was not observed over the course of 4 months. Less Ag loss was observed for larger AgNPs with more variability in the extent of loss as a function of the deployment site. Complementary laboratory experiment revealed that the initial and dominant process releasing silver was the desorption of chemisorbed Ag⁺ from the surface of AgNPs. Oxidative dissolution also likely plays a role but is a slower process. Overall, AgNPs are expected to persist in the environment at least on the order of a year but larger AgNPs and those coated with citrate would persist the longest.

The results from this study suggest that AgNPs should continue to be studied as nanomaterials in the environment since they will be present in that form at least for the medium term. Hence, research aiming at differentiating between AgNP- and Ag⁺-mediated toxicity mechanisms remains very important.

2.4 Associated Content

Details of temperature control experiment, deployment sites and materials, TEM micrograph and DLS measurements of AgNPs used in this study, IC water composition, measurements of water DO, pH and temperature and calculation of silver ions fraction released.

2.5 Acknowledgments

We would like to thank Jean-Luc Loizeau and Neil Graham from Institute Cipel in Versoix for their help in lake deployments; Daniel S. Alessi and Leia Falquet for their help on deploying and retrieving samples in the rivers. Also, we are grateful to the “inspection de la pêche du canton de Vaud” for allowing the deployment of AgNPs. Finally, we would like to thank Ruud Hovius from Horst Vogel’s Laboratory (LCPPM EPFL) for providing us with ultracentrifugation help and materials.

2.6 References

- (1) Woodrow Woodrow Wilson Center: Project on Emerging Nanotechnologies Inventory. http://www.nanotechproject.org/inventories/consumer/analysis_draft/.
- (2) Luoma, S. N. Silver Nanotechnologies and the environment: old problems or new challenges. <http://www.nanotechproject.org/publications/archive/silver/>.
- (3) Sotiriou, G. A.; Pratsinis, S. E., Antibacterial Activity of Nanosilver Ions and Particles. *Environmental Science & Technology* **2010**, *44* (14), 5649-5654.
- (4) Sharma, V. K.; Yngard, R. A.; Lin, Y., Silver nanoparticles: Green synthesis and their antimicrobial activities. *Advances in Colloid and Interface Science* **2009**, *145* (1-2), 83-96.
- (5) Lok, C. N.; Ho, C. M.; Chen, R.; He, Q. Y.; Yu, W. Y.; Sun, H.; Tam, P. K. H.; Chiu, J. F.; Che, C. M., Silver nanoparticles: partial oxidation and antibacterial activities. *Journal of Biological Inorganic Chemistry* **2007**, *12* (4), 527-534.
- (6) Marambio-Jones, C.; Hoek, E., A review of the antibacterial effects of silver nanomaterials and potential implications for human health and the environment. *Journal of Nanoparticle Research* **2010**, *12* (5), 1531-1551.
- (7) Benn, T. M.; Westerhoff, P., Nanoparticle Silver Released into Water from Commercially Available Sock Fabrics. *Environmental Science & Technology* **2008**, *42* (11), 4133-4139.
- (8) Durán, N.; Marcato, P.; Alves, O.; Da Silva, J.; De Souza, G.; Rodrigues, F.; Esposito, E., Ecosystem protection by effluent bioremediation: silver nanoparticles impregnation in a textile fabrics process. *Journal of Nanoparticle Research* **2010**, *12* (1), 285-292.
- (9) Gottschalk, F.; Nowack, B., The release of engineered nanomaterials to the environment. *Journal of Environmental Monitoring* **2011**, *13* (5), 1145-1155.
- (10) Kim, B.; Park, C. S.; Murayama, M.; Hochella, M. F., Discovery and Characterization of Silver Sulfide Nanoparticles in Final Sewage Sludge Products. *Environmental Science & Technology* **2010**, *44* (19), 7509-7514.
- (11) Blaser, S. A.; Scheringer, M.; MacLeod, M.; Hungerbühler, K., Estimation of cumulative aquatic exposure and risk due to silver: Contribution of nano-functionalized plastics and textiles. *Science of The Total Environment* **2008**, *390* (2-3), 396-409.
- (12) Liu, J. Y.; Hurt, R. H., Ion Release Kinetics and Particle Persistence in Aqueous Nano-Silver Colloids. *Environmental Science & Technology* **2010**, *44* (6), 2169-2175.
- (13) Ma, R.; Levard, C.; Marinakos, S. M.; Cheng, Y. W.; Liu, J.; Michel, F. M.; Brown, G. E.; Lowry, G. V., Size-Controlled Dissolution of Organic-Coated Silver Nanoparticles. *Environmental Science & Technology* **2012**, *46* (2), 752-759.
- (14) Lubick, N., Nanosilver toxicity: ions, nanoparticles-or both? *Environmental Science & Technology* **2008**, *42* (23), 8617-8617.
- (15) Park, E. J.; Yi, J.; Kim, Y.; Choi, K.; Park, K., Silver nanoparticles induce cytotoxicity by a Trojan-horse type mechanism. *Toxicology in Vitro* **2010**, *24* (3), 872-878.
- (16) Zhang, W.; Yao, Y.; Sullivan, N.; Chen, Y. S., Modeling the Primary Size Effects of Citrate-Coated Silver Nanoparticles on Their Ion Release Kinetics. *Environmental Science & Technology* **2011**, *45* (10), 4422-4428.
- (17) Fabrega, J.; Renshaw, J. C.; Lead, J. R. In *Silver nanoparticles in natural waters: behaviour and impact on bacterial communities*, Water - how need drives research and research underpins solutions to world-wide problems, University of Birmingham, Birmingham UK, 2008; University of Birmingham, Birmingham UK, **2008**; pp 1-3.
- (18) Navarro, E.; Piccapietra, F.; Wagner, B.; Marconi, F.; Kaegi, R.; Odzak, N.; Sigg, L.; Behra, R., Toxicity of silver nanoparticles to *Chlamydomonas reinhardtii*. *Environmental Science & Technology* **2008**, *42* (23), 8959-64.
- (19) Neal, A. L., What can be inferred from bacterium-nanoparticle interactions about the potential consequences of environmental exposure to nanoparticles? *Ecotoxicology* **2008**, *17* (5), 362-71.
- (20) Cumberland, S. A.; Lead, J. R., Particle size distributions of silver nanoparticles at environmentally relevant conditions. *Journal of Chromatography A* **2009**, *1216* (52), 9099-9105.
- (21) Fabrega, J.; Fawcett, S. R.; Renshaw, J. C.; Lead, J. R., Silver nanoparticle impact on bacterial growth: effect of pH, concentration, and organic matter. *Environmental Science & Technology* **2009**, *43* (19), 7285-90.
- (22) Gao, J.; Youn, S.; Hovsepian, A.; Llana, V. L.; Wang, Y.; Bitton, G.; Bonzongo, J.-C. J., Dispersion and Toxicity of Selected Manufactured Nanomaterials in Natural River Water Samples: Effects of Water Chemical Composition. *Environmental Science & Technology* **2009**, *43* (9), 3322-3328.

- (23) Dror-Ehre, A.; Mamane, H.; Belenkova, T.; Markovich, G.; Adin, A., Silver nanoparticle - *E. coli* colloidal interaction in water and effect on *E. coli* survival. *Journal of Colloid and Interface Science* **2009**, *339* (2), 521-6.
- (24) El Badawy, A. M.; Silva, R. G.; Morris, B.; Scheckel, K. G.; Suidan, M. T.; Tolaymat, T. M., Surface Charge-Dependent Toxicity of Silver Nanoparticles. *Environmental Science & Technology* **2011**, *45* (1), 283-287.
- (25) Fabrega, J.; Renshaw, J. C.; Lead, J. R., Interactions of Silver Nanoparticles with *Pseudomonas putida* Biofilms. *Environmental Science & Technology* **2009**, *43* (23), 9004-9009.
- (26) Morones, J. R.; Elechiguerra, J. L.; Camacho, A.; Holt, K.; Kouri, J. B.; Ramirez, J. T.; Yacaman, M. J., The bactericidal effect of silver nanoparticles. *Nanotechnology* **2005**, *16* (10), 2346-2353.
- (27) Choi, O.; Hu, Z., Size dependent and reactive oxygen species related nanosilver toxicity to nitrifying bacteria. *Environmental Science & Technology* **2008**, *42* (12), 4583-8.
- (28) Su, H. L.; Chou, C. C.; Hung, D. J.; Lin, S. H.; Pao, I. C.; Lin, J. H.; Huang, F. L.; Dong, R. X.; Lin, J. J., The disruption of bacterial membrane integrity through ROS generation induced by nanohybrids of silver and clay. *Biomaterials* **2009**, *30* (30), 5979-5987.
- (29) Kittler, S.; Greulich, C.; Diendorf, J.; Köller, M.; Epple, M., Toxicity of Silver Nanoparticles Increases during Storage Because of Slow Dissolution under Release of Silver Ions. *Chemistry of Materials* **2010**, *22* (16), 4548-4554.
- (30) Ho, C. M.; Yau, S. K. W.; Lok, C. N.; So, M. H.; Che, C. M., Oxidative Dissolution of Silver Nanoparticles by Biologically Relevant Oxidants: A Kinetic and Mechanistic Study. *Chemistry – An Asian Journal* **2010**, *5* (2), 285-293.
- (31) Liu, J. Y.; Sonshine, D. A.; Shervani, S.; Hurt, R. H., Controlled Release of Biologically Active Silver from Nanosilver Surfaces. *Acs Nano* **2010**, *4* (11), 6903-6913.
- (32) Henglein, A., Colloidal silver nanoparticles: Photochemical preparation and interaction with O₂, CCl₄, and some metal ions. *Chemistry of Materials* **1998**, *10* (1), 444-450.
- (33) Zook, J. M.; Long, S. E.; Cleveland, D.; Geronimo, C. L. A.; MacCuspie, R. I., Measuring silver nanoparticle dissolution in complex biological and environmental matrices using UV-visible absorbance. *Analytical and Bioanalytical Chemistry* **2011**, *401* (6), 1993-2002.
- (34) Jin, X.; Li, M.; Wang, J.; Marambio-Jones, C.; Peng, F.; Huang, X.; Damoiseaux, R.; Hoek, E. M. V., High-Throughput Screening of Silver Nanoparticle Stability and Bacterial Inactivation in Aquatic Media: Influence of Specific Ions. *Environmental Science & Technology* **2010**, *44* (19), 7321-7328.
- (35) Li, X.; Lenhart, J. J.; Walker, H. W., Aggregation Kinetics and Dissolution of Coated Silver Nanoparticles. *Langmuir* **2012**, *28* (2), 1095-1104.
- (36) Yang, X. Y.; Gondikas, A. P.; Marinakos, S. M.; Auffan, M.; Liu, J.; Hsu-Kim, H.; Meyer, J. N., Mechanism of Silver Nanoparticle Toxicity Is Dependent on Dissolved Silver and Surface Coating in *Caenorhabditis elegans*. *Environmental Science & Technology* **2012**, *46* (2), 1119-1127.

2.7 Supporting Information

S1: Control of temperature on AgNPs stability

Low-melt agarose requires a temperature of about 60 °C to melt. We considered the potential effect of that temperature on the release of Ag from AgNPs by exposing a suspension of AgNPs (1,000 µg/L) to 60 °C for 10 min in a water bath followed by cooling on ice to mimic the process of gel puck preparation. The concentration of Ag⁺ released was evaluated by ultrafiltration (Amicon Ultra-15 3K centrifugal units, Merck-Millipore). A 10°C control was carried at the same time. No additional release of silver was measured at the higher temperature. Therefore, the gel puck preparation cannot explain the loss observed in the field.

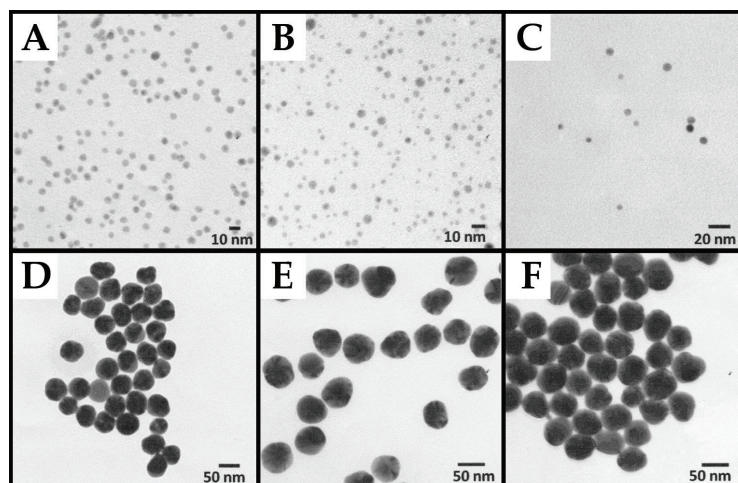


Figure S1: TEM micrograph of AgNPs used in the study: PVP-AgNPs (A, D), Tan-AgNPs (B, E), Cit-AgNPs (C, F), 5 nm (A, B), 10 nm (C) and 50 nm (D, E, F).

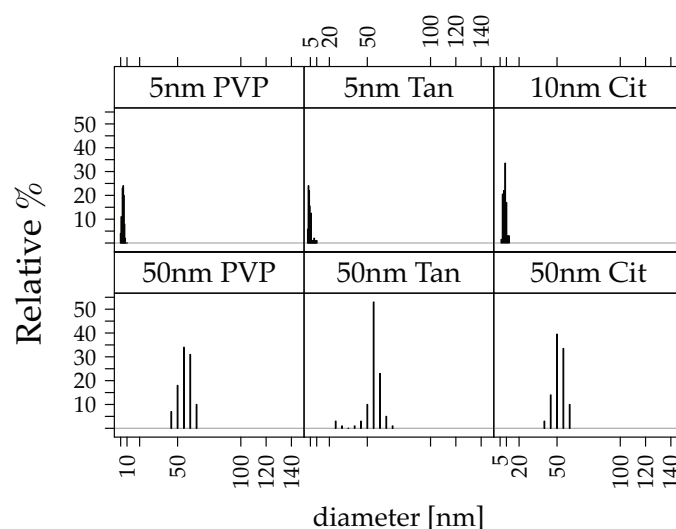


Figure S2: DLS measurements of AgNPs used in this study

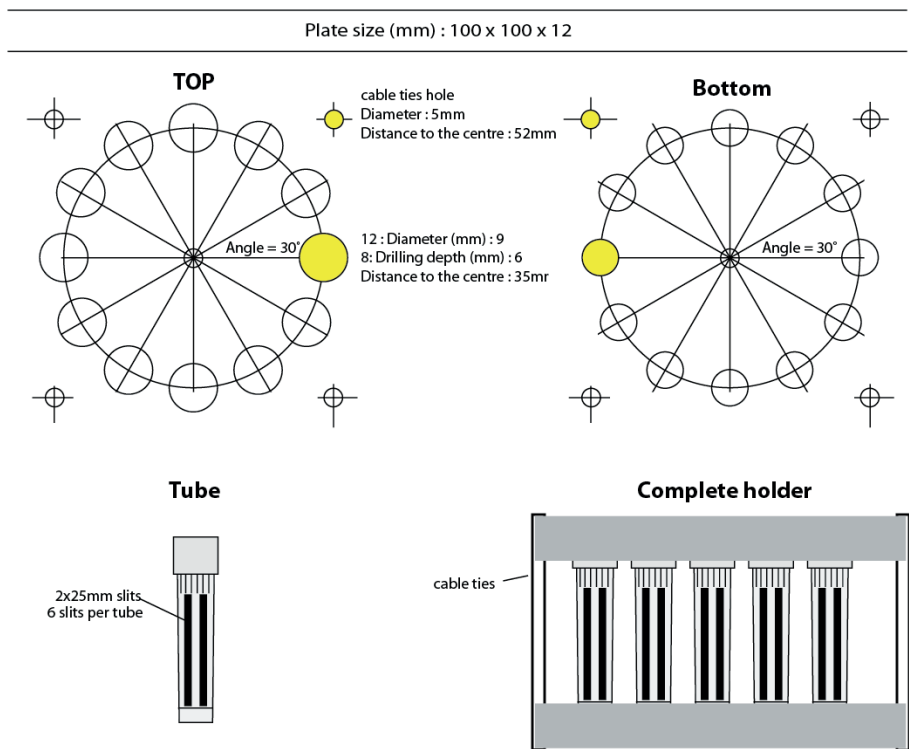


Figure S3: Schematic of deployment tubes and holders. The top two figures show the top and bottom plates of the polypropylene holder for river and lake deployment. Bottom right, tube drawing with 6 slits in the side and bottom right a schematic of the complete assembly.

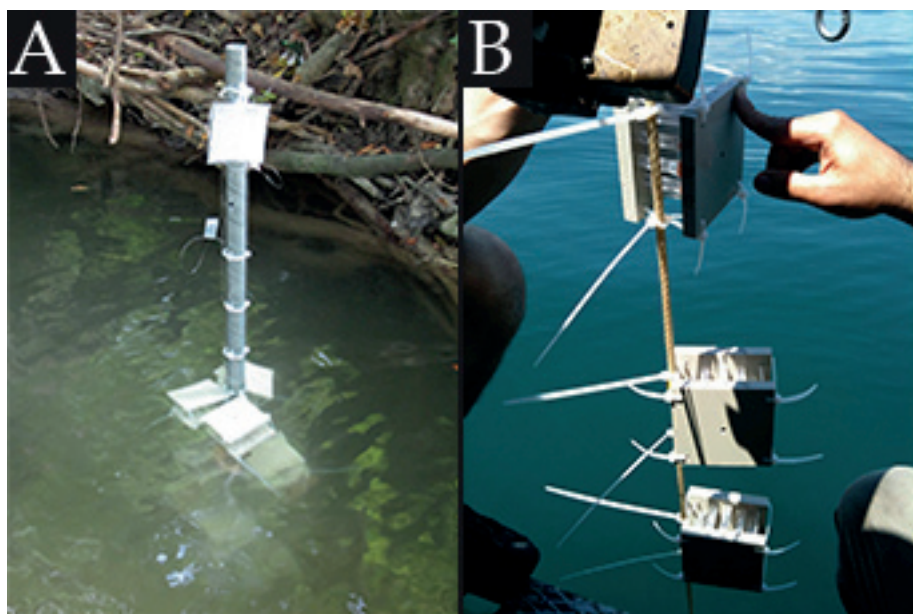


Figure S4: picture of deployment system in river (A) and Lake (B).

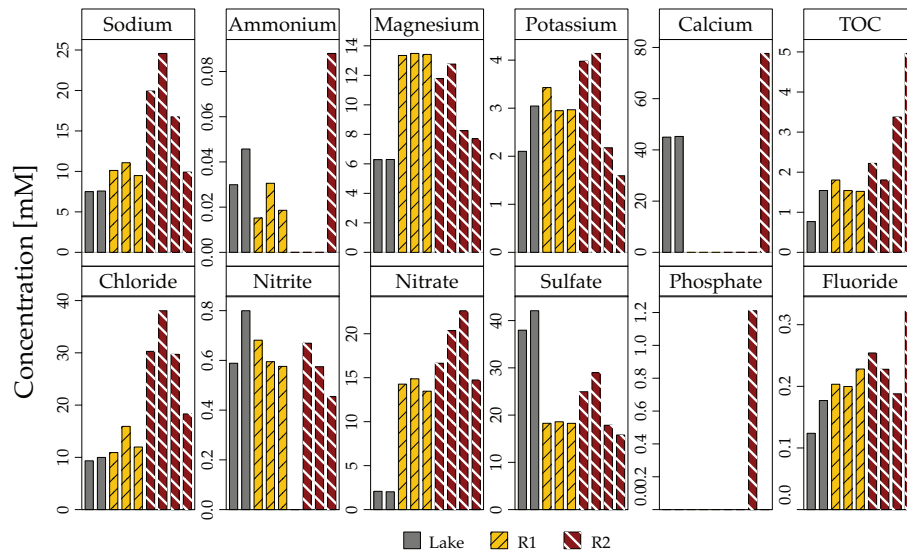


Figure S5: Composition of water collected at the time of retrieval of AgNPs. Ordinate units are concentration of respective compound in mM except for TOC that is in mg/L.

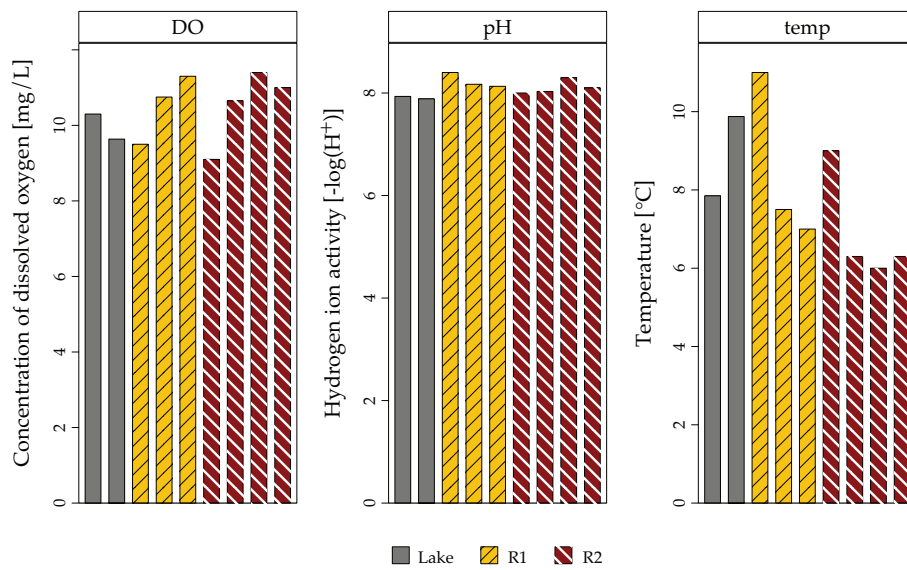


Figure S6: Measured dissolved oxygen (DO), pH and temperature (temp) at deployment and retrieval time for lake, R1 and R2 waters.

Table S1: Calculated fraction of silver ions released from PVP coated AgNPs surface for particles of 5 and 50nm

	5nm	50nm
Atomic radius of silver [nm]	0.144	
Surface Area (SA) of a silver atom [nm ²]	0.066	
Atomic Weight of silver [g/mol]	107.9	
Ag⁺ lost		
Concentration in water [μg/L]	2.0	0.5
Volume of water[L]		0.2
Amount of Ag in water after desorption [μmol]	0.004	0.001
Number of Ag⁺ ions on SA in gel		
NPs diameter measured by TEM [nm]	6.5	53.4
SA of AgNPs in gel [nm ²]	1.41E ⁺¹⁴	1.41E ⁺¹³
Number of Ag ⁺ ions on AgNP in gel	2.14E ⁺¹⁵	2.14E ⁺¹⁴
Amount of Ag potentially sorbed [μmol]	0.167	0.017
Fraction of Ag ⁺ released from the surface [%]	2.2	5.6

Chapter

3 Silver nanoparticle toxicity to *Escherichia coli* and *Bacillus subtilis*

J. Dobias and R. Bernier-Latmani

Abstract: With the increased use of silver nanoparticles (AgNPs) as a biocidal in consumer product materials, there is a growing concern about their expected release in the environment as they could potentially impact aquatic microbial communities. It is therefore of utmost importance to understand the factors governing AgNP toxicity. Here we chose to study the role of AgNP size and coating on the toxicity response of two bacterial strains with distinct characteristics: *Escherichia coli* (Gram-negative) and *Bacillus subtilis* (Gram-positive). We adopted a systematic approach, which we felt was missing from previous studies and tested AgNPs of various sizes (5, 10, 20, 50 and 100 nm) and exhibiting one of three surface coatings (polyvinylpyrrolidone [PVP-], tannic acid [Tan-] and citric acid [Cit-]). The chosen bacteria showed a distinct sensitivity to AgNPs toxicity with *E. coli* being the most sensitive. The toxicity response was shown to be dependent on the AgNPs size. The small NPs were the most toxic. The effect of the capping agent was also notable and Cit-AgNPs were shown to be much less toxic than PVP- or Tan-AgNPs. We also evaluated the mode of toxicity and proposed that Cit-AgNPs act via direct interaction to locally dispense large doses of Ag⁺ that potentially damage the membrane (i.e., the Trojan horse effect) whereas PVP- and Tan-AgNPs were more likely to act via the release of silver ions.

Keywords: Silver, nanoparticles, toxicity, *Escherichia coli*, *Bacillus subtilis*, polyvinylpyrrolidone, tannic, citrate

3.1 Introduction

The nanomaterials market was valued at \$15 billion in 2011 and is expected to reach \$37 billion in 2017¹. The contribution of silver was about \$290 million in 2011 with an expected growth to around \$1.2 billion in 2016². At the end of 2011, around 1,300 consumer goods were referenced as nanomaterial-containing products and present in almost any consumer good category from households to electronics³. Among the numerous nanomaterials, silver nanoparticles (AgNPs) represent the major fraction of available products^{3,4} and is used most often for its antimicrobial properties⁵⁻⁷, though its electric, optical and catalytic properties are of interest as well⁸. As a result, it is expected that some of these products will release AgNPs in the environment during their production, useful life or upon final disposal^{9,10}. Because AgNPs are antimicrobial¹¹, there is growing concern that their release into the environment would have an effect on microbes, significantly impacting the microbial communities in natural aquatic ecosystems^{12,13}.

Environmental conditions (pH, ionic strength, background electrolyte and exposure time) are key factors for AgNPs toxicity to bacteria¹⁴⁻²². Changes in the values of those parameters may lead to changes in aggregation^{17,18} and surface charge²⁰, which may in turn impact toxicity. Their effect, however, is mostly dependent of the NP surface characteristics, which underscores the importance of the capping agent in the behavior of AgNPs in the environment and with respect to bacterial toxicity²³.

Three mechanisms of AgNPs biocidal activity are documented in the literature: (1) Gradual release of silver ions from AgNPs^{5,15,24,25}. Previous studies have shown that AgNPs had the potential to serve as a source of Ag⁺ under oxic conditions either via direct release or as carriers for chemisorbed silver ions^{7,26,27}. The release of ionic silver has been shown to be dependent on AgNPs size^{27,28} and to correlate with the size-dependent toxicity observed in some cases^{5,29}. (2) Damage of the cell membrane by direct association with AgNPs^{23,30-34} or uptake of AgNPs (<10 nm)³¹ and (3) generation of reactive oxygen species^{29,35-38}.

A recent study described a surface area-related toxicity for phosphate-AgNPs to *E. coli*³⁹. The authors showed that the concentrations required for complete growth inhibition with the three sizes of AgNPs tested (20, 50 and 100 nm) corresponded to the same total surface area of 1E¹⁸ nm²/L. However that correlation did not hold for the model eukaryotic system considered: zebrafish embryos (*Danio rerio*).

Even though environmental relevance is claimed by most of the published studies, a closer look suggests that few investigations utilized natural or synthetic fresh/marine water. Two previous studies considered AgNP toxicity in natural systems (i.e., estuarine sediments)^{40,41}, and an additional one evaluated toxicity in a microcosm⁴². Other

recent studies also utilized natural and synthetic freshwater⁴³⁻⁴⁷ to probe the stability (aggregation and dissolution) of AgNPs. What is still lacking in the literature is a systematic study of the role of size and capping agent on the toxicity of AgNPs to bacteria under environmentally relevant conditions.

In this work, we used 14 AgNPs of discrete sizes (5, 10, 20, 50 and 100 nm) and surface coatings (polyvinylpyrrolidone (PVP), tannic acid and citric acid) and tested their toxicity potential on two laboratory bacterial strains (*Escherichia coli*, a Gram-negative and *Bacillus subtilis*, a Gram-positive bacterium) grown in synthetic lake water.

3.2 Materials and methods

3.2.1 Bacterial strains and growth conditions

The two lab strains, *Escherichia coli* K-12 (DSM-No. 498) and *Bacillus subtilis* (DSM-No. 23778), used in this study were purchased from DSMZ. Bacterial cultures were grown aerobically at 30°C under continuous shaking at 140 rpm in liquid Luria-Bertani (LB) broth [tryptone (10 g/L), sodium chloride (10 g/L), yeast extract (5 g/L)] or in artificial lake water (see below for composition) in Erlenmeyer flasks (250 mL) containing 100 mL of medium unless otherwise stated. LB broth inoculation were done with glycerol stock aliquots of 100 µL maintained at -80°C.

3.2.2 Silver nanoparticles

Spherical silver nanoparticles of various sizes and surface coatings were considered in this study: 5, 10, 20, 50 and 100 nm polyvinylpyrrolidone (PVP)-coated AgNPs (actual sizes in nm: 6.5 ± 0.8 , 7.7 ± 1.6 , 20.4 ± 1.8 , 53.4 ± 5.0 , 111.2 ± 8.1 nm); 5, 10, 20, 50 and 100 nm tannic (Tan) acid-coated AgNPs (4.3 ± 1.3 , 7.9 ± 1.2 , 21.7 ± 2.3 , 52.1 ± 7.1 , 95.8 ± 8.4) and 10, 20, 50 and 100 nm citric-acid (Cit) coated AgNPs (8.2 ± 1.2 , 19.2 ± 2.2 , 49.1 ± 4.5 , 99.1 ± 8.2 nm) were obtained from nanoComposix (San Diego, CA) as aqueous suspension and characterized by TEM and DLS (Figure S1 and S2).

3.2.3 Medium composition

A defined medium, Artificial Lake Water (ALW), whose composition was based on the composition of Lake Geneva water (courtesy of Felipe de Alencastro, EPFL) was developed. Its composition is the following (µmol/L): CaSO₄ (345.96), NaCl (99.22), Mg(C₂H₃O₂)₂ (24.87), MgSO₄ (15.77), KCl (19.55), MgCl₂ (7.32), Mg(NO₃)₂ (3.05), K₂HPO₄ (0.12), (NH₄)₂SO₄ (0.012), NaNO₂ (0.022). A 1,000x concentrate of all components (except CaSO₄) was prepared as a stock and diluted to obtain the medium.

The medium was prepared by autoclaving CaSO₄, at double the target concentration (691.92 µmol/L) in 18MΩ·cm water to ensure reasonably rapid and complete solubilization. The CaSO₄ solution was amended with the medium stock (1x final concentration), lactate (5 mM), acetate (5 mM), glucose (3 g/L) and additional 18MΩ·cm water. The pH was adjusted to a value of 8.0 with NaOH. Finally, the solution was filter-sterilized with a 0.22 µm pore size filter (GPWP 47 mm, Merck Millipore, Billerica, MA) immediately prior use.

3.2.4 *Screening experiments*

Measurements intended to screen for conditions where toxicity to bacteria was detectable were carried out with a Synergy MX microplate reader from Bio-Tek (Winooski, VT, USA) using transparent 96 well plates (300 μ L flat bottom). ALW (100 mL) was inoculated ($OD_{600} = 0.015-0.020$) with an overnight culture of bacteria grown in Luria Bertani medium at 30°C and incubated with shaking (140 rpm) for 1-2 hours at 30°C to allow the bacteria to adapt to the new medium prior to challenging them with AgNPs. Once measurable growth was detected ($OD_{600} = 0.03-0.04$) 150 μ L of culture was amended to each well that already contained 150 μ L of ALW and double the target concentration of AgNPs. The continuous shaking of the 96-well plate was interrupted every five minutes for collection of an OD_{600} reading for each well.

3.2.5 *Batch experiments*

Bacteria from an overnight culture (LB, 30°C, 140 rpm) were used to inoculate 100 mL of ALW (to a final $OD_{600} = 0.02$) in 250 mL baffled Erlenmeyers flasks. The flasks were incubated for 1-2h (30°C, 140 rpm) to allow for growth prior to the amendment of AgNPs.

3.2.6 *AgNP characterization*

Hydrodynamic radii and surface charge were measured by dynamic light scattering (DLS) and zeta potential respectively using a Malvern Instruments Zetasizer Nano ZS (Westborough, MA, USA). DLS measurements were done in 173° backscatter mode. Samples were resuspended with a manual pipettor immediately prior to measurement in order to avoid artifacts from aggregate sedimentation.

3.2.7 *Analytical approaches*

Silver in solution was measured by ICP-MS on a Perkin Elmer DRCII system. Samples and standards were prepared in 0.5% HNO_3 (final concentration).

3.3 Results and discussion

In order to compare the toxicity of the 14 different AgNPs we used in this study, we elected to first screen for the effect of various Ag concentrations on growth using a 96-well microplate reader. This allowed the identification of the AgNPs sizes, coatings and concentrations that resulted in toxicity to bacterial cultures. Those conditions could then be investigated in more detail. The microplate experiments were carried out with two strains: the Gram-negative bacterium *Escherichia coli* and the Gram-positive bacterium *Bacillus subtilis*. Figures 1 and 2 clearly show that: (1) the two strains have distinct sensitivities to AgNPs with *E. coli* being more sensitive than *B. subtilis*; (2) toxicity is dependent of AgNP size with small AgNPs being the most toxic; and (3) AgNPs coating significantly impacts the toxicity and results in the following order from most to least toxic: tannic-AgNPs, PVP-AgNPs and citric-AgNPs.

El Badawy and coworkers²³ also found a difference in toxicity between PVP- and citric-AgNPs (with PVP being more toxic than citric-AgNPs) that they attributed to the NP surface charge. To test the hypothesis that surface charge is linked to toxicity, we measured the zeta potential of the three types of AgNPs (table S1) and found that tannic-AgNPs, the most toxic NPs, have the least negative charge whereas citric-AgNPs, the least toxic NPs, show the most negative charge. PVP-AgNPs display an intermediate value. Our results provide evidence for a role for surface charge in AgNP toxicity and underscore the importance of surface coatings and the attendant link with electrostatic charge for the toxicity of AgNPs to bacteria.

Surface area has been mentioned as a potential determinant of AgNPs toxicity³⁷ instead of mass concentration. Hence, we tested the toxicity of AgNPs to *E. coli* as a function of surface area across the range of sizes of our AgNPs (5-100 nm) for PVP- and tannic-AgNPs (Figure S3). We considered several constant surface areas (assuming no aggregation) across all sizes by varying the concentration of AgNPs. We observed that the same surface area did not yield the same effect when particle size varied. Large AgNPs were more toxic than small ones due to the higher overall Ag concentration required to achieve the same surface area. Thus, our results suggest that toxicity is not a surface area-related process for the AgNPs tested. Citric-AgNPs and *Bacillus subtilis* were not tested, as they would have required concentrations higher than 1 mg/L that we considered to be outside the range of environmental relevance. Bowman *et al.*³⁹ reported that the toxicity of phosphate-coated AgNPs of 20, 50 and 110 nm correlates with the total surface area for *E. coli* but not for zebrafish. There is not necessarily a contradiction between these results and our study with respect to the role of surface area in AgNPs toxicity. The difference is attributable to the distinct capping agents used: they studied PO₄-AgNPs while we considered PVP-, Tan-, Cit-AgNPs.

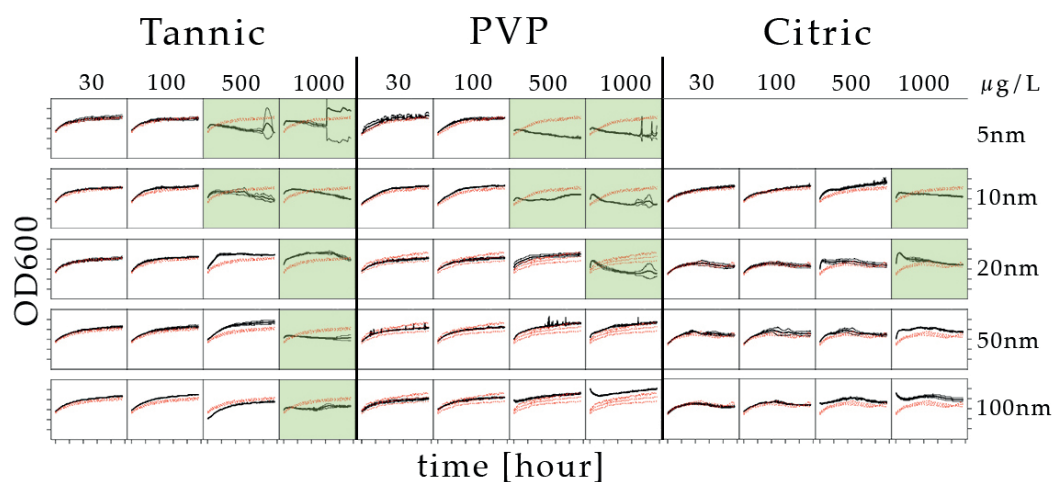


Figure 1: Microplate screening experiment for *E. coli* exposed to tannic-AgNPs, PVP-AgNPs, citric-AgNPs or to no silver (red dotted curves). Nanoparticle sizes are indicated on the right-hand side (5, 10, 20, 50 and 100 nm) and concentrations are 30, 100, 500 and 1000 $\mu\text{g/L}$ for each surface coating. Each individual panel represents the growth (OD_{600}) as a function of time (hours). Y-axis tick value (OD_{600}) = 0.00, 0.02, 0.04, 0.06, 0.08; x-axis ticks value (hours) = 5, 10, 15, 20, 25. Shaded Panels represent conditions inhibitory to growth. Detailed version of these plots can be found in figures S4-S7.

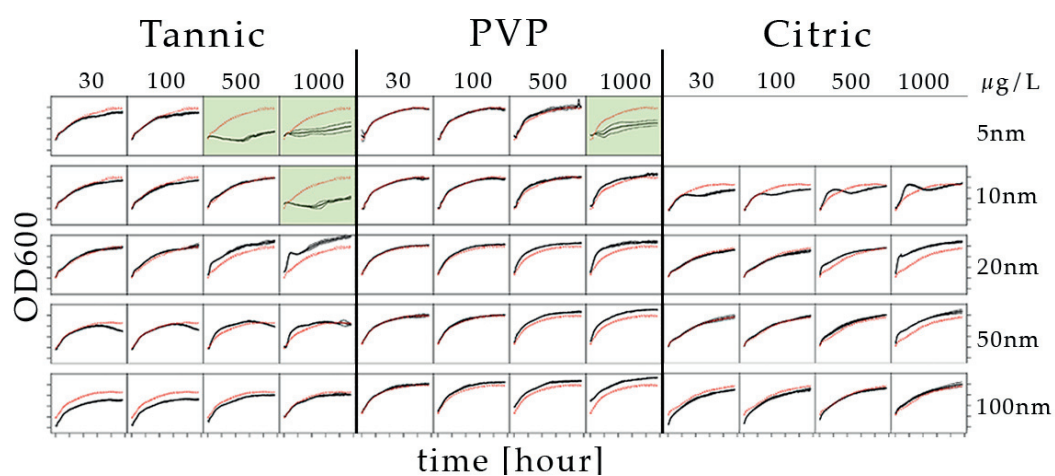


Figure 2: Microplate screening experiment for *B. subtilis* exposed to tannic-AgNPs, PVP-AgNPs, citric-AgNPs or to no silver (red dotted curves). Nanoparticle sizes are indicated on the right-hand side (5, 10, 20, 50 and 100 nm) and concentrations are 30, 100, 500 and 1000 $\mu\text{g/L}$ for each surface coating. Each individual panel represents the growth (OD_{600}) as a function of time (hours). Y-axis tick value (OD_{600}) = 0.00, 0.02, 0.04, 0.06, 0.08; x-axis ticks value (hours) = 5, 10, 15, 20, 25. Shaded Panels represent conditions inhibitory to growth. Detailed version of these plots can be found in figures S8-S11.

However, surprisingly, Bowman *et al.*'s Ag^+ control is 20-40 fold less toxic than ours. That difference may be attributed to the difference in medium. The Bowman *et al.*³⁹ study used a phosphate buffer saline (PBS) rich in chloride (0.14 M) whereas the chloride concentration in our ALW medium was 0.01 M. The high concentration of Cl⁻ leads to the precipitation of AgCl(s) and to the retention of only 0.18% of the total Ag in solution⁴⁸. We suggest that AgCl precipitation is an explanation for the dichotomy between the two studies and is consistent with the findings of decreased Ag toxicity reported for AgNPs in estuarine sediment studies^{40,41}.

In order to gain a better understanding of the processes leading to AgNP toxicity, we selected specific conditions from the microplate screening experiments and repeated them in larger volumes (250 mL Erlenmeyer flask culture) that allowed sampling for soluble Ag measurements as well as following AgNP aggregation. We selected small (5PVP, 5Tan and 10Cit) AgNPs for both *E. coli* and *B. subtilis* as these sizes were the most toxic of the set as well as mid-sized (50 nm) AgNPs, the smallest size with no observable toxicity.

First, we set up a dose-response experiment by growing bacteria in the presence of AgNPs and plotting the change in OD₆₀₀ vs. the Ag concentration (Figure 3).

Similarly to the microplate results, we found that *B. subtilis* was more resistant to AgNPs (independently from size) than *E. coli* and that the small AgNPs were more toxic than the larger ones. Two small AgNPs, 5nm PVP- and 5nm tannic-AgNPs, had distinct toxicity for *E. coli* with tannic-AgNPs eliciting a toxic response at a concentration half of that causing the same response with PVP-AgNPs. However, the two AgNPs displayed a similar toxicity response for *B. subtilis*. The larger particles, 50nm PVP- and tannic-AgNPs, exhibited a similar toxicity profile for each bacterium with *B. subtilis* showing greater resistance than *E. coli*. Finally, citric acid-coated AgNPs had the lowest toxicity response of all the surface coatings to both *E. coli* and *B. subtilis*: 10 nm citric-AgNPs were toxic at a concentration two-fold greater than that at which tannic-AgNPs were toxic to *E. coli*. Neither 10 nm nor 50 nm citric-AgNPs were toxic to *B. subtilis* up to 2 mg/L. Surprisingly, the presence of 50 nm citric-AgNPs in a *B. subtilis* culture results in a decrease in the amount of bacterial growth OD₆₀₀ (Figure 3) but not in complete growth inhibition. A similar phenomenon was observed by El Badawy *et al.*²³: A 20% decrease in cell viability was reported in the presence of 10 nm citric AgNPs at concentrations as low as 1 µg/L but was not observed with uncoated or PVP-coated AgNPs.

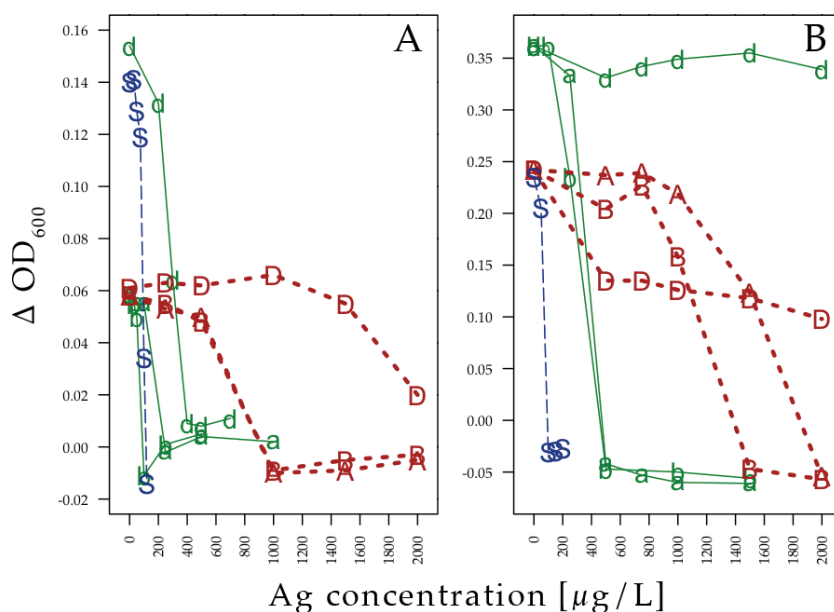


Figure 3: Dose-response curves of *E. coli* (A) and *B. subtilis* (B) to PVP-, tannic- and citric-AgNPs. Within the plots, the letters correspond to specific AgNPs: a, A= 5 and 50 nm PVP AgNPs, b, B=5 and 50 nm tannic AgNPs, d, D= 10 and 50 nm citric AgNPs. Green = small AgNPs, red = big AgNPs, blue = soluble silver. $\Delta OD_{600} = [OD_{600}]_{t24} - [OD_{600}]_{t0}$

The mode of action of AgNPs that leads to a toxicity response is still under debate and could either relate to a direct interaction of NPs with cells (i.e., Trojan horse effect) or to indirect toxicity resulting from the release of silver ions from the NPs^{5, 15, 24, 25}. In order to tackle this question, we measured soluble silver released from AgNPs suspended in the culture medium at concentrations inhibitory for bacterial growth (Figure 4) in the presence and in the absence of biomass. We observed that soluble silver was present at the first time point in the presence of *E. coli* and *B. subtilis* at concentrations ranging from 0.95 to 3.10 $\mu g/L$ for PVP-AgNPs and from 1.95 to 6.60 $\mu g/L$ for Tan-AgNPs and decreased rapidly to barely detectable levels after 24h. In contrast, citric acid-coated AgNPs released little Ag^+ (0.07 $\mu g/L$). This is consistent with a previous study in our laboratory showing that citric-AgNPs dissolve to a lesser extent than tannic- or PVP-AgNPs (Dobias *et al*, submitted). In the case of PVP- and tannic-AgNPs and *E. coli* or *B. subtilis*, the presence of soluble Ag^+ suggests that at least one of the mechanisms of toxicity may be through the soluble form of the metal. While the concentrations of Ag^+ are low (up to 6 $\mu g/L$) in comparison to those that elicit an inhibition of growth (Figure 3), Ag^+ may also be adsorbed onto cell biomass or precipitated on the cell surface. In the absence of biomass, the initial measured soluble silver was 35 and 58 $\mu g/L$ respectively for PVP- and Tan-AgNPs. However, in the case of citric-AgNPs, very low concentrations of Ag^+ are released even in the absence of biomass (2 $\mu g/L$).

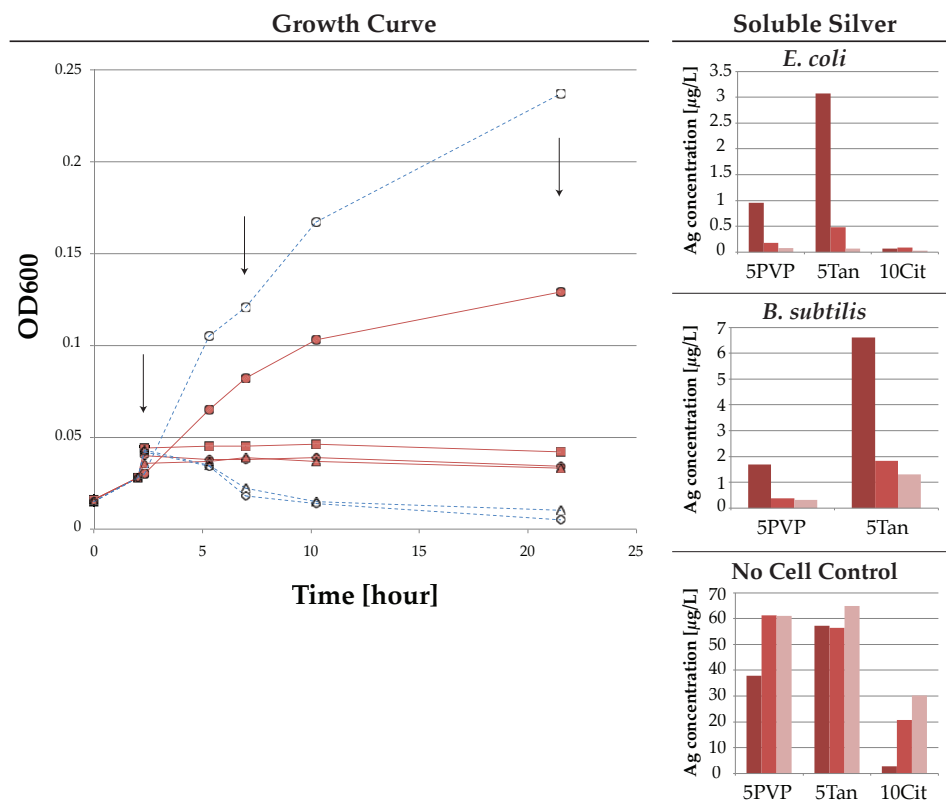


Figure 4: Measurements of bacterial growth for *E. coli* and *B. subtilis* with and without AgNPs (5nm PVP-, 5nm Tan-, 10nm Cit-AgNPs). *E. coli* was exposed to 5 nm PVP- and 5 nm Tan-AgNPs both at 250 µg/L and to 10 nm Cit-AgNPs at 500 µg/L. *B. subtilis* was exposed to 5 nm PVP- and 5 nm Tan-AgNPs at 500 µg/L. The presence of soluble silver was measured by ICP-MS at 1, 6 and 22 hours after inoculation with AgNPs (indicated by arrows). Column bars represent the soluble silver (in µg/L) for the three time points. For the growth curve, symbols are the following: *B. subtilis* (blue dashed lines- open symbols), *E. coli* (red lines – filled symbols); circles (bacteria - no AgNPs), diamonds (5nm PVP-AgNPs), triangles (5nm Tan-AgNPs) and square (10nm Cit-AgNPs)

Hence, the inhibitory mechanism preventing cell growth in the presence of citric-AgNPs (Figure 4) must involve a mechanism other than Ag^+ ion toxicity. We propose that the Trojan horse mechanism is predominant in this case: Ag^+ ions adsorbed onto the surface of the citric-AgNPs are delivered to the cells in a high, localized dose and result in toxicity. A common trend for Cit-AgNPs is to be less toxic than PVP-AgNPs to *E. coli* (this study), to *B. subtilis* (this study, El Badawy *et al.*²³) or to *Caenorhabditis elegans*⁴⁹. In *Nitrosomonas europaea*, however, Cit-AgNPs were shown to be more toxic than PVP-AgNPs⁵⁰. Our hypothesis that Ag^+ adsorbs onto Cit-AgNPs is supported by the observation that citrate has a potential for Ag^+ sorption⁴⁹ because of the formation of complexes between Ag^+ and the carboxylic groups of the organic acid²⁶. Even though Cit-AgNPs are negatively charged and theoretically should not associate with the negatively charged cell membrane, this interaction has been documented³⁰. Finally, Cit-AgNPs were shown to aggregate earlier than PVP-AgNPs⁴⁵

which may also explain their lower toxicity which was previously observed²³. We explore the aggregation potential of all three AgNPs in the next section.

Figure 4 shows a decrease in soluble silver over time. This decrease may be attributed to: (1) adsorption of Ag^+ to bacterial surfaces or to AgNPs aggregates or (2) reduction to Ag^0 . We collected samples from the same experiment as above at three time points 2, 6 and 24 hours and measured the AgNPs particle size distribution using DLS. Data were obtained within 40 minutes of sample collection. Figure 5 shows a clear trend for aggregation that is independent from NP or condition. In the absence of cells (Figure 5A, 5D and 5G), all AgNPs aggregate to final sizes of 150, 295 and 350 nm for PVP-, tannic- and citric-AgNPs respectively after 24 hours. We also observe that the capping agent on the AgNPs impacts aggregation potential with PVP showing the lowest aggregation. Its peak intensity and size in the absence of cells are smaller than in the two other cases.

Citric is the only AgNP to exhibit detectable aggregation after two hours with a broad spectrum that included peaks at 120 and 295 nm (Figure 5H). This could also explain its lower toxicity as compared to PVP and tannic AgNPs.

We also observed the effect of bacteria on NP aggregation. The presence of *E. coli* appears to inhibit aggregation. This is evident if one considers the particle size distribution of AgNPs in the presence and absence of *E. coli* (Figure 5A and 5B). In the *E. coli*-containing samples, peaks attributable to aggregates are either absent as for PVP-AgNPs or smaller than the no cell control in the case of Tan-AgNPs (Figure 5D and 5E). For PVP-AgNPs, the extent of aggregation in the presence of *B. subtilis* is comparable to that in its absence (Figure 5A and 5C).

In the presence of cit-AgNPs, an intermediary broad peak at 615nm at 6h and subsequently, a peak at 1,000 nm at 24 h may have suggested aggregation up to that size. However, the signal at 1,000 nm is a signature peak of bacterial cells. Hence, it is very unlikely that it would correspond to AgNPs aggregates in the case of cit-AgNPs only. Additionally, we observe that the bacterial cell peak is broader in the cit-AgNP than in the PVP- and Tan-AgNPs or the no silver control cases (data not shown). We suggest that the peaks detected at 615 and 1,000 nm for cit-AgNPs do not represent AgNP aggregates but rather cells displaying an unusual DLS profile due to the association of AgNPs with the cell membrane.

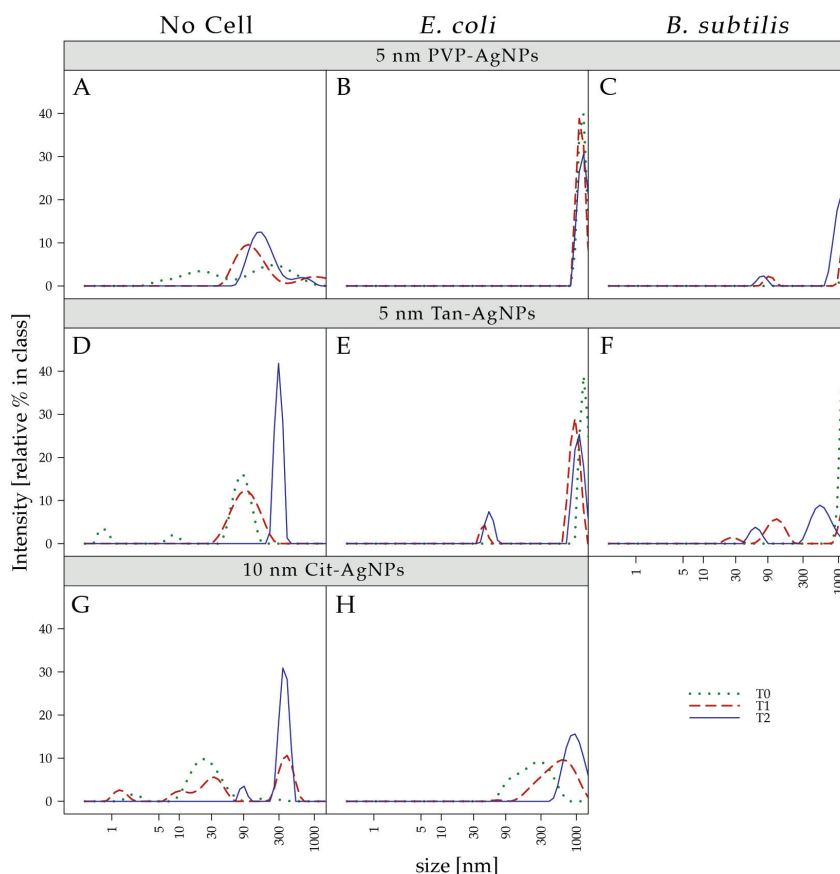


Figure 5: DLS measurements of AgNPs in ALW (no cell) and in a bacterial growth culture (*E. coli*, *B. subtilis*) at three time points (T0= 2h (green), T1=6h (red) and T2=24h (blue)) after inoculation. For *E. coli* and *B. subtilis* columns two and three, peaks at 1000 nm represent the cells.

Taken together, these results show that aggregation is likely to happen in most cases, independently of the condition but that aggregate size and aggregation speed are highly dependent on the coating, the microorganism and the medium.

The systematic approach of this study helped to explore in greater detail the toxicity of AgNPs to bacteria. Here we report a clear effect of the AgNP size, with small NPs being more toxic than large NPs, and of the capping agent with citrate coated AgNPs being considerably less toxic than PVP- and Tan-AgNPs. We suggest four major factors in the antimicrobial activity of silver nanoparticles: (1) bacterial species is the first important factor. We showed that *B. subtilis* is more resistant to AgNPs (but also to Ag^+) than *E. coli*. Their difference in cell wall composition could explain their different toxicity response, especially for Cit-AgNPs due to the direct membrane interaction invoked as a toxicity mechanism; (2) the surface charge of NPs correlates well with their toxicity. Cit-AgNPs are the most negatively charged (-40 mV) with a charge close to that of bacteria. It is therefore expected that these AgNPs should exhibit the lowest toxicity, which is what is observed; (3) the aggregation rate is also important. The relatively rapid aggregation of Cit-AgNPs as opposed to PVP- and Tan-AgNPs could

explain the lower toxicity as aggregates NPs are expected to behave similarly to large NPs and (4) the concentration of soluble silver was lower for Cit-AgNPs than for Tan- or PVP-AgNPs and DLS measurements showed signs of cell deformation of *E. coli* in the presence of Cit-AgNPs. Both these results strongly suggest that Cit-AgNPs are more likely to interact directly with bacterial cells (i.e., the Trojan horse effect^{51, 52}) whereas PVP- and Tan-AgNPs are more likely to be toxic through the release of soluble silver.

Findings in the study were revealing of the role of size and coating on toxicity as well as the role these parameters play in eliciting specific toxicity mechanisms. However, a significant limitation of the study remains that the microorganisms considered are not representative of environmental conditions. Hence, the next step is clearly to probe natural microbial communities for their toxicity response to AgNPs in order to obtain a more accurate understanding of the true environmental impact of AgNPs

3.4 Acknowledgments

We would like to thank the following people or institutes for providing us with help or access to instruments: Dr. L. F. De Alencastro (GR-CEL, EPFL) for lake Geneva water composition; the central environmental analytical laboratory (CEAL) for access to shaker-incubators, ICP-MS and ICP-OES; Dr. Lucas Bragazza (ECOS, EPFL) for access to the Synergy MX microplate reader and Prof. T. Kohn (LCE, EPFL) for access to the Malvern zetasizer nano zs.

We would also thank Prof. Massimo Trotta and Alessandra Costanza from the University of Bari for their help in the initial part of this study. We acknowledge COST Action CM0902 “Molecular machineries for ion translocation across biomembranes” for funding Alessandra Costanza’s visit as part of an STSM (Short Term Scientific Mission).

3.5 Reference:

- (1) BCC_Research Nanotechnology: A Realistic Market Assessment, NAN031E. <http://www.bccresearch.com/report/nanotechnology-market-applications-products-nan031e.html>.
- (2) Pistilli, M. Nanosilver Market Growth: Boon or Bust for Silver Prices. <http://silverinvestingnews.com/8575/nanosilver-market-growth-boon-or-bust-for-silver-prices.html>.
- (3) Woodrow Wilson Center: Project on Emerging Nanotechnologies Inventory. http://www.nanotechproject.org/inventories/consumer/analysis_draft/.
- (4) Luoma, S. N. Silver Nanotechnologies and the environment: old problems or new challenges. <http://www.nanotechproject.org/publications/archive/silver/>.
- (5) Sotiriou, G. A.; Pratsinis, S. E., Antibacterial Activity of Nanosilver Ions and Particles. *Environmental Science & Technology* **2010**, *44* (14), 5649-5654.
- (6) Sharma, V. K.; Yngard, R. A.; Lin, Y., Silver nanoparticles: Green synthesis and their antimicrobial activities. *Advances in Colloid and Interface Science* **2009**, *145* (1-2), 83-96.
- (7) Lok, C. N.; Ho, C. M.; Chen, R.; He, Q. Y.; Yu, W. Y.; Sun, H.; Tam, P. K. H.; Chiu, J. F.; Che, C. M., Silver nanoparticles: partial oxidation and antibacterial activities. *Journal of Biological Inorganic Chemistry* **2007**, *12* (4), 527-534.
- (8) Dallas, P.; Sharma, V. K.; Zboril, R., Silver polymeric nanocomposites as advanced antimicrobial agents: Classification, synthetic paths, applications, and perspectives. *Advances in Colloid and Interface Science* **2011**, *166* (1-2), 119-135.
- (9) Durán, N.; Marcato, P.; Alves, O.; Da Silva, J.; De Souza, G.; Rodrigues, F.; Esposito, E., Ecosystem protection by effluent bioremediation: silver nanoparticles impregnation in a textile fabrics process. *Journal of Nanoparticle Research* **2010**, *12* (1), 285-292.
- (10) Benn, T. M.; Westerhoff, P., Nanoparticle Silver Released into Water from Commercially Available Sock Fabrics. *Environmental Science & Technology* **2008**, *42* (11), 4133-4139.
- (11) Marambio-Jones, C.; Hoek, E., A review of the antibacterial effects of silver nanomaterials and potential implications for human health and the environment. *Journal of Nanoparticle Research* **2010**, *12* (5), 1531-1551.
- (12) Gottschalk, F.; Nowack, B., The release of engineered nanomaterials to the environment. *Journal of Environmental Monitoring* **2011**, *13* (5), 1145-1155.
- (13) Blaser, S. A.; Scheringer, M.; MacLeod, M.; Hungerbühler, K., Estimation of cumulative aquatic exposure and risk due to silver: Contribution of nano-functionalized plastics and textiles. *Science of The Total Environment* **2008**, *390* (2-3), 396-409.
- (14) Fabrega, J.; Renshaw, J. C.; Lead, J. R. In *Silver nanoparticles in natural waters: behaviour and impact on bacterial communities*, Water - how need drives research and research underpins solutions to world-wide problems, University of Birmingham, Birmingham UK, 2008; University of Birmingham, Birmingham UK, **2008**; pp 1-3.
- (15) Navarro, E.; Piccapietra, F.; Wagner, B.; Marconi, F.; Kaegi, R.; Odzak, N.; Sigg, L.; Behra, R., Toxicity of silver nanoparticles to *Chlamydomonas reinhardtii*. *Environmental Science & Technology* **2008**, *42* (23), 8959-64.
- (16) Neal, A. L., What can be inferred from bacterium-nanoparticle interactions about the potential consequences of environmental exposure to nanoparticles? *Ecotoxicology* **2008**, *17* (5), 362-71.
- (17) Cumberland, S. A.; Lead, J. R., Particle size distributions of silver nanoparticles at environmentally relevant conditions. *Journal of Chromatography A* **2009**, *1216* (52), 9099-9105.
- (18) Fabrega, J.; Fawcett, S. R.; Renshaw, J. C.; Lead, J. R., Silver nanoparticle impact on bacterial growth: effect of pH, concentration, and organic matter. *Environmental Science & Technology* **2009**, *43* (19), 7285-90.
- (19) Gao, J.; Youn, S.; Hovsepian, A.; Llaneza, V. L.; Wang, Y.; Bitton, G.; Bonzongo, J.-C. J., Dispersion and Toxicity of Selected Manufactured Nanomaterials in Natural River Water Samples: Effects of Water Chemical Composition. *Environmental Science & Technology* **2009**, *43* (9), 3322-3328.
- (20) El Badawy, A. M.; Luxton, T. P.; Silva, R. G.; Scheckel, K. G.; Suidan, M. T.; Tolaymat, T. M., Impact of Environmental Conditions (pH, Ionic Strength, and Electrolyte Type) on the Surface Charge and Aggregation of Silver Nanoparticles Suspensions. *Environmental Science & Technology* **2010**, *44* (4), 1260-1266.

- (21) Jin, X.; Li, M.; Wang, J.; Marambio-Jones, C.; Peng, F.; Huang, X.; Damoiseaux, R.; Hoek, E. M. V., High-Throughput Screening of Silver Nanoparticle Stability and Bacterial Inactivation in Aquatic Media: Influence of Specific Ions. *Environmental Science & Technology* **2010**, *44* (19), 7321-7328.
- (22) Huynh, K. A.; Chen, K. L., Aggregation Kinetics of Citrate and Polyvinylpyrrolidone Coated Silver Nanoparticles in Monovalent and Divalent Electrolyte Solutions. *Environmental Science & Technology* **2011**, *45* (13), 5564-5571.
- (23) El Badawy, A. M.; Silva, R. G.; Morris, B.; Scheckel, K. G.; Suidan, M. T.; Tolaymat, T. M., Surface Charge-Dependent Toxicity of Silver Nanoparticles. *Environmental Science & Technology* **2011**, *45* (1), 283-287.
- (24) Lok, C. N.; Ho, C. M.; Chen, R.; He, Q. Y.; Yu, W. Y.; Sun, H. Z.; Tam, P. K. H.; Chiu, J. F.; Che, C. M., Proteomic analysis of the mode of antibacterial action of silver nanoparticles. *Journal of Proteome Research* **2006**, *5* (4), 916-924.
- (25) Kittler, S.; Greulich, C.; Diendorf, J.; Köller, M.; Epple, M., Toxicity of Silver Nanoparticles Increases during Storage Because of Slow Dissolution under Release of Silver Ions. *Chemistry of Materials* **2010**, *22* (16), 4548-4554.
- (26) Liu, J. Y.; Hurt, R. H., Ion Release Kinetics and Particle Persistence in Aqueous Nano-Silver Colloids. *Environmental Science & Technology* **2010**, *44* (6), 2169-2175.
- (27) Ma, R.; Levard, C.; Marinakos, S. M.; Cheng, Y. W.; Liu, J.; Michel, F. M.; Brown, G. E.; Lowry, G. V., Size-Controlled Dissolution of Organic-Coated Silver Nanoparticles. *Environmental Science & Technology* **2012**, *46* (2), 752-759.
- (28) Zhang, W.; Yao, Y.; Sullivan, N.; Chen, Y. S., Modeling the Primary Size Effects of Citrate-Coated Silver Nanoparticles on Their Ion Release Kinetics. *Environmental Science & Technology* **2011**, *45* (10), 4422-4428.
- (29) Choi, O.; Hu, Z., Size dependent and reactive oxygen species related nanosilver toxicity to nitrifying bacteria. *Environmental Science & Technology* **2008**, *42* (12), 4583-8.
- (30) Sondi, I.; Salopek-Sondi, B., Silver nanoparticles as antimicrobial agent: a case study on *E. coli* as a model for Gram-negative bacteria. *Journal of Colloid and Interface Science* **2004**, *275* (1), 177-182.
- (31) Morones, J. R.; Elechiguerra, J. L.; Camacho, A.; Holt, K.; Kouri, J. B.; Ramirez, J. T.; Yacaman, M. J., The bactericidal effect of silver nanoparticles. *Nanotechnology* **2005**, *16* (10), 2346-2353.
- (32) Pal, S.; Tak, Y. K.; Song, J. M., Does the Antibacterial Activity of Silver Nanoparticles Depend on the Shape of the Nanoparticle? A Study of the Gram-Negative Bacterium *Escherichia coli*. *Applied and Environmental Microbiology* **2007**, *73* (6), 1712-1720.
- (33) Dror-Ehre, A.; Mamane, H.; Belenkova, T.; Markovich, G.; Adin, A., Silver nanoparticle - *E. coli* colloidal interaction in water and effect on *E. coli* survival. *Journal of Colloid and Interface Science* **2009**, *339* (2), 521-6.
- (34) Fabrega, J.; Renshaw, J. C.; Lead, J. R., Interactions of Silver Nanoparticles with *Pseudomonas putida* Biofilms. *Environmental Science & Technology* **2009**, *43* (23), 9004-9009.
- (35) Kim, J. S.; Kuk, E.; Yu, K. N.; Kim, J.-H.; Park, S. J.; Lee, H. J.; Kim, S. H.; Park, Y. K.; Park, Y. H.; Hwang, C.-Y.; Kim, Y.-K.; Lee, Y.-S.; Jeong, D. H.; Cho, M.-H., Antimicrobial effects of silver nanoparticles. *Nanomedicine: Nanotechnology, Biology and Medicine* **2007**, *3* (1), 95-101.
- (36) Hwang, E. T.; Lee, J. H.; Chae, Y. J.; Kim, Y. S.; Kim, B. C.; Sang, B. I.; Gu, M. B., Analysis of the toxic mode of action of silver nanoparticles using stress-specific bioluminescent bacteria. *Small* **2008**, *4* (6), 746-750.
- (37) Park, M. V. D. Z.; Neigh, A. M.; Vermeulen, J. P.; de la Fonteyne, L. J. J.; Verharen, H. W.; Briedé, J. J.; van Loveren, H.; de Jong, W. H., The effect of particle size on the cytotoxicity, inflammation, developmental toxicity and genotoxicity of silver nanoparticles. *Biomaterials* **2011**, *32* (36), 9810-9817.
- (38) Su, H. L.; Chou, C. C.; Hung, D. J.; Lin, S. H.; Pao, I. C.; Lin, J. H.; Huang, F. L.; Dong, R. X.; Lin, J. J., The disruption of bacterial membrane integrity through ROS generation induced by nanohybrids of silver and clay. *Biomaterials* **2009**, *30* (30), 5979-5987.
- (39) Bowman, C. R.; Bailey, F. C.; Elrod-Erickson, M.; Neigh, A. M.; Otter, R. R., Effects of silver nanoparticles on zebrafish (*Danio rerio*) and *Escherichia coli* (ATCC 25922): A comparison of toxicity based on total surface area versus mass concentration of particles in a model eukaryotic and prokaryotic system. *Environmental Toxicology and Chemistry* **2012**, *31* (8), 1793-1800.
- (40) Bradford, A.; Handy, R. D.; Readman, J. W.; Atfield, A.; Muhling, M., Impact of silver nanoparticle contamination on the genetic diversity of natural bacterial assemblages in estuarine sediments. *Environmental Science & Technology* **2009**, *43* (12), 4530-6.

-
- (41) Muhling, M.; Bradford, A.; Readman, J. W.; Somerfield, P. J.; Handy, R. D., An investigation into the effects of silver nanoparticles on antibiotic resistance of naturally occurring bacteria in an estuarine sediment. *Marine Environmental Research* **2009**, *68* (5), 278-283.
- (42) Bone, A. J.; Colman, B. P.; Gondikas, A. P.; Newton, K. M.; Harrold, K. H.; Cory, R. M.; Unrine, J. M.; Klaine, S. J.; Matson, C. W.; Di Giulio, R. T., Biotic and Abiotic Interactions in Aquatic Microcosms Determine Fate and Toxicity of Ag Nanoparticles: Part 2-Toxicity and Ag Speciation. *Environmental Science & Technology* **2012**, *46* (13), 6925-6933.
- (43) Li, X.; Lenhart, J. J., Aggregation and Dissolution of Silver Nanoparticles in Natural Surface Water. *Environmental Science & Technology* **2012**, *46* (10), 5378-5386.
- (44) Piccapietra, F.; Sigg, L.; Behra, R., Colloidal Stability of Carbonate-Coated Silver Nanoparticles in Synthetic and Natural Freshwater. *Environmental Science & Technology* **2012**, *46* (2), 818-825.
- (45) Tejamaya, M.; Romer, I.; Merrifield, R. C.; Lead, J. R., Stability of Citrate, PVP, and PEG Coated Silver Nanoparticles in Ecotoxicology Media. *Environmental Science & Technology* **2012**, *46* (13), 7011-7017.
- (46) Lowry, G. V.; Espinasse, B. P.; Badireddy, A. R.; Richardson, C. J.; Reinsch, B. C.; Bryant, L. D.; Bone, A. J.; Deonarine, A.; Chae, S.; Therezien, M.; Colman, B. P.; Hsu-Kim, H.; Bernhardt, E. S.; Matson, C. W.; Wiesner, M. R., Long-Term Transformation and Fate of Manufactured Ag Nanoparticles in a Simulated Large Scale Freshwater Emergent Wetland. *Environmental Science & Technology* **2012**, *46* (13), 7027-7036.
- (47) Unrine, J. M.; Colman, B. P.; Bone, A. J.; Gondikas, A. P.; Matson, C. W., Biotic and Abiotic Interactions in Aquatic Microcosms Determine Fate and Toxicity of Ag Nanoparticles. Part 1. Aggregation and Dissolution. *Environmental Science & Technology* **2012**, *46* (13), 6915-6924.
- (48) Zook, J. M.; Long, S. E.; Cleveland, D.; Geronimo, C. L. A.; MacCuspie, R. I., Measuring silver nanoparticle dissolution in complex biological and environmental matrices using UV-visible absorbance. *Analytical and Bioanalytical Chemistry* **2011**, *401* (6), 1993-2002.
- (49) Yang, X. Y.; Gondikas, A. P.; Marinakos, S. M.; Auffan, M.; Liu, J.; Hsu-Kim, H.; Meyer, J. N., Mechanism of Silver Nanoparticle Toxicity Is Dependent on Dissolved Silver and Surface Coating in *Caenorhabditis elegans*. *Environmental Science & Technology* **2012**, *46* (2), 1119-1127.
- (50) Arnaout, C. L.; Gunsch, C. K., Impacts of Silver Nanoparticle Coating on the Nitrification Potential of *Nitrosomonas europaea*. *Environmental Science & Technology* **2012**, *46* (10), 5387-5395.
- (51) Lubick, N., Nanosilver toxicity: ions, nanoparticles-or both? *Environmental Science & Technology* **2008**, *42* (23), 8617-8617.
- (52) Park, E. J.; Yi, J.; Kim, Y.; Choi, K.; Park, K., Silver nanoparticles induce cytotoxicity by a Trojan-horse type mechanism. *Toxicology in Vitro* **2010**, *24* (3), 872-878.

3.6 Supporting Information

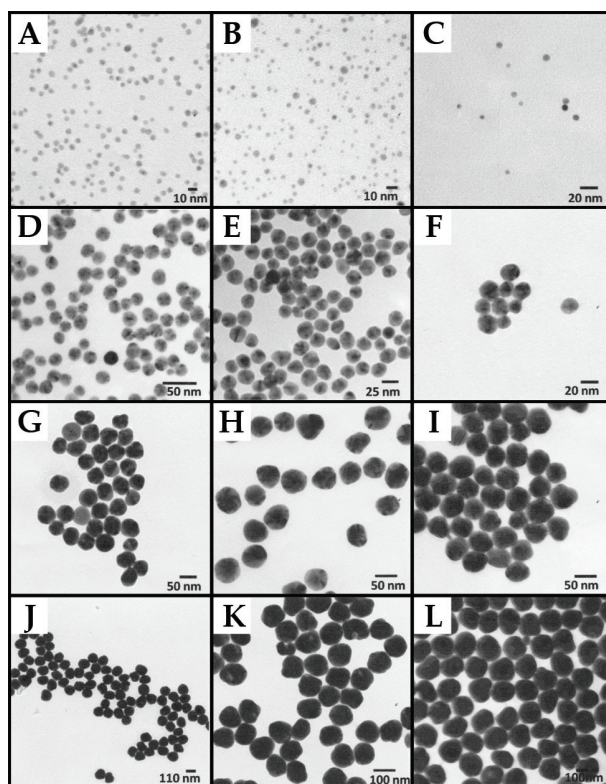


Figure S1: TEM micrograph of AgNPs used in the study: PVP-AgNPs (A, D, G, J), Tan-AgNPs (B, E, H, K), Cit-AgNPs (C, F, I, L), 5 nm (A, B), 10 nm (C) and 20 nm (D, E, F), 50 nm (G, H, I) and 100 nm (J, K, L).

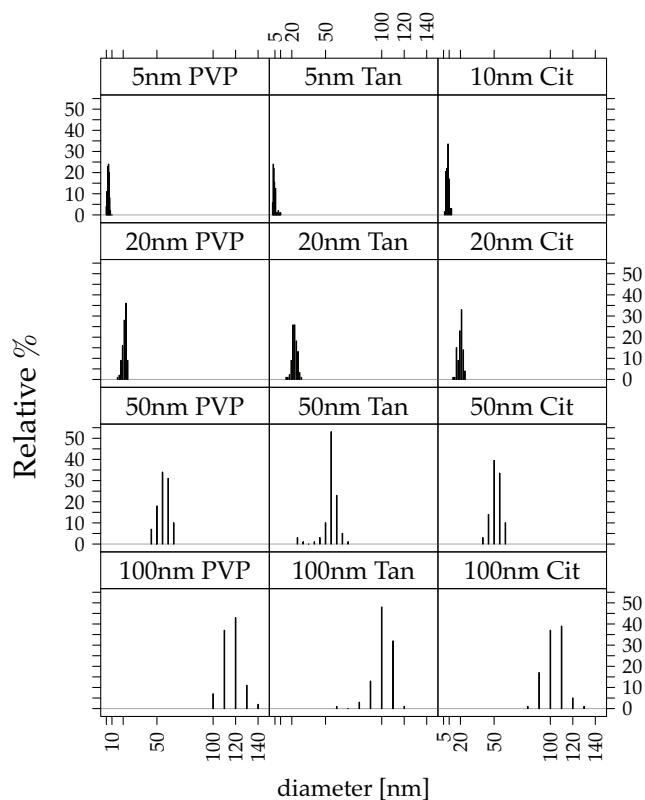


Figure S2: DLS measurements of AgNPs used in this study.

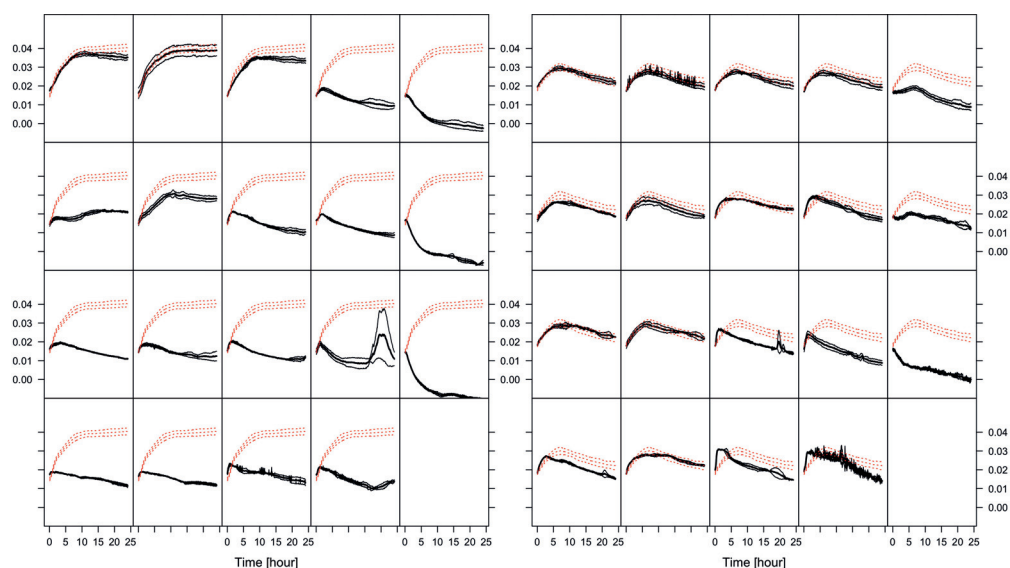


Figure S3: Surface area effect of PVP-AgNPs (left panel) and tannic-AgNPs (right panel) on *E. coli*. Columns in each panel represent different sizes (left to right): 5, 10, 20, 50 and 100 nm. Rows in each panel represent different total surface area (top to bottom): 1.71, 2.57, 3.43 and 6.86 mm². Each individual panel represents the growth (OD₆₀₀) as a function of time (hours). Red dotted curves represent the control growth in absence of AgNPs and the black one the tested conditions. Each curve is made of a mean \pm the standard deviation for triplicates.

Table S1: ζ potential measurements for silver nanoparticles used in this study in ALW medium.

Coating	Size	ζ potential [mV]
Tannic	5 nm	-12.8
Tannic	10 nm	-16.5
Tannic	20 nm	-15.5
Tannic	50 nm	-17.0
Tannic	100 nm	-23.0
PVP	5 nm	-20.2
PVP	10 nm	-11.4
PVP	20 nm	-19.5
PVP	50 nm	-22.7
PVP	100 nm	-27.6
Citric	10 nm	-27.3
Citric	20 nm	-34.1
Citric	50 nm	-42.7
Citric	100 nm	-44.7

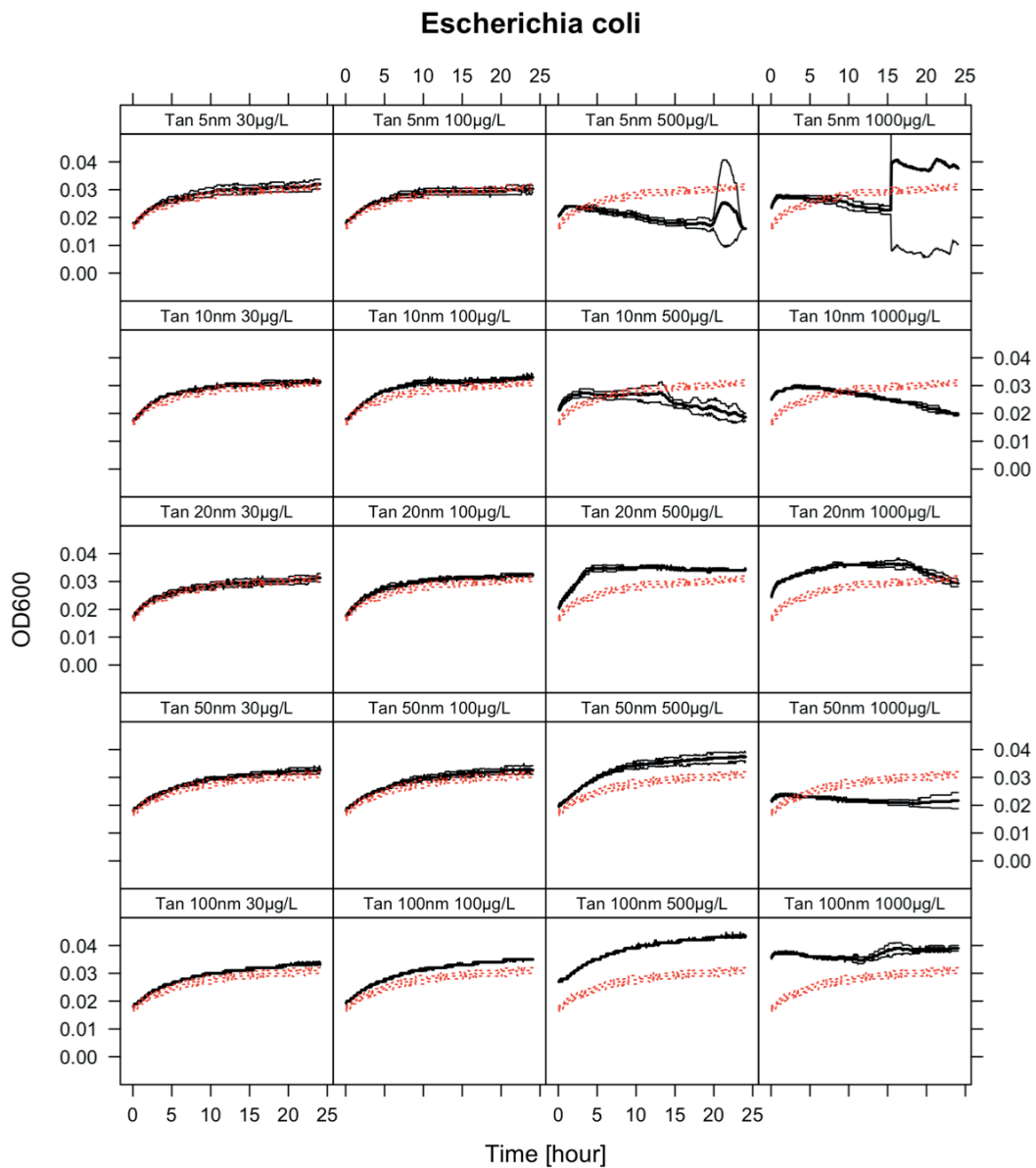


Figure S4: Microplate screening experiment for *E. coli* exposed to tannic-AgNPs.

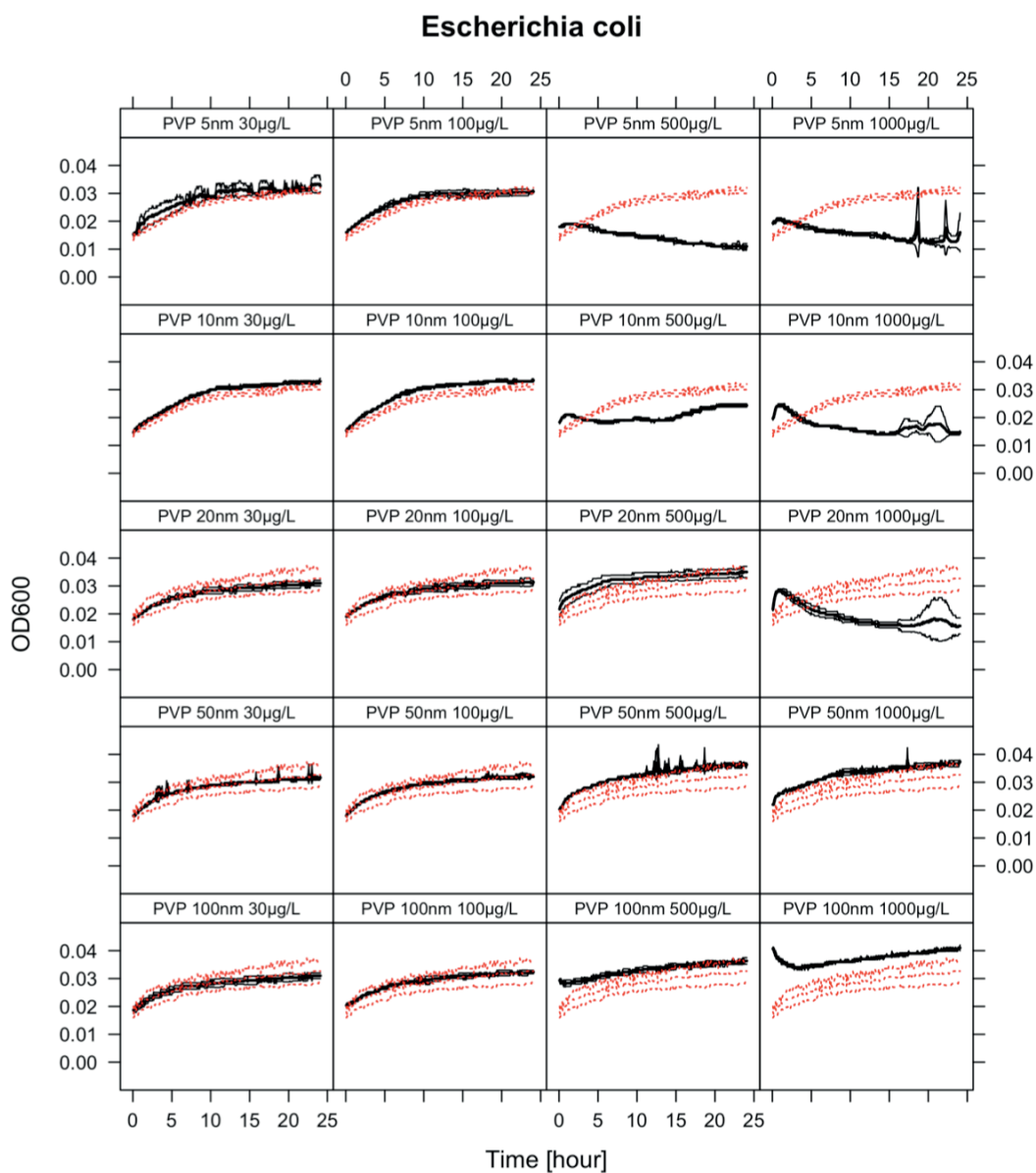


Figure S5: Microplate screening experiment for *E. coli* exposed to PVP-AgNPs.

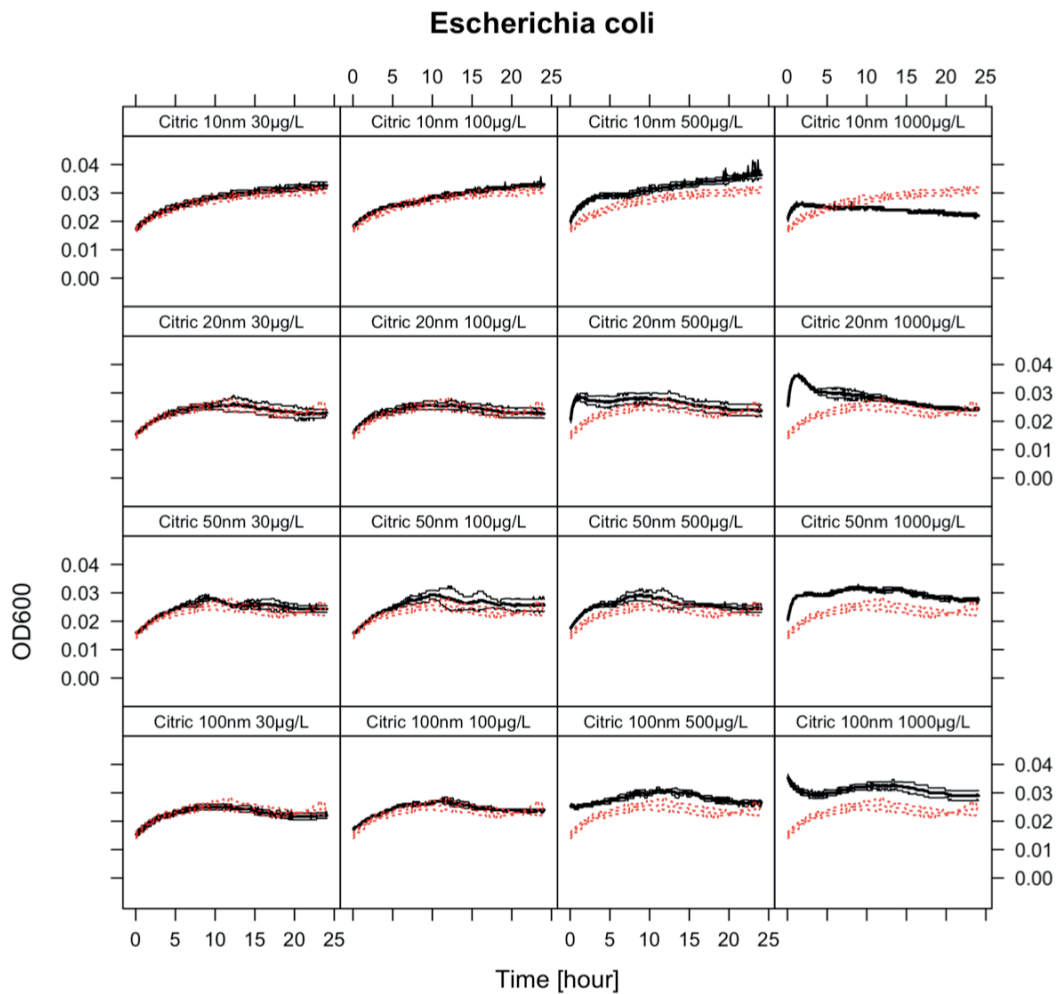


Figure S6: Microplate screening experiment for *E. coli* exposed to citric-AgNPs.

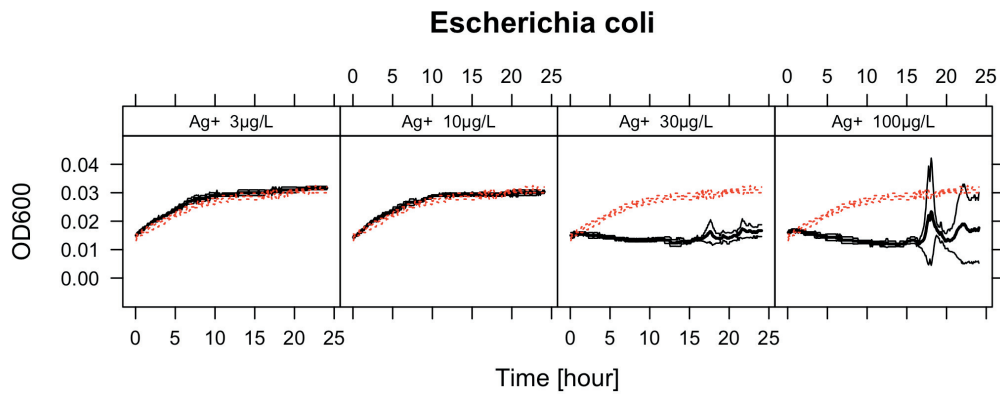


Figure S7: Microplate screening experiment for *E. coli* exposed to Ag_2SO_4 .

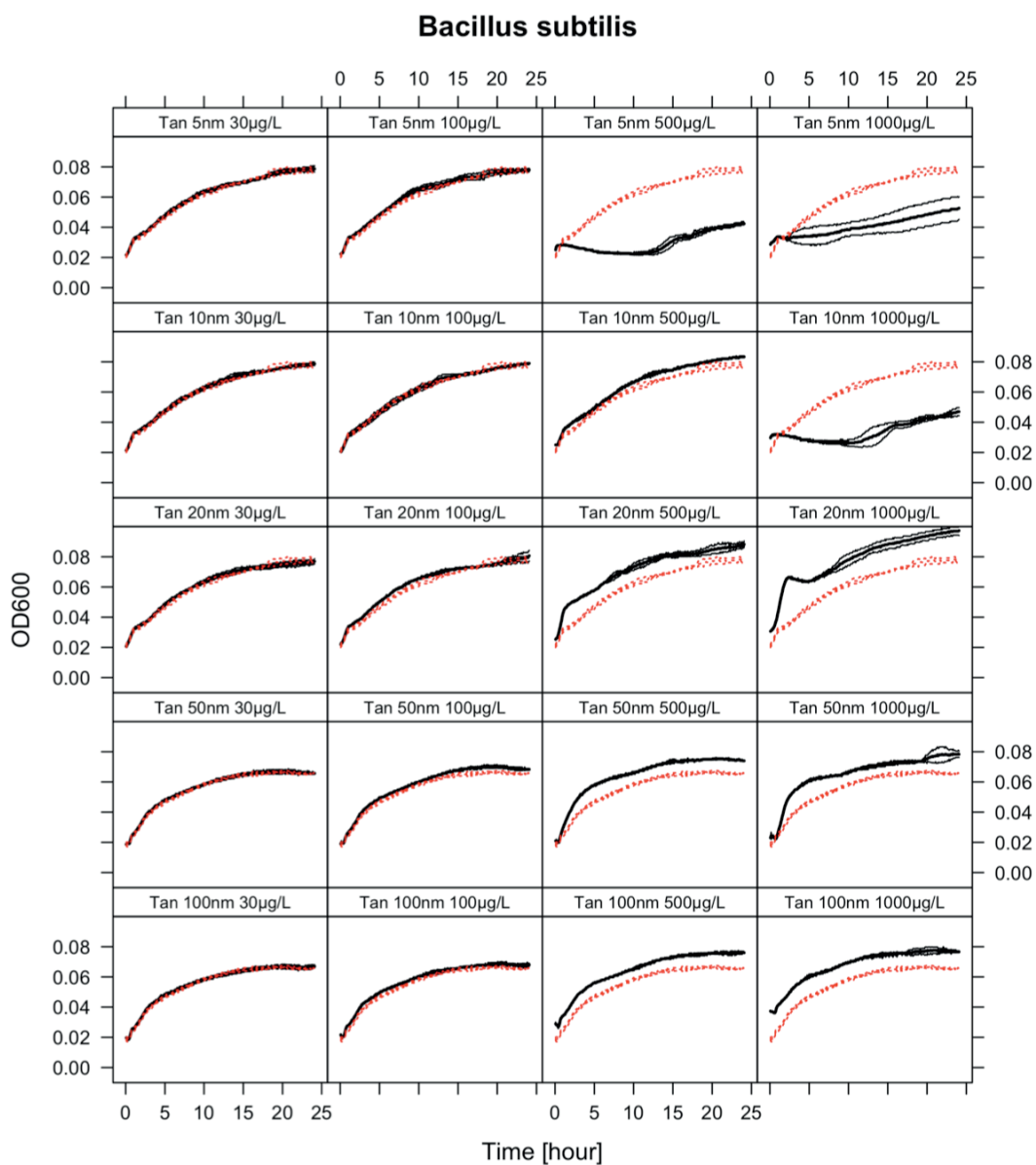


Figure S8: Microplate screening experiment for *B. subtilis* exposed to tannic-AgNPs.

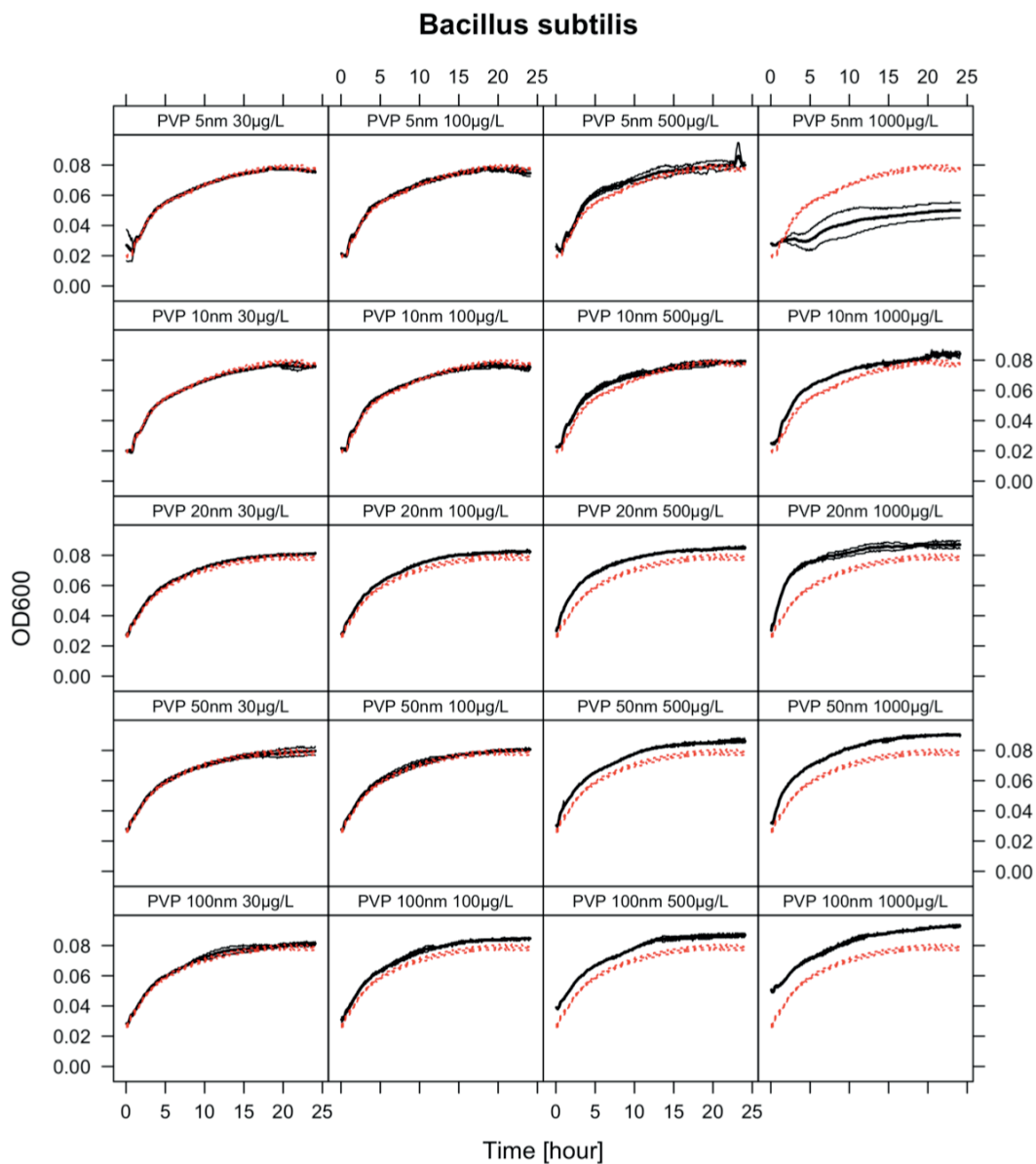


Figure S9: Microplate screening experiment for *B. subtilis* exposed to PVP-AgNPs.

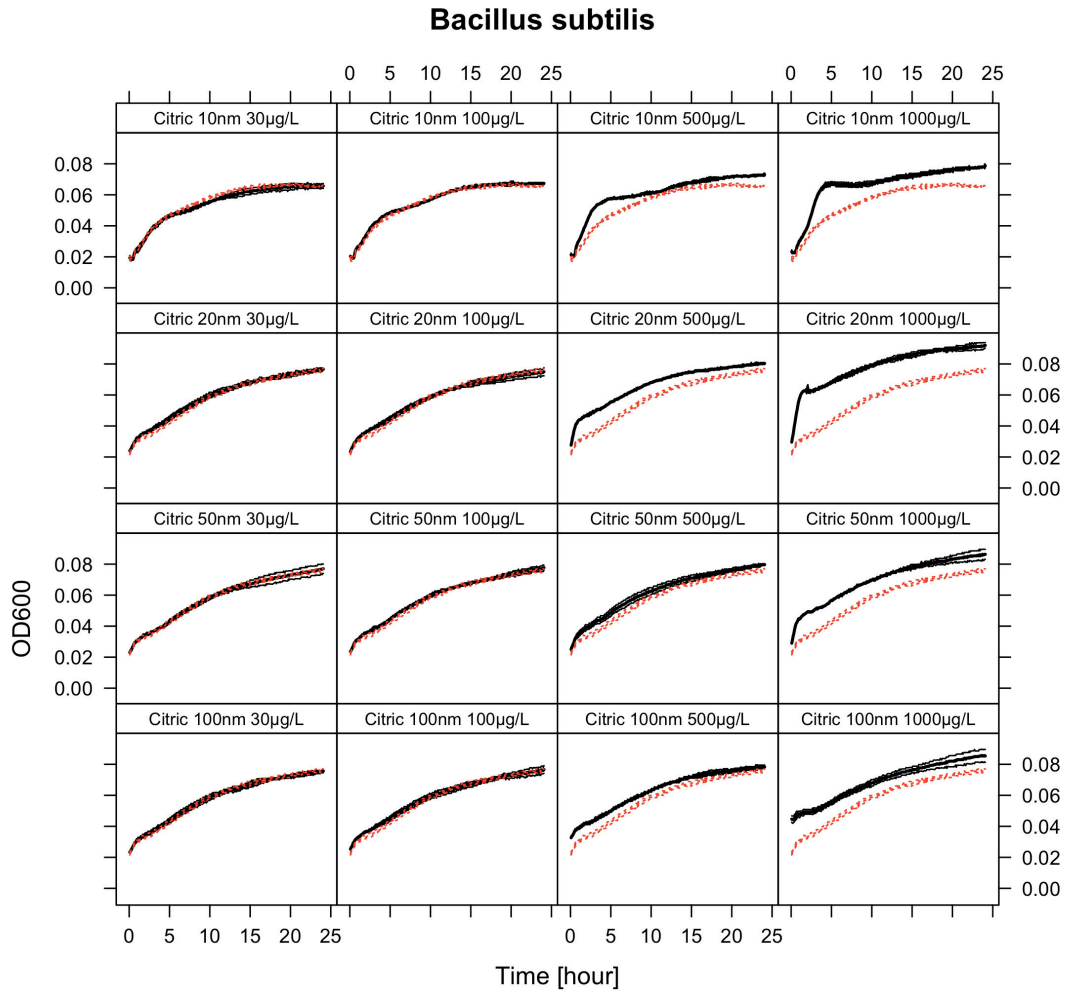


Figure S10: Microplate screening experiment for *B. subtilis* exposed to citric-AgNPs.

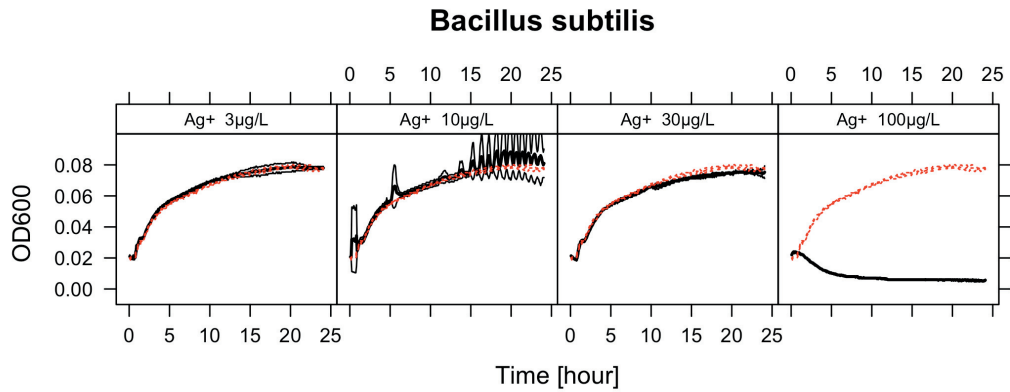


Figure S11: Microplate screening experiment for *B. subtilis* exposed to Ag_2SO_4 .

Chapter

4 Effect of silver nanoparticles on microbial communities from Lake Geneva

J. Dobias, A. Bagnoud and R. Bernier-Latmani

Abstract: For the past 15 years, there has been growing interest from industry for the use of nanomaterials in a variety of applications. This increased use has raised concerns within the scientific community as well as regulators and led them to consider in greater detail the potential harmful effect of the release of nanomaterials into the environment. Silver nanoparticles, in particular, have been under scrutiny for a few years, even though ionic silver has been used for a century for its strong bactericidal effect. Little is known about the impact of nanosilver colloids on aquatic environments. Here, we report the effect of 5 nm polyvinylpyrrolidone (PVP)-coated AgNPs on the diversity of a microbial community from Lake Geneva. We carried out high-throughput pyrosequencing of DNA from the same microbial community exposed to various concentrations of AgNPs. The study showed a shift in bacterial community composition correlating with the concentration of AgNPs added. In contrast, no correlation was observed for fungi communities. This study suggests that AgNPs may significantly impact microbial communities in aquatic environments

Keywords: microbes, bacteria, fungi, 16S rRNA, 18S rRNA, tagged pyrosequencing, microbial diversity, lake, freshwater

4.1 Introduction

In the past 20 years, nanotechnology has become a sought-after science as it opened a world of new materials with unique electrical, mechanical, optical or chemical properties. Concomitantly industry sensed the commercial opportunities and started developing and branding an increasing number of products that represent hundreds of tons of nanomaterials produced per year^{1,2}. Silver nanoparticles (AgNPs) account for a large fraction of the nanomaterials used in consumer goods³. Even though silver nanoparticles show interesting electrical, optical and catalytic properties⁴, they are mostly used for their strong antimicrobial effect⁵⁻⁸. The release of nanoparticles from consumer products has been documented⁹⁻¹² and with their steadily increasing production and use, a growing concern is emerging linking their release to the environment to their impact on microbial communities^{11,13-16}.

Whereas many human health standards include studies (already from the early 20th century) that considered nanosilver materials, environmental standards do not consider nanosilver materials but rather are based on the impact of ionic silver¹⁷. Therefore, there is a need for the re-evaluation of environmental standards for the release of AgNPs based on nanosilver-based studies. However, an evident limitation in this re-evaluation is the very limited number of available studies that considered the effect of NPs on the environment under realistic conditions¹⁸⁻²⁴. The numerous laboratory-based studies that considered AgNPs include the following microorganisms: *Escherichia coli*^{5,7,25-34} (this thesis), *Bacillus subtilis*^{26,35} (this thesis), *Shewanella oneidensis* MR-1^{26,36}, *Pseudomonas fluorescens* SBW25³⁷, *P. putida*³⁸, *P. aeruginosa*^{30,39}, *Cupriavidus metallidurans* CH34²⁹, *Staphylococcus epidermidis*³⁹, *S. aureus*³⁰⁻³², *Streptococcus pyogenes*³⁰, *Nitrosomonas europae*⁴⁰ and nitrifying bacteria enrichments⁴¹ (further types of NPs and organism are discussed in Marambio-Jones and Hoeck⁸ and in Sharma *et al.*⁶). All of these studies are individually valuable but it is difficult to extract information relevant to microbial communities from this work due to differences in the nanosilver materials used and in the considered conditions.

Whereas mechanistic aspects of AgNPs toxicity were discussed in the previous chapter, here we report the impact of 5 nm polyvinylpyrrolidone (PVP)-coated AgNPs on freshwater microbial communities obtained from enrichments from Lake Geneva water. We chose to focus on small AgNPs as they were evidenced (Chapter 2) to be the most toxic to both Gram-positive and Gram-negative bacteria and therefore the most relevant for this toxicity study. The work is based on the high-throughput sequencing of 16S (bacteria) and 18S (fungi) rRNA of lakewater enrichments exposed to various concentrations of AgNPs. The results showed a correlation between the bacterial

community composition and the silver concentration, whereas no correlation was observed in the case of fungi.

4.2 Materials and methods

4.2.1 *Lakewater enrichments*

The enrichments were obtained from Lake Geneva water sampled at the Vidy Bay (VD, Switzerland) shore (latitude 46.518, longitude 6.589, elevation 372 m). Samples were collected in February (F) and in June (J) in an area where flow was evident and at around 20 cm below the water surface.

Water samples were transferred to Artificial Lake Water (ALW, see below) at a 1:10 ratio of inoculum (lakewater sample) to fresh medium. Enrichments were transferred to fresh medium every week for at least 6 weeks prior to being exposed to AgNPs.

4.2.2 *Silver nanoparticles*

The silver nanoparticles, from nanoComposix (San Diego, CA), considered in this study were from the same batch as in Chapter 3. Here we used 5 nm polyvinylpyrrolidone-coated AgNPs (PVP-AgNPs) (actual size in nm: 6.5 ± 0.8).

4.2.3 *Medium composition*

A defined medium, Artificial Lake Water (ALW), was prepared as described in Chapter 3 (medium composition) but with the following modifications: Glucose was used at 1 g/L and effluent from the Vidy wastewater treatment plant filtered with a 3 μm pore size filter (SSWP 47 mm, Merck Millipore, Billerica, MA) was added to the final medium at a 1:10 ratio to serve as a supplementary carbon source. Finally, the solution was filter-sterilized with a 0.22 μm pore size filter (GPWP 47 mm, Merck Millipore, Billerica, MA) immediately prior use.

4.2.4 *Enrichment cultures for DNA purification*

The two final enrichments (F and J from February and June, respectively) were transferred to 100 mL of ALW medium containing the following concentration of AgNPs: 0, 25, 50, 75 and 100 $\mu\text{g/L}$, and incubated at 25°C with continuous shaking (130 rpm) in 250 mL baffled Erlenmeyer flasks. Growth was followed spectrophotometrically and samples were taken for protein content quantification. When no further growth could be detected, a 50 mL volume of culture was centrifuged for 20 min at 5,000 rcf at 20°C. The pellet was re-suspended in 400 μL TE pH 8.0 containing: 0.1N NaCl, 0.5% Triton™ X-100, 0.7 mg/ml lysozyme from hen egg and 200 $\mu\text{g/ml}$ Proteinase K. The solution was allowed to incubate at 37°C for 2 hours with gentle mixing every 15 minutes. After the incubation period, FastDNA® SpinKit for Soil (MP Biomedicals LLC, Solon OH, USA) was used to physically break the cell.

After the first step of bead beating (40 sec., intensity 5) the tubes were centrifuged and the supernatant used for DNA purification on a Promega Maxwell® system with the Maxwell® 16 Tissue DNA Purification Kit. The DNA was then concentrated by ethanol precipitation and tested by PCR amplification with the following primers: Eub 9-27 (F) GAG TTT GAT CCT GGC TCA G and Eub 1542 ® AGA AAG GAG GTG ATC CAG CC (PCR specific conditions were: 50°C for the annealing temperature, 1'30'' of elongation and 30 cycles). Finally, the amplified DNA was sent to Research and Testing Laboratory (Lubbock TX, USA) for high throughput sequencing against 16S 28F-519R (bacterial communities assay b.2) and 18S 515F-1100 (fungi communities assay F.2) assays.

4.2.5 *DNA Sequence analysis*

The analysis of the DNA sequences was done with MacQIIME ⁴² (qiime.org) and following section (1) “overview” of the tutorial (<http://qiime.org/tutorials/tutorial.html>) for general file handling, (2) “Denoising of 454 Data Sets” (http://qiime.org/tutorials/denoising_454_data.html) for denoising the sequences and (3) “Chimera checking sequences with QIIME” (http://qiime.org/tutorials/chimera_checking.html) for the removal of the potential chimeric sequences. Briefly, the data analysis was carried out as follows: data were extracted from sff raw files and a library of sequences was created for each sample excluding sequences that were too short, contained reading errors in the primer regions or were of low quality; sequences with poor terminal quality were truncated. A denoising step was then applied to each library where sequences were compared to each other, the ones with similarities >97% were grouped together and for each group a mean sequence (centroid) was calculated. Then operational taxonomic units (OTU) are selected with a similarity threshold of 97%. The OTUs are aligned with Pynast, which is a template of already aligned sequences from greengenes (core_set_aligned.fasta.imputed for bacteria and core_Silva_aligned.fasta for fungi). Potentially chimeric sequences were identified with the same two latter databases and removed from the OTU alignment sets. Finally, phylogenetic assignments were carried out with the ribosomal database project (RDP) classifier with the default 16S database and the QIIME r104 database for 18S fungal RNA (<http://www.arb-silva.de/download/archive/qiime/>).

Taxa plots, PCoA analysis and rarefaction plots were computed using QIIME tools in the “overview” tutorial (see above).

Krona plots were generated with Krona ⁴³ tools (<http://sourceforge.net/p/krona/home/krona/>) applied to the non-chimeric OTU output file of QIIME.

4.2.6 *Analytical methods*

Cell growth was measured by photometric absorbance at a wavelength of 600 nm (OD_{600}) on a Shimadzu UV-2501 PC spectrophotometer (Shimadzu, Reinach BL, Switzerland).

Protein and DNA content were measured with a benchtop Qubit® fluorometer (LuBioScience GmbH, Lucerne, Switzerland) with the Protein and dsDNA HS Assay respectively. For protein content measurements, two samples of 2 mL were centrifuged and 1.95 mL was removed without disturbing the pellet. The pellet was then frozen to help break the cells, thawed and dispersed in the remaining solution which volume was measured with a manual pipettor to account for any experimental imprecision in expected concentrating factors. Finally, the suspension was used for proteins quantitation with the Qubit® Protein Assay.

4.3 Results and discussion

In order to probe the effect of silver nanoparticles on bacterial communities, we established enrichments from Lake Geneva water collected in February (F) and June (J) 2012. The enrichments were exposed to various concentrations of AgNPs. The microbial community diversity was then estimated by using pyrosequencing.

The enrichments were established by weekly transfer to fresh Artificial Lake water (ALW) medium for several weeks prior to use in AgNPs experiments. The two enrichments (F and J) were then subsampled and exposed to increasing concentrations of silver nanoparticles (0, 25, 50, 75, 100 $\mu\text{g/L}$ of 5 nm PVP-AgNPs). Measurements of total silver by ICP-MS confirmed that the concentrations were close to expected values (Table S1). Growth was monitored by measuring the optical density at 600 nm (Figure 1) but also by sampling the solutions for protein content analysis (Figure S1).

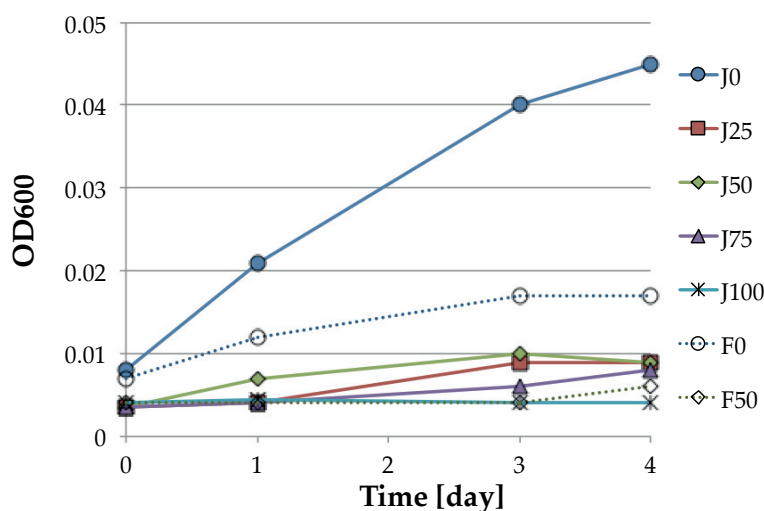


Figure 1: Measurements of bacterial growth by measurement of the absorbance at 600 nm for Lake Geneva enrichments from February (F) and June (J) amended with 5 nm PVP-AgNPs at: 0, 25, 50, 75 and 100 $\mu\text{g/L}$. Legend key: F=February, J=June, numbers = AgNPs concentration in $\mu\text{g/L}$

Similarly to what was observed in Chapter 3, microbial enrichments growth inhibition appeared to be a function of AgNP concentration. Compared to the sensitivity of *Escherichia coli* and *Bacillus subtilis* to AgNPs that was described in that chapter, respectively 200-250 $\mu\text{g/L}$ and 500 $\mu\text{g/L}$, both enrichments displayed toxicity at lower concentrations. A concentration of 100 $\mu\text{g/L}$ was sufficient to completely inhibit their growth. Additionally, the growth inhibition of natural enrichments is striking at 25 $\mu\text{g/L}$, a concentration considerably below laboratory strain sensitivity. As a consequence, one would expect to observe a change in the microbial community between enrichment not exposed to AgNPs and that exposed to 25 $\mu\text{g/L}$. This higher sensitivity of environmental microorganisms was expected, as the two laboratory strains

considered previously were obtained from the DSMZ repository, and have been maintained and propagated for the last 40 years. This selection likely made them more resistant than wild type organisms to a variety of injuries.

To track the shift in bacterial community diversity, the 16S rRNA genes in purified genomic DNA (gDNA) were sequenced and compared to databases to reconstruct the microbial population composition. It should be noted that this approach is partially quantitative. An abundant microbial population is more likely to be identified as its amount of total genetic material is going to be greater than that of a less abundant species. However, although the amplification is done with universal primers present in a consensus genomic sequence, the gDNA templates are not equally amplifiable leading to potential over/under estimation of some species.

In order to estimate the representativeness of the species identified by the sequenced amplicons, rarefaction plots were produced. Figure 2A shows that the June enrichment has a poorer rarefaction than February and additional sequencing could have been beneficial for more accurate estimation of the diversity. However, the June rarefaction plot is lowered by sample J25. In Figure 2B (rarefaction curve as a function of the sample), J25 has the lowest number of available sequences by far, thus decreasing the overall rarefaction value of the other samples. From an individual perspective, however, J25 is clearly a sample with a low diversity as is indicated by the plateau reached by its rarefaction curve.

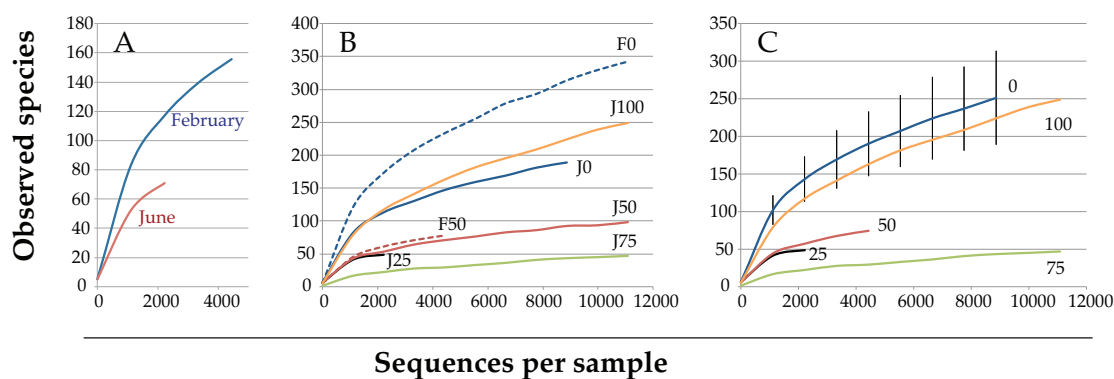


Figure 2: Rarefaction analysis for 16S rRNA sequenced amplicons from February and June enrichments exposed to PVP-AgNPs at 0, 25, 50, 75 and 100 $\mu\text{g/L}$ clustered by (A) sample origin, (B) sample ID and (C) AgNPs concentrations. The legend numbers correspond to the AgNPs concentration in $\mu\text{g/L}$ and February samples are labeled with an “F” and June samples with a “J”

This leveling off of the number of observed species as additional sequences are considered suggests that the entire diversity of the sample has been described. In contrast, all other samples would have benefited from additional sequences as their curves have positive slopes. Finally, both Figure 2B and 2C indicate that the rarefaction

is correlated with AgNP concentration as the number of species decreases when the AgNP concentration increases, except for J100 that is close to J0. An explanation for the behavior of J100 is that the species found in that sample derive from the inoculum itself since no growth was observed (Figure 1).

We used an unweighted principal coordinate analysis (PCoA) in Fast Unifrac to visualize the differences between microbial communities for each sample (Figure 3). Bacterial communities from the February enrichment clustered together and were different from the June enrichment (Figure 3A). Two other clusters can be seen in Figure 3A: (1) J0 and J100, (2) J25, J50 and J75. From Figure 3A, PC1 that accounts for 27% of the variation between samples, indicates that the difference between F and J samples come from the sample origin more than from the exposure to silver. PC2 (22% of variation) clearly points to the effect of AgNPs on the difference in community diversity between J0, J100 and J25, J50, J75. Finally, PC3 (Figure 3B and 3C) explains the difference between the samples J25, J50, and J75 but also the similarities between J0, F0 and J25. J100 and F50 are closely related too on this axis.

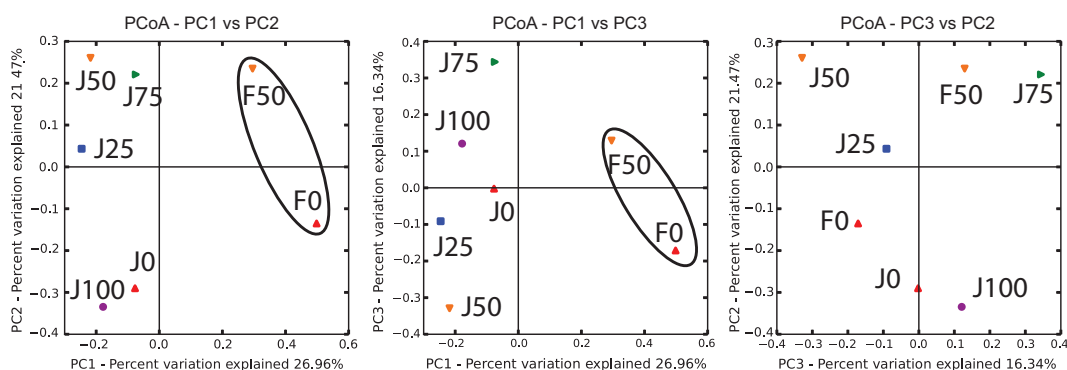


Figure 3: Fast Unifrac principal coordinate analysis (PCoA) for bacterial population from February (F) and June (J) enrichments exposed to 0, 25, 50, 75 and 100 $\mu\text{g/L}$ of 5 nm PVP-AgNPs. The plot legend key numbers correspond to the AgNPs concentration in $\mu\text{g/L}$.

The phylogeny of bacteria associated with the various treatments was determined by 454-sequencing of the 16S rRNA amplicon. A complete representation of the microbial community composition for all the treatments is available in the associated content Figure S5, and was obtained with Krona⁴³ tools (<http://sourceforge.net/p/krona/home/krona/>). The bacterial population is mainly divided into two groups: Bacteroidetes and Proteobacteria (Figure 4). Both phyla are Gram-negative bacteria widely distributed in the environment, including soil, sediments, and seawater but also present in the gut and on the skin of animals (including humans). Surprisingly, almost no Gram-positive bacteria were found. Low contributions of Gram-positive bacteria (Actinobacteria) were observed in J0, J100 and F50 (0.1%, 0.02% and 0.02% respectively). No members of the phylum Firmicutes were detected at all. The Gram staining bias may come from the

enrichment procedure or may reflect the prevalence of Gram-negative bacteria in lakewater as Gram-positive bacteria are associated more readily with soil environments.

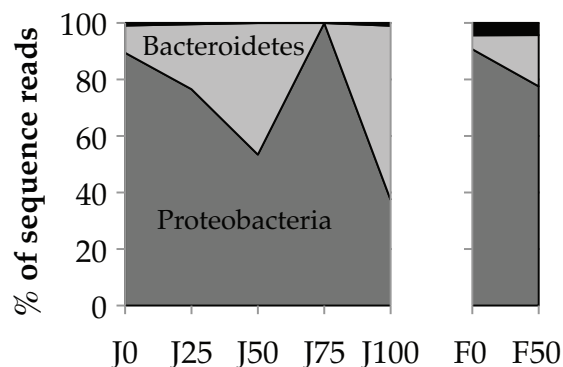


Figure 4: Phylum composition of enrichments from February (F) and June (J) exposed to no silver (0) and increasing concentrations of 5 nm PVP-AgNPs (25, 50, 75 and 100 $\mu\text{g/L}$). Phyla representing less than 0.005% (OP10, Actinobacteria, Verrucomicrobia, Planctomycetes, Acidobacteria, Chloroflexi, OD1, TM7, Unclassified - Other) are not included in this plot. Legend key: F=February, J=June, numbers = AgNPs concentration in $\mu\text{g/L}$.

The relative abundance of the Bacteroidetes and Proteobacteria phyla described, in Figure 4, correlates well with the increase of AgNPs throughout the range of used concentrations, except for the J75 sample. As the AgNP concentration increases, Proteobacteria become less abundant and the community is dominated by Bacteroidetes. Sample J75 is quite peculiar, as it is dominated (98%) by *Novosphingobium*, a genus belonging to Alphaproteobacteria Sphingomonadales' order. Interestingly, Sphingomonadales are bacteria with a large fraction of sphingolipids in the outer membrane of their cell wall. Sphingolipids are a special class of lipids, whose features are, among others, stability and resistance. They are designed to provide a protective barrier to the cell by creating an outer shell resistant to both mechanical and chemical attacks⁴⁴⁻⁴⁶. Therefore, we propose two potential explanations for the break in the decreasing trend of Proteobacteria in Figure 4: (1) experimental artifacts could have been introduced during the sampling, DNA extraction or sequencing processes. The rarefaction plots displays more than 10,000 sequences and a trend towards flattening of the curve (Figure 2), which would suggest that additional sequences would not impact the final result very much. Hence, sequencing is not likely to explain this observation. Nonetheless, it is conceivable that an amplification artifact favoring this particular species could have been introduced during the PCR step. (2) *Novosphingobium* is unlikely to outcompete other bacteria under normal environmental conditions. However, its specific cell wall composition could provide it with a competitive advantage in the presence of AgNPs when the concentration reaches 75 $\mu\text{g/L}$. We propose that the latter explanation is the most likely. The sample amended with 100 $\mu\text{g/L}$ AgNP does not follow the trend because no growth was observed in that

case and the microbial community closely resembles that in the absence of AgNPs. The cells are not viable but their DNA remains.

Details of the microbial community composition at the Class level are given in Figure 5. Alphaproteobacteria and Betaproteobacteria are the dominant groups (Figure 5A). Alphaproteobacteria appear to be more resistant to AgNPs as their occurrence increases with the increase of silver concentration while the contribution of Betaproteobacteria steadily decreases with increasing AgNP concentration. The February enrichments are only dominated by Alphaproteobacteria, which is the main difference with the June enrichments. In both cases silver has a negative impact on community diversity.

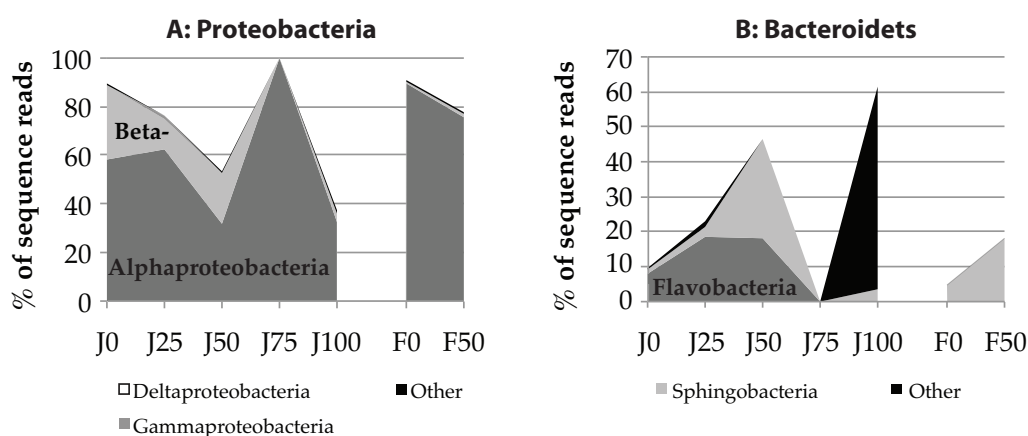


Figure 5: Class composition of enrichments exposed to no silver (0) and increasing concentrations of 5 nm PVP-AgNPs (25, 50, 75 and 100 $\mu\text{g/L}$). Classes representing less than 0.005% (OP10 genera incertae sedis, Actinobacteria, Verrucomicrobiae, Planctomycetacia, Deltaproteobacteria, Acidobacteria Gp3, Anaerolineae, OD1 genera incertae sedis, TM7 genera incertae sedis, Other (Unclassified)) have been merged together (Other).

In the case of Bacteroidetes (Figure 5B), two groups are present in all the samples, Flavobacteria and Sphingobacteria, except for June 100 $\mu\text{g/L}$ (J100), where unknown sub-class species are present. Sphingobacteria seem to display higher tolerance for AgNPs as compared to Flavobacteria. Interestingly, Sphingobacteria is also a class containing bacteria with higher sphingolipid cell wall content and therefore are morphologically similar to the *Novosphingobium* genus discussed above.

No additional trends were found in the analysis of the lower phylogenetic levels (order, family and genus), thus details of identified species are not discussed in additional detail.

A similar analysis was performed with the 18S rRNA amplicon 454-sequencing specific for fungi. Rarefaction plots (Figure S2) indicate that a higher number of sequenced amplicons would have added valuable information to uncover a larger number of observed species. No trend can be observed in these fungal rarefaction plots in terms of observed species as function of AgNPs. The PCoA analysis (Figure S3) showed that

98% of the diversity is accounted for by the sample origin, therefore AgNPs had no influence on the fungal population whatsoever. Finally, the speciation of the order level revealed that the fungal population of the enrichments is dominated at 98% by Dikary and an unreferenced fungal species for February and June enrichments respectively (Figure S4). OTU corresponding to the unknown species were analyzed with BLAST and the output was that it is an “uncultured fungus clone D53 18S ribosomal RNA gene” (GenBank: JN054692.1) isolated from activated sludge. The Dikarya blast results indicated the present species to be *Engyodontium album* strain IHEM4198 (JF797223.1).

The present study is the first to our knowledge to probe the impact of AgNPs on the microbial community composition in freshwater. A study had attempted to evaluate this impact on estuarine sediments and found no impact¹⁸. This was likely due to the mitigating effect of chloride on Ag toxicity. In this study, we obtained promising results showing a clear impact of AgNPs on microbial enrichments from lakewater. The first significant finding was that the greater sensitivity of natural microbial consortia to AgNPs as compared to that to laboratory stains was clearly established. A concentration as low as 25 µg/L is sufficient to alter the microbial community and induce a shift first to Bacteroides then to a specific Proteobacterium, *Novosphingobium*. The second major finding was that a sufficiently high AgNP concentration effects a significant change in the community with greater resistance to the toxic metal (Bacteroides and *Novosphingobium*). These findings underscore the critical importance of studying environmentally relevant microbial communities and AgNP concentrations when impact assessments are performed.

Additionally, the study leaves open the possibility that the enrichments that were used represented only a fraction of the microbial community in lakewater. In particular, it is noteworthy that a very small number of Gram-positive bacteria was detected in the entire study. Further studies utilizing lakewater directly without enrichment will be performed in the future to account for this possibility.

Finally, the fungal diversity study suggested that fungi might be more resistant to AgNPs than bacteris as no shift in fungal community composition was detected for the AgNP concentrations considered.

Overall, this study provides a first glimpse of the impact of AgNPs on microbial ecosystems and suggests that significant damage to the community can result from exposure to low levels of AgNPs.

4.4 Associated Content

Soluble silver measurements, Proteins content analysis, fungal rarefaction plots, fungal PCoA Unifrac plots, Fungal order phylogenic level composition, Krona representation of bacterial phylogeny associated to the tested conditions.

4.5 Acknowledgments

We would like to thank the central environmental analytical laboratory (CEAL) for granting access to shaker-incubators and ICP-MS instruments.

4.6 References

- (1) Kumar, N.; Shah, V.; Walker, V. K., Influence of a nanoparticle mixture on an arctic soil community. *Environmental Toxicology and Chemistry* **2012**, *31* (1), 131-135.
- (2) Mueller, N. C.; Nowack, B., Exposure modeling of engineered nanoparticles in the environment. *Environmental Science & Technology* **2008**, *42* (12), 4447-4453.
- (3) Woodrow Woodrow Wilson Center: Project on Emerging Nanotechnologies Inventory. http://www.nanotechproject.org/inventories/consumer/analysis_draft/.
- (4) Dallas, P.; Sharma, V. K.; Zboril, R., Silver polymeric nanocomposites as advanced antimicrobial agents: Classification, synthetic paths, applications, and perspectives. *Advances in Colloid and Interface Science* **2011**, *166* (1-2), 119-135.
- (5) Sotiriou, G. A.; Pratsinis, S. E., Antibacterial Activity of Nanosilver Ions and Particles. *Environmental Science & Technology* **2010**, *44* (14), 5649-5654.
- (6) Sharma, V. K.; Yngard, R. A.; Lin, Y., Silver nanoparticles: Green synthesis and their antimicrobial activities. *Advances in Colloid and Interface Science* **2009**, *145* (1-2), 83-96.
- (7) Lok, C. N.; Ho, C. M.; Chen, R.; He, Q. Y.; Yu, W. Y.; Sun, H.; Tam, P. K. H.; Chiu, J. F.; Che, C. M., Silver nanoparticles: partial oxidation and antibacterial activities. *Journal of Biological Inorganic Chemistry* **2007**, *12* (4), 527-534.
- (8) Marambio-Jones, C.; Hoek, E., A review of the antibacterial effects of silver nanomaterials and potential implications for human health and the environment. *Journal of Nanoparticle Research* **2010**, *12* (5), 1531-1551.
- (9) Benn, T. M.; Westerhoff, P., Nanoparticle Silver Released into Water from Commercially Available Sock Fabrics. *Environmental Science & Technology* **2008**, *42* (11), 4133-4139.
- (10) Durán, N.; Marcato, P.; Alves, O.; Da Silva, J.; De Souza, G.; Rodrigues, F.; Esposito, E., Ecosystem protection by effluent bioremediation: silver nanoparticles impregnation in a textile fabrics process. *Journal of Nanoparticle Research* **2010**, *12* (1), 285-292.
- (11) Gottschalk, F.; Nowack, B., The release of engineered nanomaterials to the environment. *Journal of Environmental Monitoring* **2011**, *13* (5), 1145-1155.
- (12) Kim, B.; Park, C. S.; Murayama, M.; Hochella, M. F., Discovery and Characterization of Silver Sulfide Nanoparticles in Final Sewage Sludge Products. *Environmental Science & Technology* **2010**, *44* (19), 7509-7514.
- (13) Blaser, S. A.; Scheringer, M.; MacLeod, M.; Hungerbühler, K., Estimation of cumulative aquatic exposure and risk due to silver: Contribution of nano-functionalized plastics and textiles. *Science of The Total Environment* **2008**, *390* (2-3), 396-409.
- (14) Handy, R. O.; Richard, Viewpoint: Formulating the Problems for Environmental Risk Assessment of Nanomaterials. *Environmental Science & Technology* **2007**, *41* (16), 5582-5588.
- (15) Nowack, B.; Bucheli, T. D., Occurrence, behavior and effects of nanoparticles in the environment. *Environmental Pollution* **2007**, *150* (1), 5-22.
- (16) Wiesner, M. R.; Lowry, G. V.; Jones, K. L.; Hochella, J. M. F.; Di Giulio, R. T.; Casman, E.; Bernhardt, E. S., Decreasing Uncertainties in Assessing Environmental Exposure, Risk, and Ecological Implications of Nanomaterials. *Environmental Science & Technology* **2009**, *43* (17), 6458-6462.
- (17) Nowack, B.; Krug, H. F.; Height, M., 120 Years of Nanosilver History: Implications for Policy Makers. *Environmental Science & Technology* **2011**, *45* (4), 1177-1183.
- (18) Bradford, A.; Handy, R. D.; Readman, J. W.; Atfield, A.; Muhling, M., Impact of silver nanoparticle contamination on the genetic diversity of natural bacterial assemblages in estuarine sediments. *Environmental Science & Technology* **2009**, *43* (12), 4530-6.
- (19) Johansen, A.; Pedersen, A. L.; Jensen, K. A.; Karlson, U.; Hansen, B. M.; Scott-Fordsmand, J. J.; Winding, A., Effects of C60 fullerene nanoparticles on soil bacteria and protozoans. *Environmental Toxicology and Chemistry* **2008**, *27* (9), 1895-1903.
- (20) Kumar, N.; Shah, V.; Walker, V. K., Perturbation of an arctic soil microbial community by metal nanoparticles. *Journal of Hazardous Materials* **2011**, *190* (1-3), 816-822.
- (21) Mishra, V. K.; Kumar, A., Impact of metal nanoparticles on the plant growth promoting rhizobacteria. *Digest Journal of Nanomaterials and Biostructures* **2009**, *4* (3), 587-592.
- (22) Muhling, M.; Bradford, A.; Readman, J. W.; Somerfield, P. J.; Handy, R. D., An investigation into the effects of silver nanoparticles on antibiotic resistance of naturally occurring bacteria in an estuarine sediment. *Marine Environmental Research* **2009**, *68* (5), 278-283.

- (23) Plassart, P.; Akpa Vincelas, M.; Gangneux, C.; Mercier, A.; Barray, S.; Laval, K., Molecular and functional responses of soil microbial communities under grassland restoration. *Agriculture, Ecosystems & Environment* **2008**, *127* (3-4), 286-293.
- (24) Bone, A. J.; Colman, B. P.; Gondikas, A. P.; Newton, K. M.; Harrold, K. H.; Cory, R. M.; Unrine, J. M.; Klaine, S. J.; Matson, C. W.; Di Giulio, R. T., Biotic and Abiotic Interactions in Aquatic Microcosms Determine Fate and Toxicity of Ag Nanoparticles: Part 2-Toxicity and Ag Speciation. *Environmental Science & Technology* **2012**, *46* (13), 6925-6933.
- (25) Dror-Ehre, A.; Mamane, H.; Belenkova, T.; Markovich, G.; Adin, A., Silver nanoparticle - *E. coli* colloidal interaction in water and effect on *E. coli* survival. *Journal of Colloid and Interface Science* **2009**, *339* (2), 521-6.
- (26) Suresh, A. K.; Pelletier, D. A.; Wang, W.; Moon, J.-W.; Gu, B.; Mortensen, N. P.; Allison, D. P.; Joy, D. C.; Phelps, T. J.; Doktycz, M. J., Silver Nanocrystallites: Biofabrication using *Shewanella oneidensis*, and an Evaluation of Their Comparative Toxicity on Gram-negative and Gram-positive Bacteria. *Environmental Science & Technology* **2010**, *44* (13), 5210-5215.
- (27) Bowman, C. R.; Bailey, F. C.; Elrod-Erickson, M.; Neigh, A. M.; Otter, R. R., Effects of silver nanoparticles on zebrafish (*Danio rerio*) and *Escherichia coli* (ATCC 25922): A comparison of toxicity based on total surface area versus mass concentration of particles in a model eukaryotic and prokaryotic system. *Environmental Toxicology and Chemistry* **2012**, *31* (8), 1793-1800.
- (28) Sondi, I.; Salopek-Sondi, B., Silver nanoparticles as antimicrobial agent: a case study on *E. coli* as a model for Gram-negative bacteria. *Journal of Colloid and Interface Science* **2004**, *275* (1), 177-182.
- (29) Simon-Deckers, A.; Loo, S.; Mayne-L'Hermite, M.; Herlin-Boime, N.; Menguy, N.; Reynaud, C.; Gouget, B.; Carriere, M., Size-, Composition- and Shape-Dependent Toxicological Impact of Metal Oxide Nanoparticles and Carbon Nanotubes toward Bacteria. *Environmental Science & Technology* **2009**, *43* (21), 8423-8429.
- (30) Su, H. L.; Chou, C. C.; Hung, D. J.; Lin, S. H.; Pao, I. C.; Lin, J. H.; Huang, F. L.; Dong, R. X.; Lin, J. J., The disruption of bacterial membrane integrity through ROS generation induced by nanohybrids of silver and clay. *Biomaterials* **2009**, *30* (30), 5979-5987.
- (31) Park, H. J.; Kim, J. Y.; Kim, J.; Lee, J. H.; Hahn, J. S.; Gu, M. B.; Yoon, J., Silver-ion-mediated reactive oxygen species generation affecting bactericidal activity. *Water Research* **2009**, *43* (4), 1027-1032.
- (32) Jung, W. K.; Koo, H. C.; Kim, K. W.; Shin, S.; Kim, S. H.; Park, Y. H., Antibacterial activity and mechanism of action of the silver ion in *Staphylococcus aureus* and *Escherichia coli*. *Applied and Environmental Microbiology* **2008**, *74* (7), 2171-2178.
- (33) Pal, S.; Tak, Y. K.; Song, J. M., Does the Antibacterial Activity of Silver Nanoparticles Depend on the Shape of the Nanoparticle? A Study of the Gram-Negative Bacterium *Escherichia coli*. *Applied and Environmental Microbiology* **2007**, *73* (6), 1712-1720.
- (34) Rispoli, F.; Angelov, A.; Badia, D.; Kumar, A.; Seal, S.; Shah, V., Understanding the toxicity of aggregated zero valent copper nanoparticles against *Escherichia coli*. *Journal of Hazardous Materials* **2010**, *180* (1-3), 212-216.
- (35) El Badawy, A. M.; Silva, R. G.; Morris, B.; Scheckel, K. G.; Suidan, M. T.; Tolaymat, T. M., Surface Charge-Dependent Toxicity of Silver Nanoparticles. *Environmental Science & Technology* **2011**, *45* (1), 283-287.
- (36) Wang, H.; Law, N.; Pearson, G.; van Dongen, B. E.; Jarvis, R. M.; Goodacre, R.; Lloyd, J. R., Impact of Silver(I) on the Metabolism of *Shewanella oneidensis*. *Journal of Bacteriology* **2010**, *192* (4), 1143-1150.
- (37) Fabrega, J.; Fawcett, S. R.; Renshaw, J. C.; Lead, J. R., Silver nanoparticle impact on bacterial growth: effect of pH, concentration, and organic matter. *Environmental Science & Technology* **2009**, *43* (19), 7285-90.
- (38) Fabrega, J.; Renshaw, J. C.; Lead, J. R., Interactions of Silver Nanoparticles with *Pseudomonas putida* Biofilms. *Environmental Science & Technology* **2009**, *43* (23), 9004-9009.
- (39) Kalishwaralal, K.; BarathManiKanth, S.; Pandian, S. R. K.; Deepak, V.; Gurunathan, S., Silver nanoparticles impede the biofilm formation by *Pseudomonas aeruginosa* and *Staphylococcus epidermidis*. *Colloids and Surfaces B: Biointerfaces* **2010**, *79* (2), 340-344.
- (40) Arnaout, C. L.; Gunsch, C. K., Impacts of Silver Nanoparticle Coating on the Nitrification Potential of *Nitrosomonas europaea*. *Environmental Science & Technology* **2012**, *46* (10), 5387-5395.
- (41) Choi, O.; Hu, Z., Size dependent and reactive oxygen species related nanosilver toxicity to nitrifying bacteria. *Environmental Science & Technology* **2008**, *42* (12), 4583-8.

-
- (42) Caporaso, J. G.; Kuczynski, J.; Stombaugh, J.; Bittinger, K.; Bushman, F. D.; Costello, E. K.; Fierer, N.; Pena, A. G.; Goodrich, J. K.; Gordon, J. I.; Huttley, G. A.; Kelley, S. T.; Knights, D.; Koenig, J. E.; Ley, R. E.; Lozupone, C. A.; McDonald, D.; Muegge, B. D.; Pirrung, M.; Reeder, J.; Sevinsky, J. R.; Turnbaugh, P. J.; Walters, W. A.; Widmann, J.; Yatsunenko, T.; Zaneveld, J.; Knight, R., QIIME allows analysis of high-throughput community sequencing data. *Nat Meth* **2010**, *7* (5), 335-336.
 - (43) Ondov, B. D.; Bergman, N. H.; Phillippy, A. M., Interactive metagenomic visualization in a Web browser. *Bmc Bioinformatics* **2011**, *12*.
 - (44) Gault, C. R.; Obeid, L. M.; Hannun, Y. A., An overview of sphingolipid metabolism: from synthesis to breakdown. *Adv Exp Med Biol* **2010**, *688*, 1-23.
 - (45) Christie, W. W. Sphingolipids: an introduction to sphingolipids and membrane rafts. <http://lipidlibrary.aocs.org>.
 - (46) Chavis, J. C. What is a Sphingolipid? <http://www.wisegeek.com/what-is-a-sphingolipid.htm>.

4.7 Supporting Information

Expected concentration in $\mu\text{g/L}$	Measured concentration in $\mu\text{g/L}$	
	February enrichment	June enrichment
0	1	1
25	24	27
50	52	50
75	65	72
100	89	91

Table S1: Concentration of silver in solution measured by ICP-MS for February and June enrichments exposed to 5 nm PVP-AgNPs at expected concentrations of 0, 25, 50, 75, 100 $\mu\text{g/L}$.

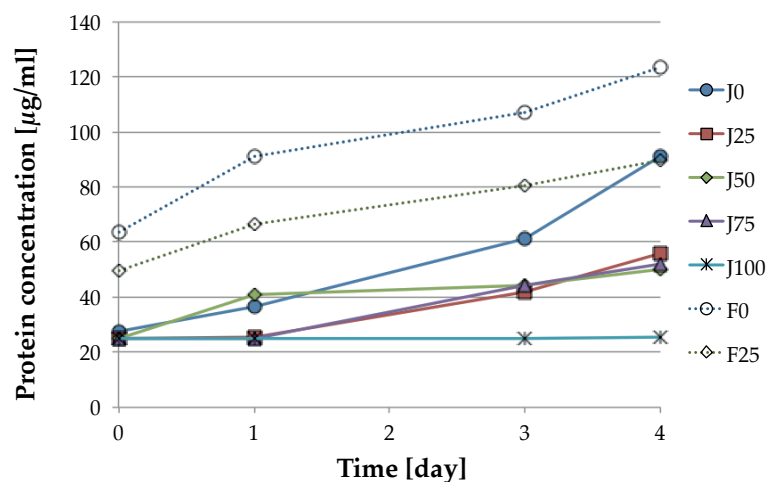


Figure S1: Time resolved protein concentration measurements corresponding to bacterial growth of figure 1 (lake Geneva enrichment from February (F) and June (J) under concentration of 5 nm PVP-AgNPs: 0, 25, 50, 75 and 100 $\mu\text{g/L}$). Legend key: F=February, J=June, numbers = AgNPs concentration in $\mu\text{g/L}$.

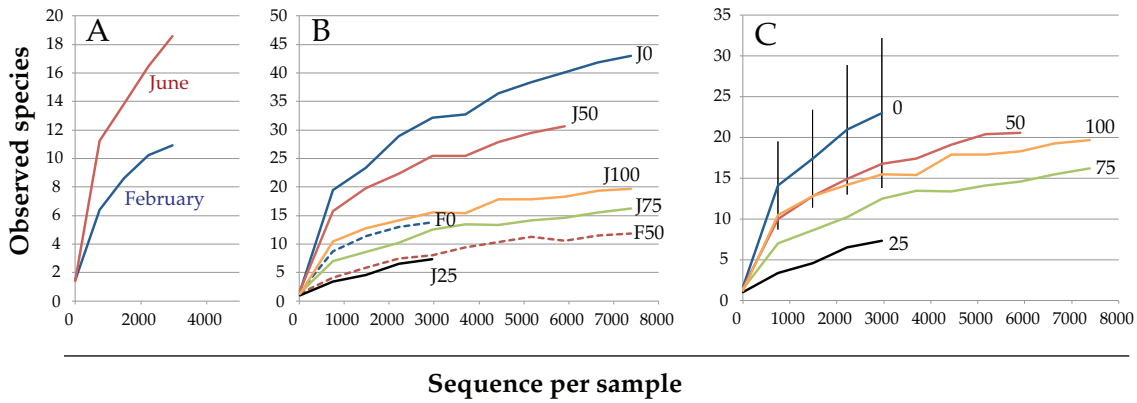


Figure S2: Rarefaction analysis for 18S rRNA sequenced amplicons from February and June enrichment exposed to PVP-AgNPs at 0, 25, 50, 75 and 100 $\mu\text{g/L}$, as a function of (A) sample origin, (B) sample ID and (C) AgNPs concentrations. The legend numbers correspond to the AgNPs concentration in $\mu\text{g/L}$ and February samples are labeled with an “F” and June samples with “J”.

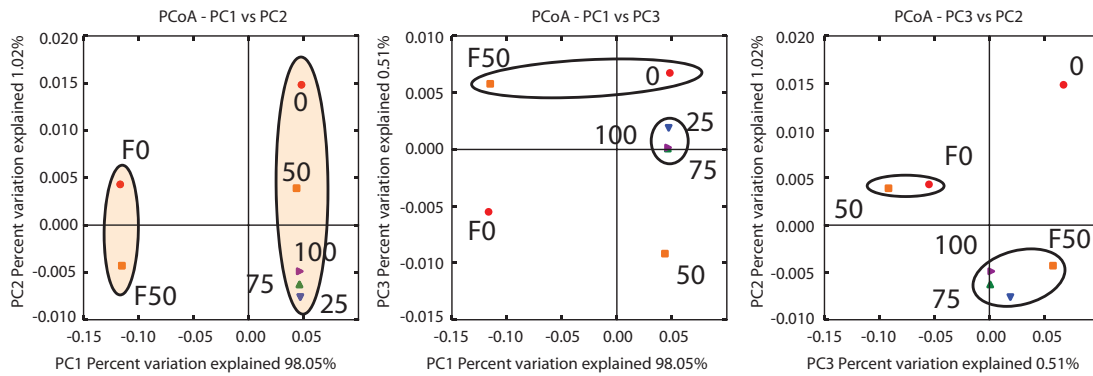


Figure S3: Fast Unifrac principal coordinate analysis (PCoA) for fungal population from February (F) and June enrichments exposed to 0, 25, 50, 75 and 100 $\mu\text{g/L}$ of 5 nm PVP-AgNPs. The plot legend key numbers correspond to the AgNPs concentration in $\mu\text{g/L}$ and February samples are labeled with an “F”.

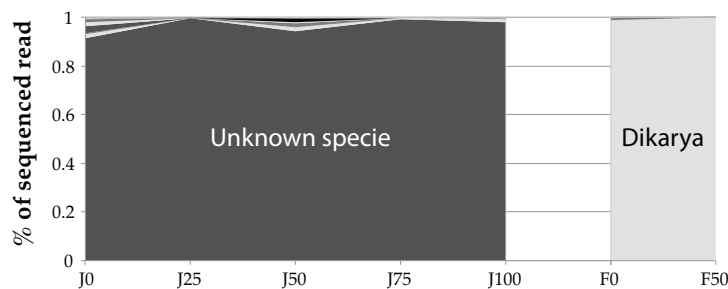
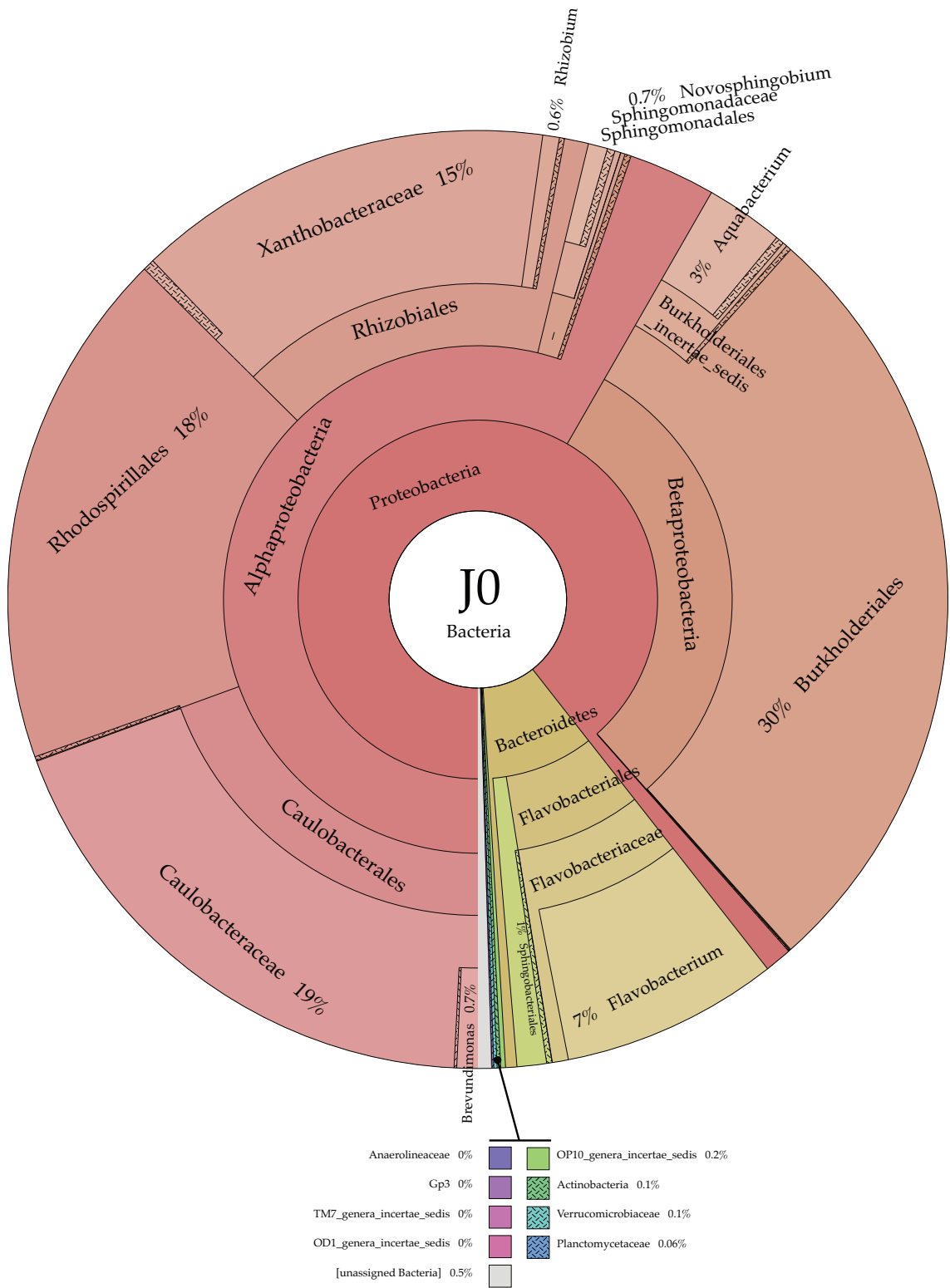
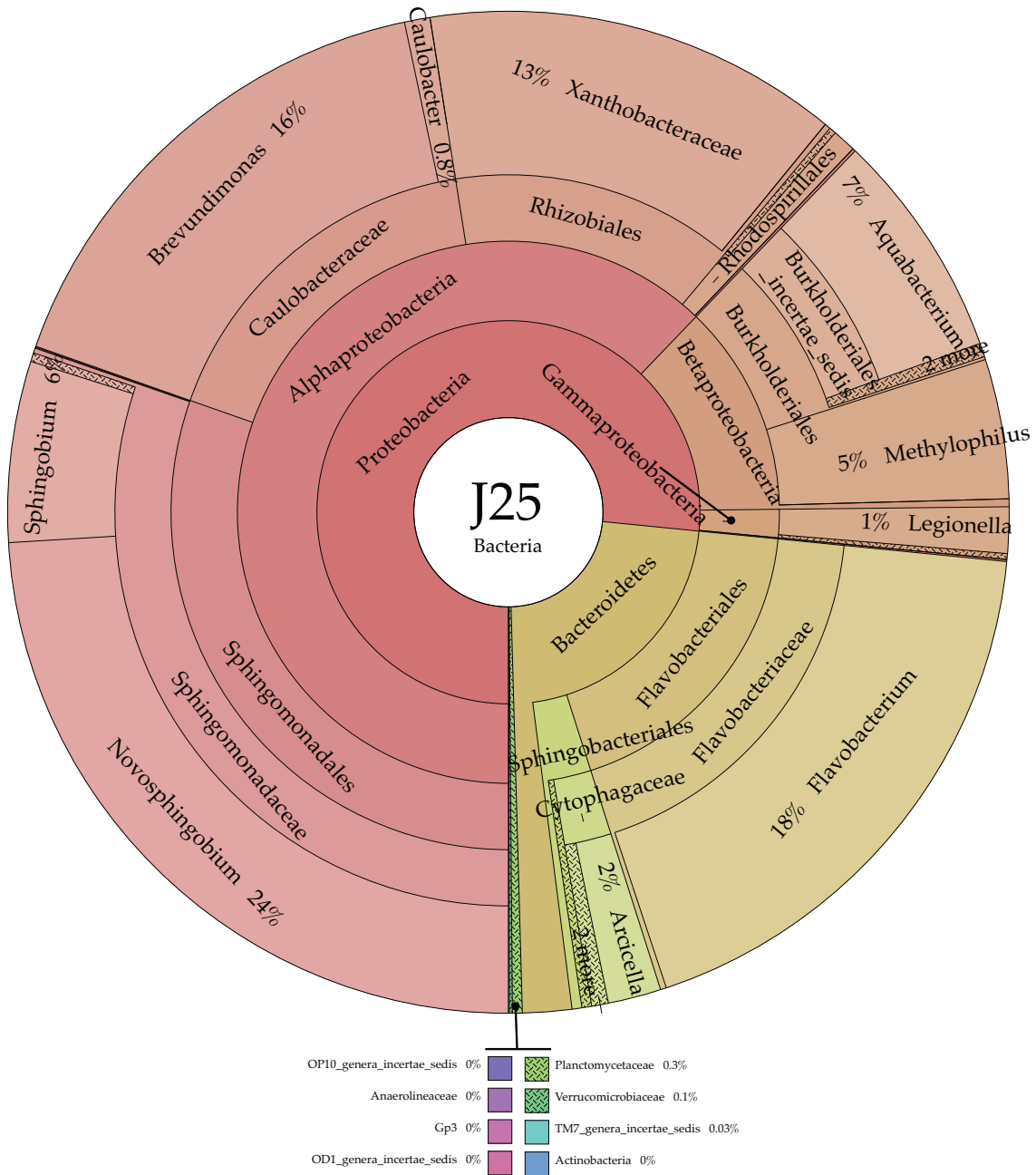
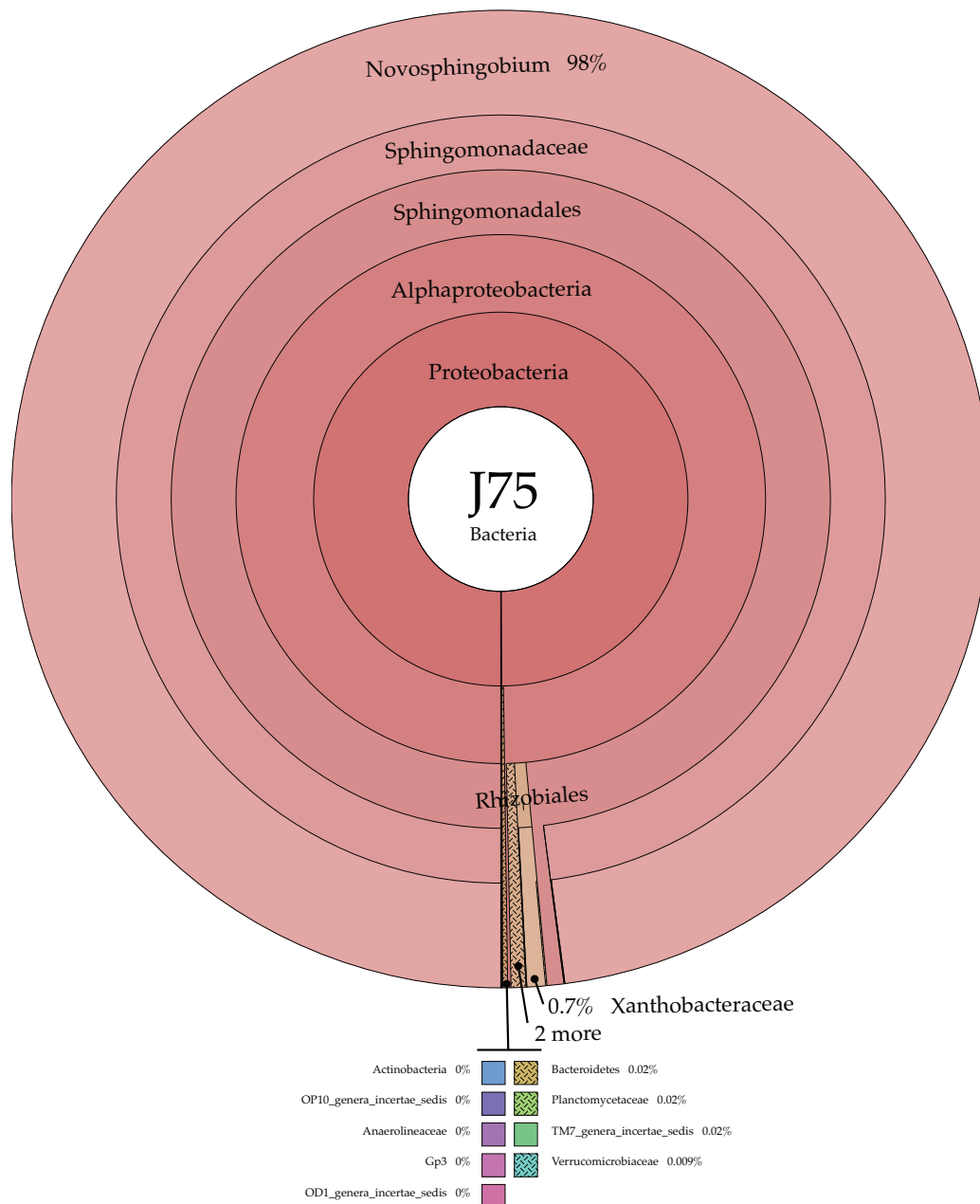


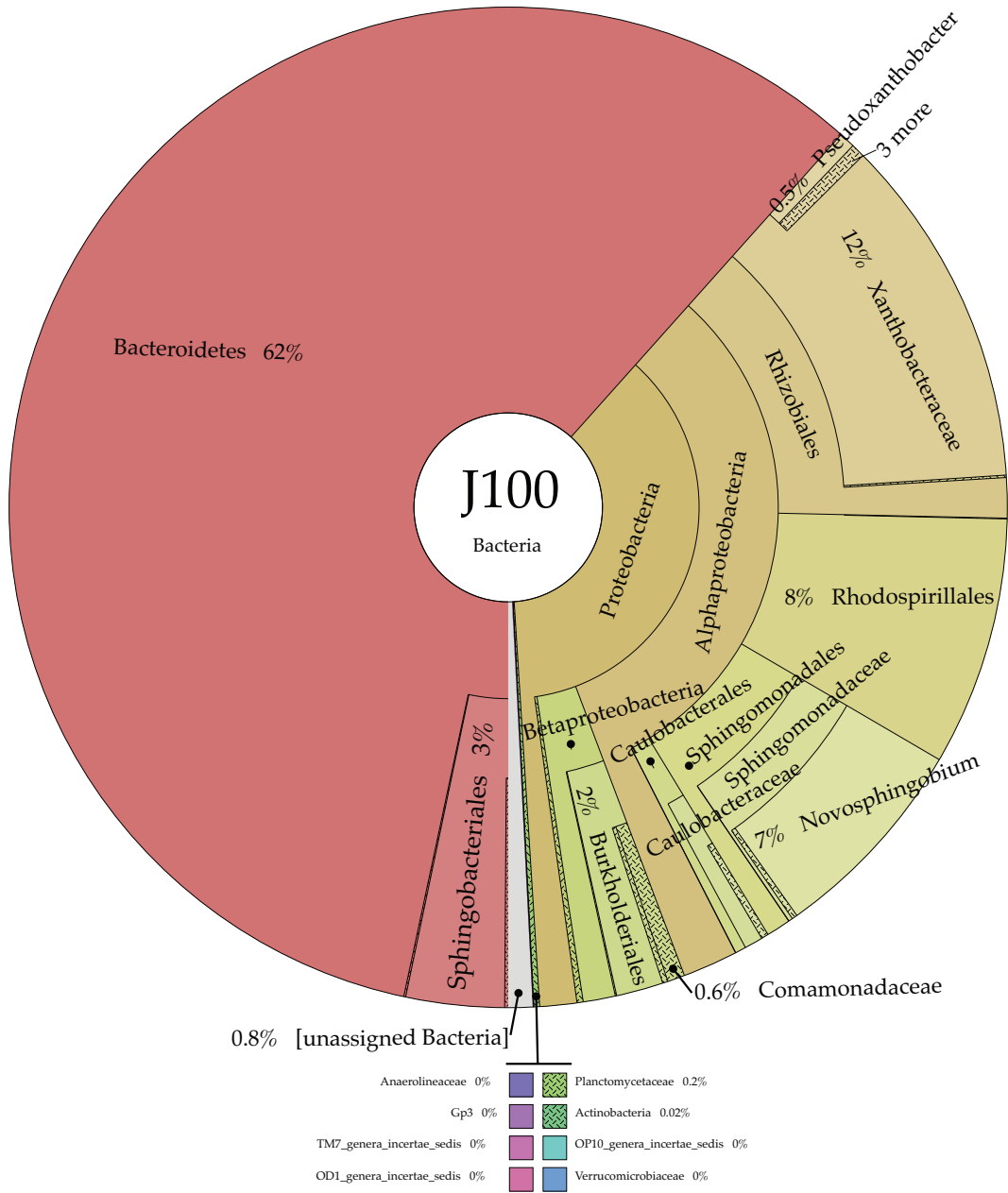
Figure S4: Order level composition for fungal analysis of enrichments exposed to no silver (0) and increasing concentrations of 5 nm PVP-AgNPs (25, 50, 75 and 100 $\mu\text{g/L}$).

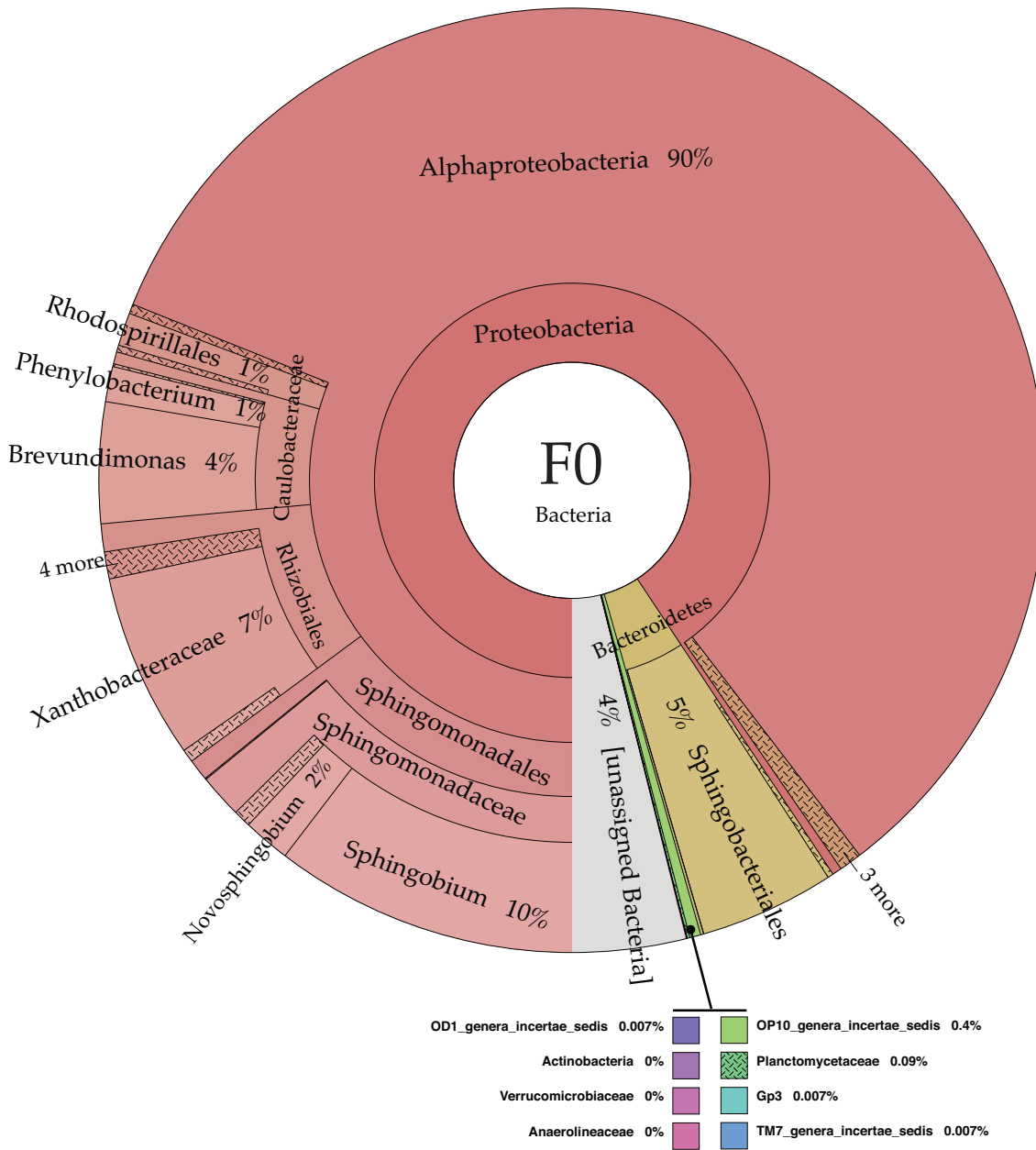
Figure S5: Complete representation of bacterial phylogenetic levels, using Krona plots, of samples J0, J25, J50, J75, J100, F0 and F50. The considered phylogenetic levels from the center to the outside are: Kingdom, Phylum, Class, Order, Family, and Genus.

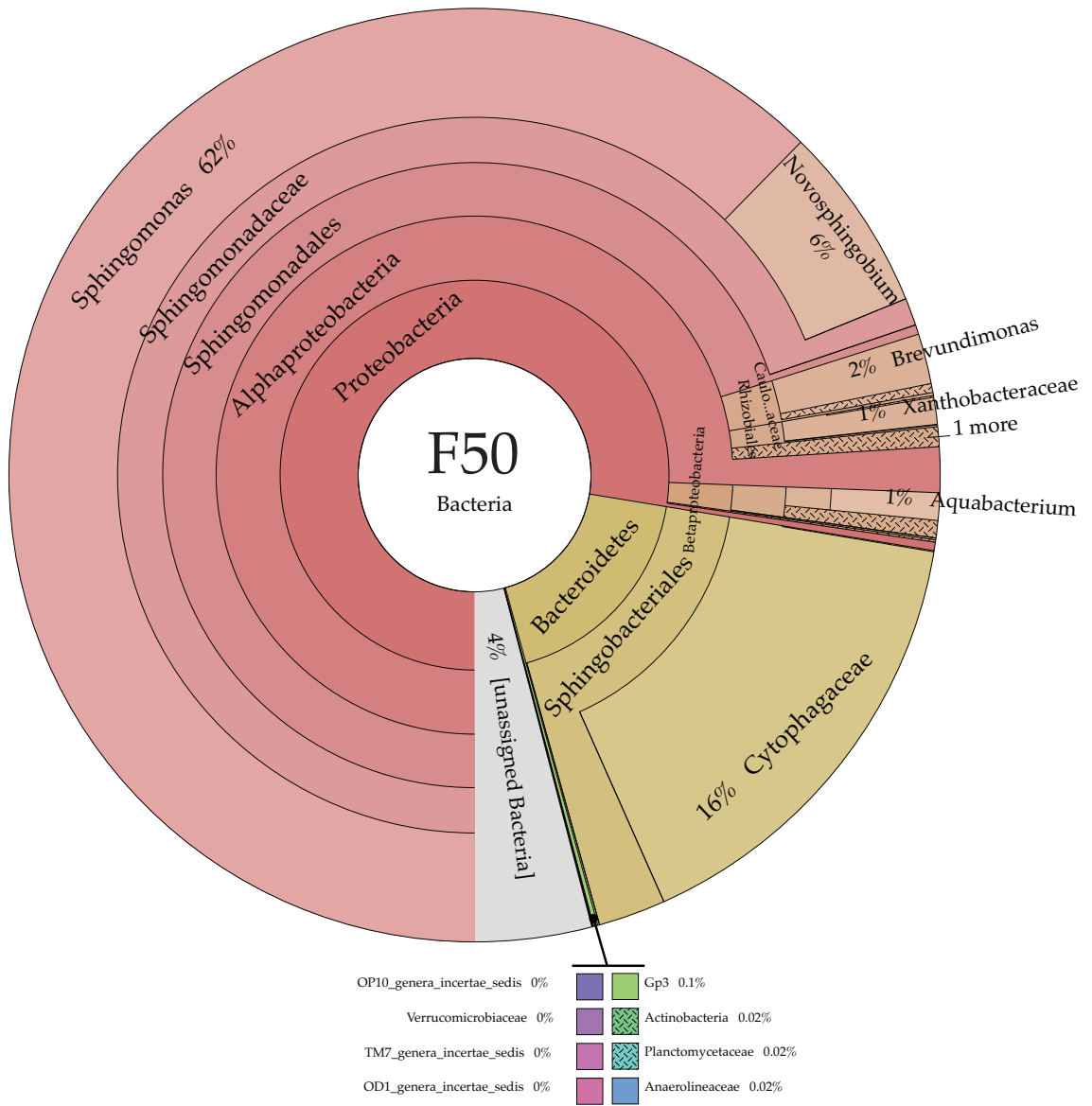












5 Conclusions

5.1 Chapter 1

In this chapter, we investigated the potential for bacterial proteins to control the size distribution and morphology of chemogenic selenium nanoparticles (chemo-SeNPs). We showed that a large number of proteins (in quantity and in diversity) were tightly associated to *E. coli* biogenic SeNPs (bio-SeNPs). A proteomic study was conducted and proteins associated to bio-SeNPs were compared to *E. coli* cell free extract proteins binding to chemo-SeNPs and to magnetite nanoparticles.

The proteomic study uncovered a large variety of proteins associated with NPs of which four proteins (AdhP, Idh, OmpC, AceA) were specific to SeNPs. None of the identified proteins had a reported function related to NP formation or metal reduction, but were rather implicated in energy, carbohydrate or fatty acid metabolism. Similarly, no shared chemical properties (i.e., isoelectric point, cofactor or size) were identified. We concluded that the binding ability of the proteins were dependent either on their spatial configuration and/or their physico-chemical properties of some amino acid(s). Finally, we showed that chemo-SeNPs synthesized in the presence of proteins exhibited a narrower size distribution and a more spherical morphology as compared to chemo-SeNPs synthesized in the absence of proteins.

One protein in particular, the alcohol dehydrogenase, propanol-preferring protein (AdhP), was studied in more detail. To do so, we cloned the coding gene of the protein and purified the protein for *in-vitro* experiments. *In-vitro* experiments confirmed the strong affinity of AdhP for the SeNP surface and revealed a potential for controlling the size distribution of the SeNPs, which showed a three-fold narrower size distribution.

The findings of this study are of primary importance as they support the assertion that protein may become an important tool for biologically based, semi-synthetic production of NPs of uniform size and properties. This study confirmed that the synthesis of NPs in simple aqueous system and under standard ambient temperature and pressure conditions is possible via the interaction with biomolecules such as bacterial proteins. This approach may even represent a valuable economic alternative to conventional chemical synthesis and calls for a detailed cost analysis.

5.2 Chapter 2

In chapter 2 we studied the release of silver from silver nanoparticles (AgNPs) in more realistic conditions than previously reported. We conducted the experiment in river and lake water for up to several months. AgNPs of 5, 10, 20, 50 and 100 nm were considered in this study. Additionally, each size except for 5 and 10 nm, was available in three different coatings: polyvinylpyrrolidone (PVP), tannic acid (Tan) and citric acid (Cit). We showed that important differences could be observed between small (5, 10 nm) and large (50 nm) AgNPs. The 50 nm particles were more resistant to dissolution in oxic water on a mass basis. Also, even though the total loss could be important (>90%), we never observed complete dissolution of the initially deployed AgNPs. This was in agreement with previously reported long-term laboratory dissolution experiments. We also highlighted the effect of surface area. A normalization of silver loss to total surface area showed a decrease in the difference between small and large AgNPs, suggesting an important role of surface area in controlling Ag loss.

In most situations, an initial rapid loss was observed, whereas in some cases an additional slower process was detected. Laboratory experiments were conducted to test two hypotheses to account for Ag loss: an oxidative dissolution process or the release of chemisorbed Ag^+ . Briefly, AgNPs were embedded in agarose gel pucks, exposed to oxic and anoxic river water and silver content of the solution analyzed by ICP-MS. We observed no difference between oxic and anoxic condition and observed a rapid (5 min.) appearance of soluble Ag^+ in solution. We evaluated the nature of the soluble silver by ultracentrifugation and showed that it was indeed Ag^+ and not AgNPs lost from the gel. Altogether, the results point to a rapid initial Ag^+ loss attributable to desorption of Ag^+ from nanoparticle surfaces rather than a loss due to oxidative dissolution. Nonetheless, we are unable to rule out the contribution of oxidative dissolution to silver loss observed in the deployment experiment due to its much slower rate. Additionally, AgNP coatings were shown to play a role on dissolution. PVP- and Tan-AgNPs were more prone to Ag^+ release than Cit-AgNPs.

This study clearly showed that small AgNPs (5nm - PVP and Tan) dissolve rapidly and almost completely, while larger ones (50nm) and ones coated with citric acid had the potential to persist in natural waters for extended periods of time: on the order of a year for small AgNPs and much longer for big ones or ones coated with citrate. Therefore, released AgNPs in the environment could serve as a continuous source of Ag ions and studies trying to unravel whether the mechanism of toxicity of AgNPs involves Ag^+ ions remain of primary importance.

5.3 Chapter 3

In this chapter, we evaluated the role of AgNP size and coating on the toxicity response of *Escherichia coli* and *Bacillus subtilis*. These bacteria are laboratory strains, well studied and represent model organisms for Gram-negative and Gram-positive bacteria. Their relevance on the environmental level is not obvious, but their study could help identify conditions for which AgNPs might be toxic.

We chose to study the effect of size and coating by systematically varying one factor at a time. We selected AgNPs of 5, 10, 20, 50 and 100nm exhibiting one of three surface coatings (polyvinylpyrrolidone [PVP-], tannic acid [Tan-] and citric acid [Cit-]), totaling 14 different tested AgNPs in this study.

We showed that the toxicity response was correlated to the AgNP concentration and inversely proportional to the size (small NPs are the most toxic ones). Dose-response experiments revealed that 50 nm AgNPs (PVP-, Tan-) were 2-4 fold less toxic than 5 nm and 10nm AgNPs in the case of *E. coli* and 3-4 time less toxic in the case of *Bacillus*. Cit-AgNPs exhibited a much lower toxicity as compared to their PVP and tannic counterparts of about 3 fold for 50nm Cit- in *E. coli* and >5 fold in *B. subtilis*. 10 nm Citric AgNPs showed no toxicity to *Bacillus* in the range of tested concentration and were 2 fold less toxic than PVP- and Tan- to *E. coli*. These findings point to the major role played by AgNPs size and capping agent in their toxicity.

We conducted a time-resolved Dynamic Light Scattering (DLS) experiment to assess the aggregation potential of AgNPs in the presence of bacterial cells. We showed that all had a tendency for aggregation, but 10 nm Cit-AgNPs aggregated the fastest, providing a potential explanation for their low toxicity. Additionally, measurements of zeta potential (under experimental conditions) suggested that the surface charge could be also be implicated in the toxicity potential of NPs. Cit-AgNPs had a charge (-30 to -40mV) close to that of bacterial cells and therefore, electrostatic repulsion might limit direct interaction. Moreover, soluble silver was measured and found to be extremely low for Cit-AgNPs both in the presence and absence of cells. These findings, plus the observation of potential morphological change of bacterial cells by DLS, suggest that direct interaction must exist and that Cit-AgNPs serve as a highly localized source of Ag^+ , potentially damaging the membrane (i.e., the Trojan horse effect). Although it is still mechanistically unclear, interaction of negatively charged NPs and bacterial was previously reported and the results here are in accordance to that observation.

As mentioned above, the microorganisms considered in this study are clearly not representative of environmental conditions. Therefore, a necessary alternative is to test natural microbial communities for their toxicity response to AgNPs in order to obtain a more accurate understanding of the true environmental impact of AgNPs.

5.4 Chapter 4

In this part, we tackled the question of the impact of nanosilver colloids on aquatic environments, for which very little is known so far. We tested the effect of 5 nm polyvinylpyrrolidone (PVP)-coated AgNPs on the diversity of a microbial community from Lake Geneva. The bacterial diversity was evaluated by high-throughput 454-sequencing of 16S rRNA (bacteria) and 18S rRNA (fungi) amplicons from gDNA extracted from microbial enrichments exposed to various concentrations of AgNPs. Two sets of enrichments were tested. One was set up from lake Geneva water collected in February 2012 and the other was from water collected in June 2012.

Biodiversity analysis showed a shift in the bacterial populations correlated to the concentration of AgNPs, whereas fungal differences in diversity were due to sample origin (Feb. vs June) as shown by PCoA analysis. Secondly, the concentration required for cell growth inhibition were much lower (25-75 $\mu\text{g/L}$) than the one required for the laboratory strain used in chapter 3 (220-500 $\mu\text{g/L}$). These low toxic concentrations are compatible with the results from the biodiversity analysis that showed that bacterial communities were composed only of Proteobacteria and Bacteroidetes. The latter exhibited a higher tolerance for silver nanoparticles, except in the case of 75 $\mu\text{g/L}$ Ag condition in which a single genus, *Novosphingobium*, dominated the community at 98%. Interestingly, the *Novosphingobium* genus, but also the Bacteroidetes Sphingobacteria, includes bacteria that exhibit sphingolipids on their outer membrane. Sphingolipids are lipids that are unusually stable and resistant. A large amount of these in the cell wall is known to provide a protective barrier against a large variety of mechanical and chemical stresses. It is therefore, very possible that this peculiar cell wall composition provide them with a competitive advantage in the presence of AgNPs. The drawback of the absence of Gram-positive bacteria in the consortia raised a concern about the experimental setup. It is puzzling that Gram-positive bacteria, some of which are ubiquitous, were not present in the bacterial diversity at least at a low fraction. Further experiments would be required to identify the factors responsible for that negative selection effect of Gram-positive bacteria.

Nonetheless, concentration related findings are fundamental as they highlight the inadequacy between concentration used in many published studies that were above the mg/L of silver and their environmental relevance.

DOBIAS JAN

ADDRESS: CH. DE BEAU-VAL 3 • 1012 LAUSANNE

PHONE NUMBER: +41 76 520 75 42 • E-MAIL: JANDOBIAS@BLUEWIN.CH

CIVIL STATUS

Family Status : Single
Nationality : Swiss
Date of Birth : 26 - 02 - 1978
Place of Birth : Prague

EDUCATION

2008 – 2012 : Ecole polytechnique fédérale de Lausanne (EPFL) Lausanne
Doctoral studies in the environmental program EDEN
2002 – 2004 : University Geneva
Master's Degree in Biology
1999 – 2002 : University Geneva
Bachelor's Degree in Biology

LANGUAGES PROFICIENCY

French : Mother Tongue
English : Good written and oral skills
Czech : Fluent Conversation

PUBLICATIONS

Dobias, J. and Bernier-Latmani, R., Silver release from silver nanoparticles in natural waters *Environmental Science & Technology* **2012**, submitted
Dobias, J.; Suvorova, E. I.; Bernier-Latmani, R., Role of proteins in controlling selenium nanoparticle size. *Nanotechnology* **2011**, 22 (19), 195605.
Wigginton, N. S.; De Titta, A.; Piccapietra, F.; Dobias, J.; Nesatty, V. J.; Suter, M. J. F.; Bernier-Latmani, R., Binding of Silver Nanoparticles to Bacterial Proteins Depends on Surface

Modifications and Inhibits Enzymatic Activity. *Environmental Science & Technology* **2010**, 44 (6), 2163-2168.

Passardi, F.; Dobias, J.; Valerio, L.; Guimil, S.; Penel, C.; Dunand, C., Morphological and physiological traits of three major *Arabidopsis thaliana* accessions. *Journal of plant physiology* **2007**, 164 (8), 980-92.

ORAL PRESENTATION

Dobias J., Costanza A., Suvorova E., Trotta M. & Bernier-Latmani R., Toxicity of Silver Nanoparticles to Environmental Microbial Consortia. *Goldschmidt* **2011**, Prague, CZ

Dobias J., Suvorova E.I. & Bernier-Latmani R. Role of Proteins in Controlling Nanoparticle Size Distribution. *Goldschmidt* **2010**, Knoxville, TN, USA

POSTER PRESENTATION

Dobias J. & Bernier-Latmani R., Role of Proteins in the Formation of Selenium Nanoparticles. *Goldschmidt* **2009**, Davos, GR, CH

DIPLOMA WORK: FUNCTION AND LOCALISATION OF ATRPX42, A CLASS III PEROXIDASE

The main aspect of the work was to understand the role of Atrpx42 in *Arabidopsis thaliana* (*A.th.*). In order to do so, I used three complementary techniques: hairpin knockout, CaMV35S overexpression and GFP fusion (Green Fluorescent Protein). I designed and created most of the cloning vectors needed for the study. I introduced these vectors in plants and observed the effect of the genetic modification. Atrpx42 seems to have an implication in the growth control pathway of the plant. The size of aerial and radicular structures is altered in absence of the gene. He is largely expressed in roots and possessed a specific localisation.

PROFESSIONAL EXPERIENCE

- Mar. 2006 – Nov. 2012 : Environmental Microbiology Laboratory (EML) EPFL Lausanne
 IT responsible
 Environmental Microbiology lab course, teaching assistant
 Programing and design of the EML website
- Nov. – Dec. 2005 : Administrative Assistant at Philip Morris International Lausanne
 Filing works (OMNI RIM system)
- Oct. – Nov. 2005 : Consulting for ITSC-E (Philip Morris International) Renens/VD
 Czech Language Expert for SAP upgrade to Unicode standard
- Feb. 2003 – Sep. 2004 : University Geneva
 Assistant professor, in charge of vegetal physiology practical work
 for 2nd year students and of molecular biology (laboratory practical
 work) for 3rd year students.
- Oct. 2001 – Jul. 2002 : Arcor sécurité S.A. Geneva
 Security agent at Caterpillar Inc.
- Summer 2001 : University Geneva
 Work in the printing department
- Fall 2000 : Citec SA Geneva
 Data Capture
- Summer 2000 : EPFL (Federal Polytechnical School of Lausanne) Geneva
 Office Work

HOBBIES

Music, cinema, literature, photography, painting, computers, guitar & piano playing.